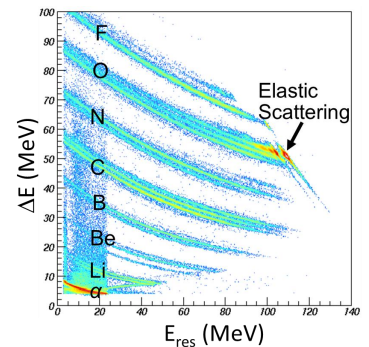
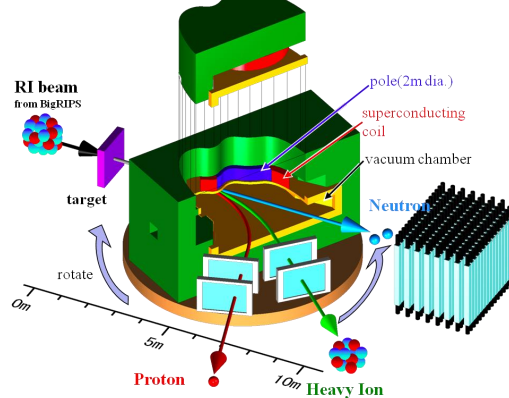
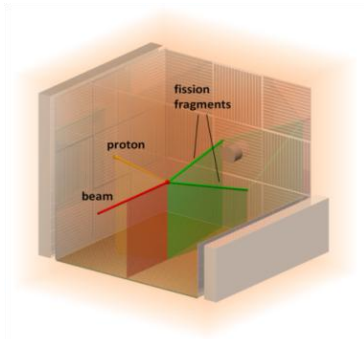
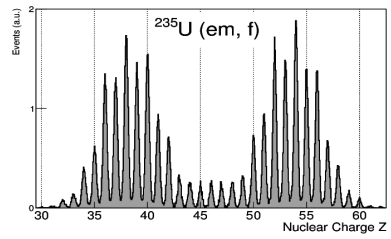
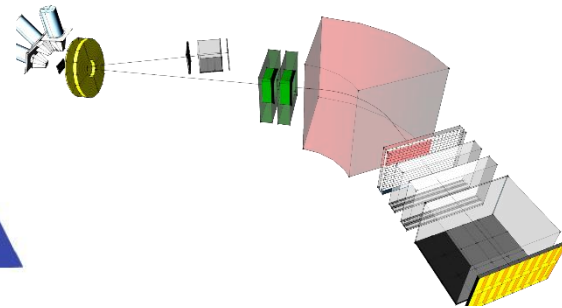
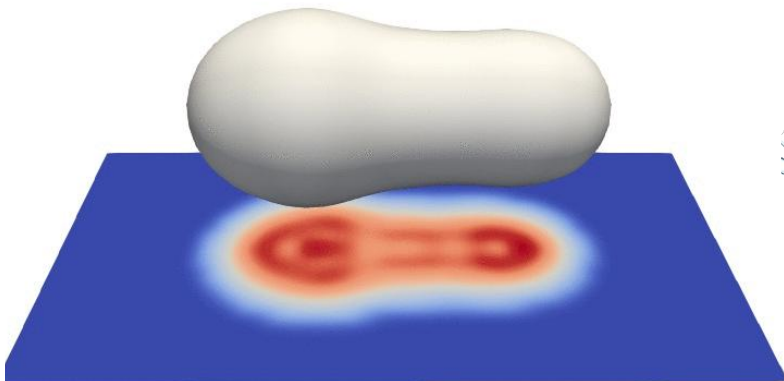
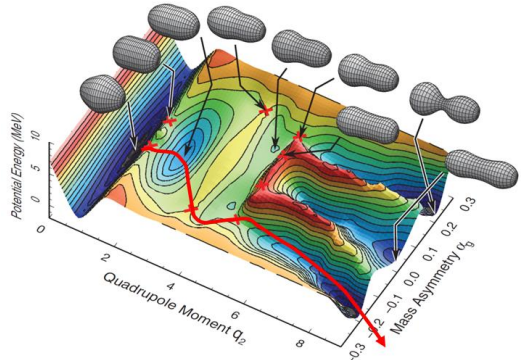


Nuclear Fission in the 21st Century (mapping Low-Energy Fission with RIBs)

Andrei Andreyev
University of York, UK



York city (UK), ~150.000 population



10 UK NP groups:

Birmingham, Brighton, Daresbury, Edinburgh, Glasgow, Liverpool, Manchester, Surrey, West of Scotland, York

University of York (est. 1963)

Academic staff	2,295
Students	23,420
<u>Undergraduates</u>	15,350
<u>Postgraduates</u>	8,070

York's Nuclear Physics group

10 “academics” (staff ☺)
10+ postdocs
25+ PhD students

Some fun ☺

陕西地图VS英国地图

35 million



陕西

69 million



英国

面积：20.6万平方公里

北部：黄土高原

著名建筑：钟楼、大雁塔

邻居：河南

资源：煤、石油、天然气

代表食品：肉夹馍

别称：大唐不夜城

艺人：郭达



面积：20.9万平方公里

北部：苏格兰高地

著名建筑：大笨钟、伦敦塔

邻居：荷兰

资源：煤、石油、天然气

代表食品：汉堡包

别称：日不落帝国

艺人：杰森斯坦森



York-Zhuhai Collaboration: Nuclear structure in heavy exotic nuclei (C.F.Jiao et al)

PHYSICAL REVIEW C 112, 024328 (2025)

August 2025

β - and α -decay spectroscopy of ^{182}Au

J. Miščík^{1,*}, B. Andel¹, A. N. Andreyev^{2,3}, A. E. Barzakh⁴, J. G. Cubiss^{2,†}, A. Algora^{5,6}, S. Antalic¹, M. Athanasakis-Kaklamanakis⁷, M. Au⁷, S. Bara⁸, R. A. Bark⁹, M. J. G. Borge¹⁰, A. Camaiani¹⁰, K. Chrysalidis⁷, T. E. Cocilios⁸, C. Costache¹³, H. De Witte⁸, R. Y. Dong¹⁴, D. V. Fedorov⁴, V. N. Fedossev¹⁷, L. M. Fraile¹⁵, H. O. U. Fynbo¹⁶, R. Grzywacz¹⁷, R. Heinke⁷, C. F. Jiao¹⁴, J. Johnson⁸, P. M. Jones⁹, D. S. Judson¹⁸, D. T. Kattikat Melcom¹⁹, M. M. Khan^{8,20}, J. Klimo⁸, A. Korgul²¹, M. Labiche²², R. Lică¹³, Z. Liu²³, M. Madurga¹⁷, N. Marginean¹³, P. Marini^{19,‡}, B. A. Marsh^{7,§}, C. Mihai¹³, P. L. Molkanov⁴, E. Nácher⁵, C. Neacsu¹³, J. N. Orce²⁴, R. D. Page¹⁸, J. Pakarinen^{25,28}, P. Papadakis²², S. Pascu¹³, A. Pereia¹⁰, M. Piera-Sifkowska²¹, Zs. Podolyák²⁶, M. D. Seliverstov⁴, A. Sitarčík¹, E. Stamatı^{7,27}, A. Stoica¹³, A. Stott², M. Stryjczyk^{25,28,29}, O. Tengblad¹⁰, I. Tsekhanovich¹⁹, A. Turturea¹³, J. M. Urdas¹⁵, P. Van Duppen⁸, N. Warr³⁰, and A. Youssef⁸

(ISOLDE Decay Station Collaboration)

¹Department of Nuclear Physics and Biophysics, Comenius University in Bratislava, 84248 Bratislava, Slovakia

²School of Physics, Engineering and Technology, University of York, York YO10 5DD, United Kingdom

³Advanced Science Research Center, Japan Atomic Energy Agency, Tokai-mura, Ibaraki 319-1195, Japan

⁴Affiliated with an institute covered by a cooperation agreement with CERN at the time of the experiment

⁵Instituto de Física Corpuscular, CSIC-Universidad de Valencia, E-46071 Valencia, Spain

⁶Institute of Nuclear Research (ATOMKI), P.O.Box 51, H-4001 Debrecen, Hungary

⁷CERN, CH-1211 Geneve 23, Switzerland

⁸KU Leuven, Instituut voor Kern- en Stralingsfysica, 3001 Leuven, Belgium

⁹iThemba LABS, National Research Foundation, P. O. Box 722, Somerset West 7129, South Africa

¹⁰Instituto de Estructura de la Materia, CSIC, 28006 Madrid, Spain

¹¹Dipartimento di Fisica, Università di Firenze, I-50019 Sesto Fiorentino, Italy

¹²Istituto Nazionale di Fisica Nucleare, Sezione di Firenze, I-50019 Sesto Fiorentino, Italy

¹³Horia Hulubei National Institute of Physics and Nuclear Engineering (IFIN-HH), R-077125 Bucharest, Romania

¹⁴School of Physics and Astronomy, Sun Yat-sen University, Zhuhai 519082, China

¹⁵Grupo de Física Nuclear and IPARCOS, Universidad Complutense de Madrid, CEI Moncloa, E-28040 Madrid, Spain

Competition between shape-coexisting $11/2^-$ states in neutron-deficient odd-mass thallium isotopes **In preparation 2026**

R. Y. Dong^{a,b}, C. F. Jiao^{a,b,*}, A. N. Andreyev^{c,d}, A. E. Barzakh^e, Z. Liu^{f,g}, S. Y. Zhang^h

^aSchool of Physics and Astronomy, Sun Yat-sen University, Zhuhai 519082, China

^bGuangdong Provincial Key Laboratory of Quantum Metrology and Sensing, Sun Yat-sen University, Zhuhai 519082, China

^cDepartment of Physics, University of York, York, YO10 5DD, United Kingdom

^dAdvanced Science Research Center (ASRC), Japan Atomic Energy Agency, Tokai-mura, Japan

^ePetersburg Nuclear Physics Institute, NRC Kurchatov Institute, Gatchina 188300, Russia

^fInstitute of Modern Physics, Chinese Academy of Sciences, Lanzhou 730000, China

^gUniversity of Chinese Academy of Sciences, Beijing 100049, China

^hSchool of Physics and State Key Laboratory of Nuclear Physics and Technology, Peking University, Beijing 100871, China

Abstract

Unlike the near-constant excitation energies of low-lying $I\pi = 11/2^-$ states in neighboring Au isotopes, an anomalous suppression in the excitation energies of one-proton $11/2^-$ states is observed in neutron-deficient Tl isotopes. We study the evolution of low-lying one-proton states in neutron-deficient odd-mass Tl isotopes, in particular the $11/2^-$ states, by means of configuration-

York-Zhuhai Collaboration: Probing the shell evolution in heavy nuclei (C.Yuan et al.)

Phys. Lett. B 871 (2025) 140013

November 2025



Contents lists available at ScienceDirect

Physics Letters B

journal homepage: www.elsevier.com/locate/physletb



Letter

Electromagnetic moments of $^{215,217}\text{Bi}$: Probing shell evolution beyond $N = 126$



A. N. Andreyev ^{1,2}, A. Barzakh ^{1,3,*}, M. D. Seliverstov ¹, Z. Yue ¹, Menglan Liu ^{1,4},
Cenxi Yuan ^{1,4}, A. Algora ^{1,5}, B. Andel ^{1,6}, S. Antalic ^{1,6}, M. Al Monthery ^{1,7}, D. Atanasov ^{1,8},
J. Benito ¹, G. Benzoni ¹, T. Berry ¹, M. L. Bissell ¹, K. Blaum ^{1,9}, M. J.
K. Chrysalidis ^{1,10}, C. Clisu ^{1,10}, T. E. Cocolios ^{1,10}, C. Costache ^{1,10}, J. G. Cub
T. Day Goodacre ^{1,11,supplementary}, G. J. Farooq-Smith ^{1,11,supplementary}, D. V. Fedorov ^{1,10}, V
L. M. Fraile ¹, H. O. U. Fynbo ¹, V. Gadelshin ¹, L. P. Gaffney ^{1,12}, R. F G
C. Granados ^{1,13}, P. T. Greenlees ¹, R. D. Harding ^{1,14}, L. J. Harkness-Bren
A. Herlert ^{1,15}, M. Huyse ¹, A. Illana ^{1,16}, J. Jolie ^{1,17}, D. S. Judson ¹, J. Kai
P. Larmonier ¹, I. Lazarus ^{1,18}, D. Leimbach ^{1,19}, R. Lică ¹, Z. Liu ^{1,20,af}, D. Li
M. Madurga ^{1,21}, V. Manea ¹, N. Marginean ¹, R. Marginean ¹, B. A. Mars
P. Molkanov ¹, P. Mosat ¹, M. Mougeot ¹, J. R. Murias ¹, E. Nacher ¹, A.
L. Nies ¹, R. D. Page ¹, S. Pascu ¹, A. Perea ¹, V. Pucknell ^{1,22}, P. Rahkila ¹
E. Rapisarda ¹, K. Rezynkina ¹, M. Rosenbush ^{1,23,ak}, R. E. Rossel ¹, S. Rotl
V. Sánchez-Tembleque ¹, K. Schomacker ^{1,24}, L. Schweikhard ^{1,25}, C. Seiffe
L. Stan ¹, M. Stryjczyk ^{1,26,al}, D. Studer ¹, J. Sundberg ^{1,ac}, C. Sürder ^{1,am},
P. Van Duppen ^{1,10}, V. Vedia ¹, M. Verlinde ¹, S. Viñals ¹, N. Warr ^{1,ab}, A.
F. Wienholtz ^{1,aj,am}, R. N. Wolf ^{1,h,aj,ao}

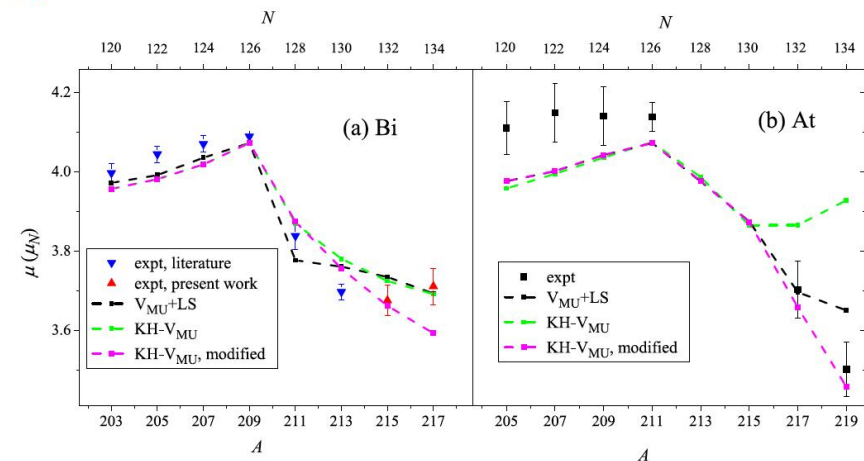


Fig. 5. Comparison of μ values from experiment and CISM calculations for $I^\pi = 9/2^-$ states of bismuth and astatine isotopes. (a) Bismuth isotopes. Upward triangles:

^a School of Physics, Engineering and Technology, University of York, YO10 5DD, York, United Kingdom

^b Affiliated with an institute covered by a cooperation agreement with CERN at the time of the experiment, Russia

^c Sino-French Institute of Nuclear Engineering and Technology, Sun Yat-Sen University, 519082, Zhuhai Guangdong, China

^d Instituto de Física Corpuscular, CSIC - Universidad de Valencia, E-46980, Valencia, Spain

^e HUN-REN Institute of Nuclear research (ATOMKI), P.O.Box 51, H-4001, Debrecen, Hungary

Nuclear Fission in the 21st Century

(from an experimentalist's point of view)

- Fission in the new" regions of the Nuclear Chart" -why?
- Brief (experimental) review on low-energy fission
- Beta-Delayed Fission at ISOLDE (CERN) **at 60 keV**
- d,pf transfer -induced fission with post-accelerated RIBs with ACTAR and ISS at HIE-ISOLDE at **Coulomb energies** (ANL example)
- Multi-nucleon transfer-induced fission at **Coulomb energies** (VAMOS@GANIL, JAEA)
- Coulex-induced fission with SOFIA@GSI at **relativistic 1 AGeV energies**,
- **Conclusions**
- Spontaneous fission (SF) in heavy/SHE nuclei
- Fusion-fission with heavy ions at Coulomb energies (Dubna, ANU, India..)
- n_ToF, n-induced fission experiments (ILL,n_ToF, LANSCE,J-PARC....)
- Future techniques: Photofission at ELI-NP with CBS-technique
- Future techniques: Fission in collision geometry with electrons (**SCRIT@RIKEN**)?

A.N. Andreyev, K. Nishio, K.-H. Schmidt, Reports on Progress in Physics, 1 (2018) Experimental review

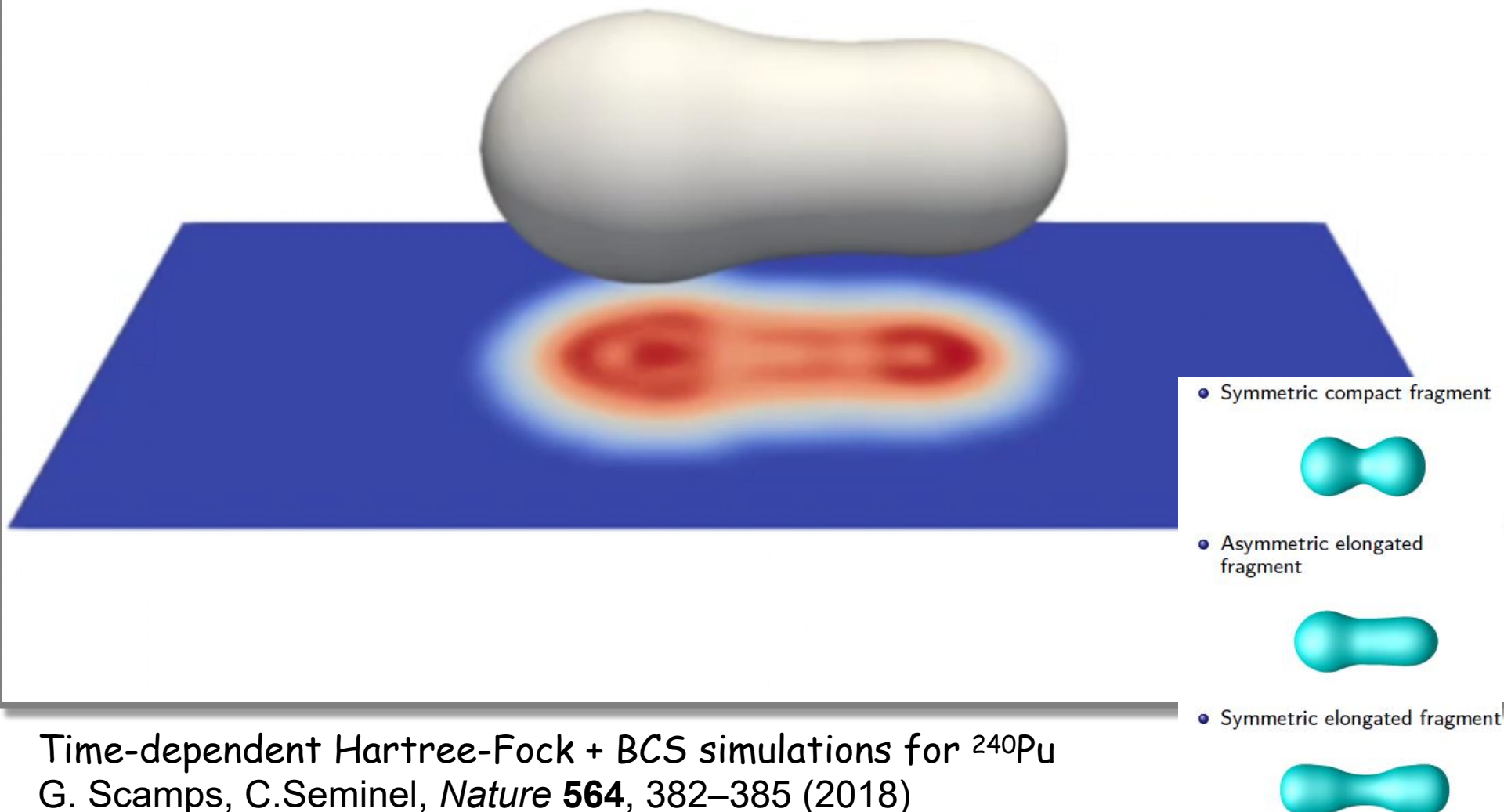
N. Schunck, L. M. Robledo, Rep. Prog. Phys. 79, 116301 (2016) Theory review

F.-P. Hessberger. Eur. Phys. J. A, 53, 75 (2017) SF review

N. Colonna et al., Eur. Phys. J. A56, 48 (2020) CERN n_ToF CERN fission program (and similar)

What is Fission?

Time scale for fission from ‘compound nucleus’ to scission ~ 20 zs ($\sim 20 \times 10^{-21}$ s)



Some Historical Milestones In Fission

- 1932 Discovery of neutron (J. Chadwick)
- 1937 Development of the Liquid Drop Model (N. Bohr)
- 1938 Neutron-induced fission (O. Hahn and F. Strassmann)
 - Explanation of fission (L. Meitner and O.R. Frisch)
- 1939 Spontaneous fission (^{238}U , G.N. Flerov and K.A. Petrzhak)
- 1942 First self-sustaining chain reaction (E. Fermi)
- 1945 First nuclear bomb (The Manhattan project)
- 1946 Alpha accompanied (ternary) fission
- 1962 Fission shape isomers (V.M. Polikanov et al.)
- 1966 Beta-delayed fission (V.I Kuznetzov et al.)
- 1967 Macroscopic-microscopic method (V. Strutinsky)
- ~1994 In-flight Coulex fission of radioactive ion beams (GSI)
- ~2008 beta-delayed fission studies with RIBs at ISOLDE

(Some of) Applications of Fission

- **Energy production**, ~11% of the world's electricity came from nuclear power (~450 reactors)
 - ~15% in the UK, 16 reactors
 - ~75% in France, 57 reactors
 - ~5%, in China, 59 operating (+28 being constructed)



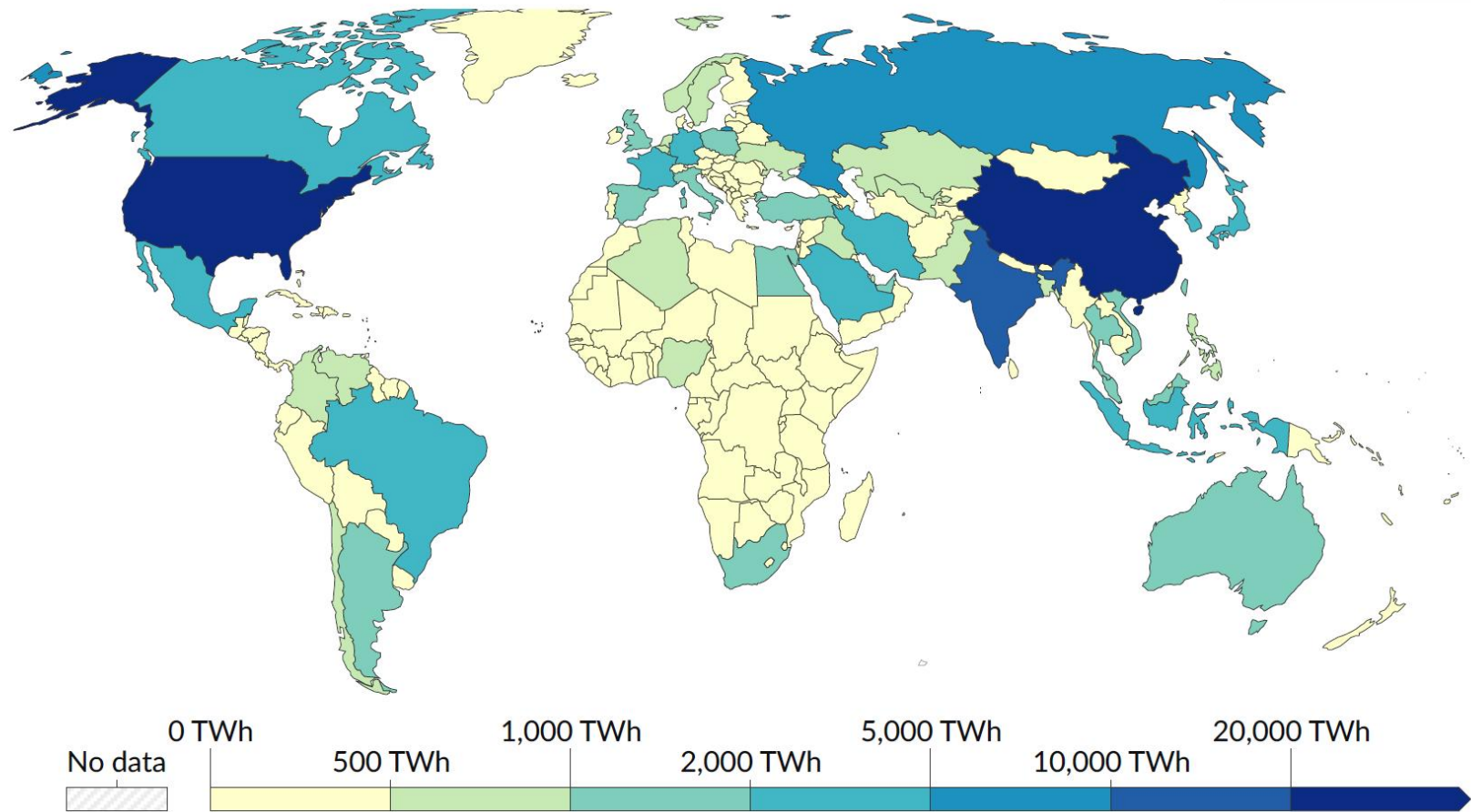
- **Medical isotope production**, e.g. $^{99}\text{Mo}/^{99}\text{Tc}$ for nuclear medicine. At present, six reactors provide more than 95% of the $^{99}\text{Mo}/^{99}\text{Tc}$ supply worldwide. 40 million procedures each year.

- **Nuclear propulsion** (mostly military so far)



- **Fundamental research** (nuclear physics and nuclear astrophysics, RIBs production, r-process termination by fission etc....) ~225 research reactors world-wide

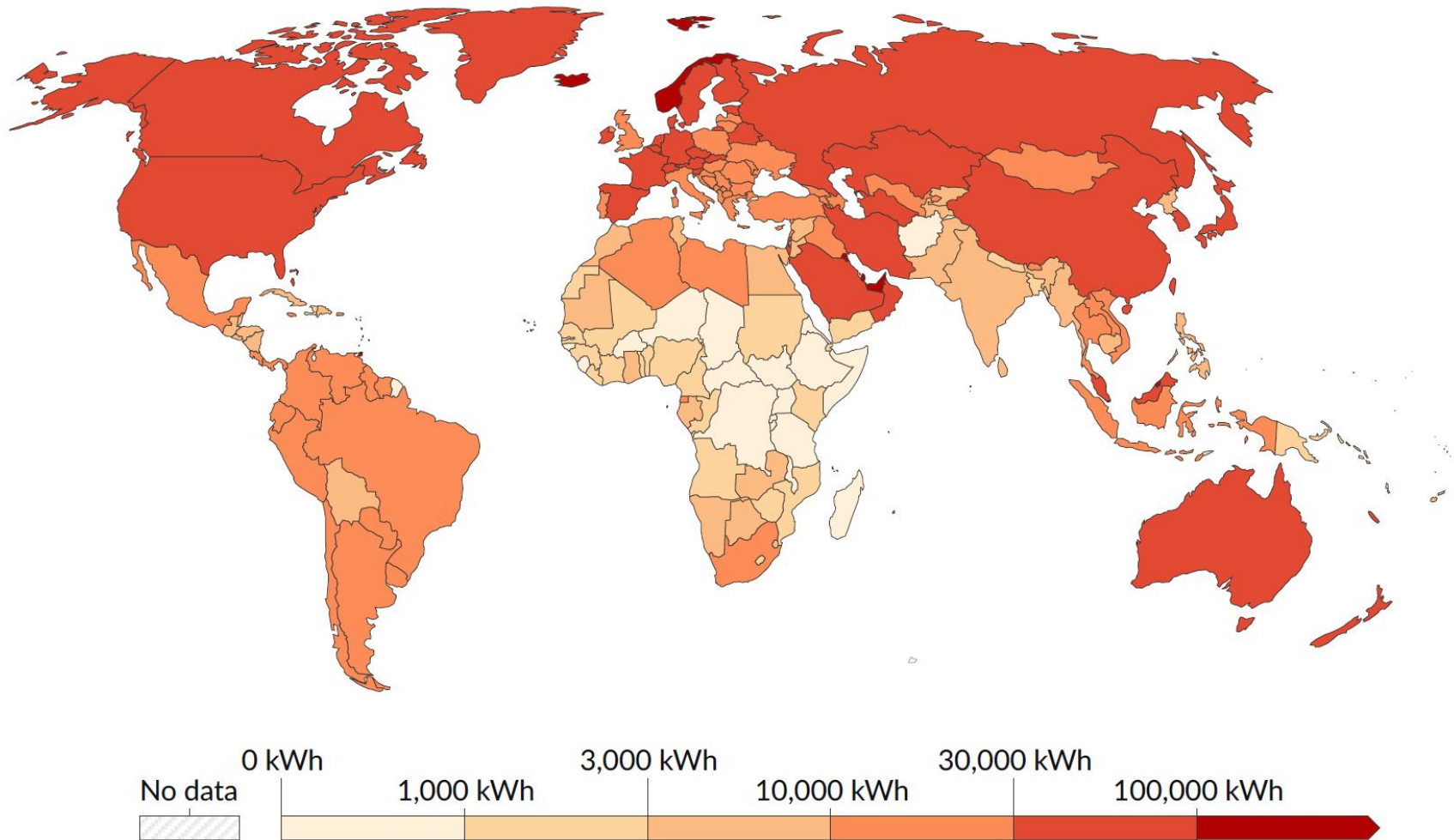
Energy use per country



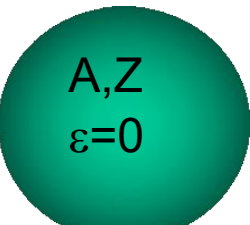
1965

2023

Energy use per person, 2023



Fission Barrier in LDM



$$R = r_o A^{1/3}$$

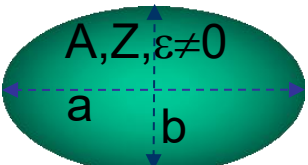


$$\begin{aligned} \text{Ellipsoidal} \\ \text{deformation } \varepsilon \\ a = R(1+\varepsilon) \\ b = R(1+\varepsilon)^{-1/2} \end{aligned}$$

$$\text{BE} = \cancel{a_V A} - a_S A^{2/3} - a_C \frac{Z(Z-1)}{A^{1/3}} - \cancel{a_A \frac{(A-2Z)^2}{A}} + \delta(A, Z)$$

Diagram illustrating the components of the Binding Energy (BE) formula:

- $\cancel{a_V A}$: Volume term, proportional to $\sim R^3$
- $-a_S A^{2/3}$: Surface term, proportional to $\sim R^2$
- $-a_C \frac{Z(Z-1)}{A^{1/3}}$: Coulomb term, proportional to $\sim 1/R$
- $\cancel{a_A \frac{(A-2Z)^2}{A}}$: Asymmetry term, proportional to $\sim 1/A$
- $+\delta(A, Z)$: Pairing term



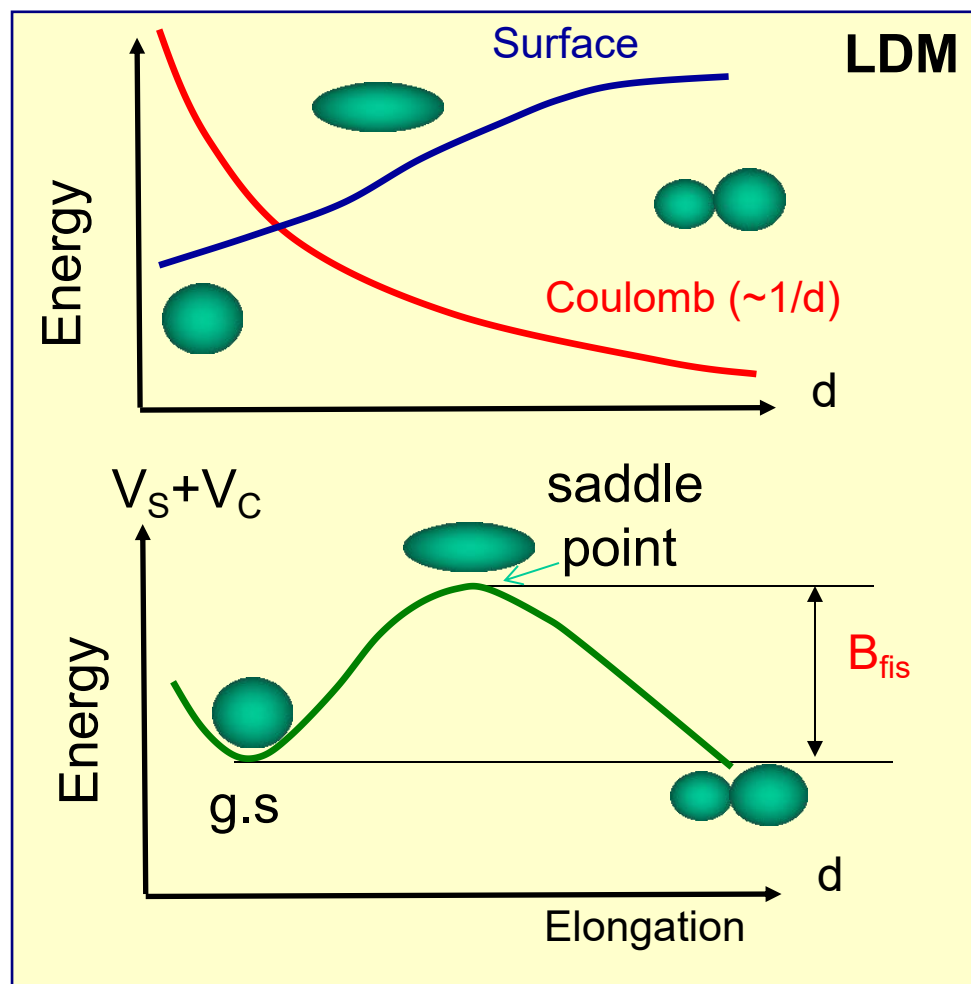
When deformed (assuming **incompressibility!** $R^3 = ab^2$):
No need to remember expressions, **but must know the trends!**

- Volume, Asymmetry and Pairing \sim constant
- Surface term **increases** (thus tries to inhibit deformation) from $S = 4\pi R^2$ to $S = 4\pi R^2(1 + \frac{2}{5}\varepsilon^2)$, thus BE decreases
- Coulomb **decreases** $\sim (1 - 1/5\varepsilon^2)$, thus BE increases
- Difference in BE: $\Delta BE = BE(\varepsilon=0) - BE(\varepsilon)$

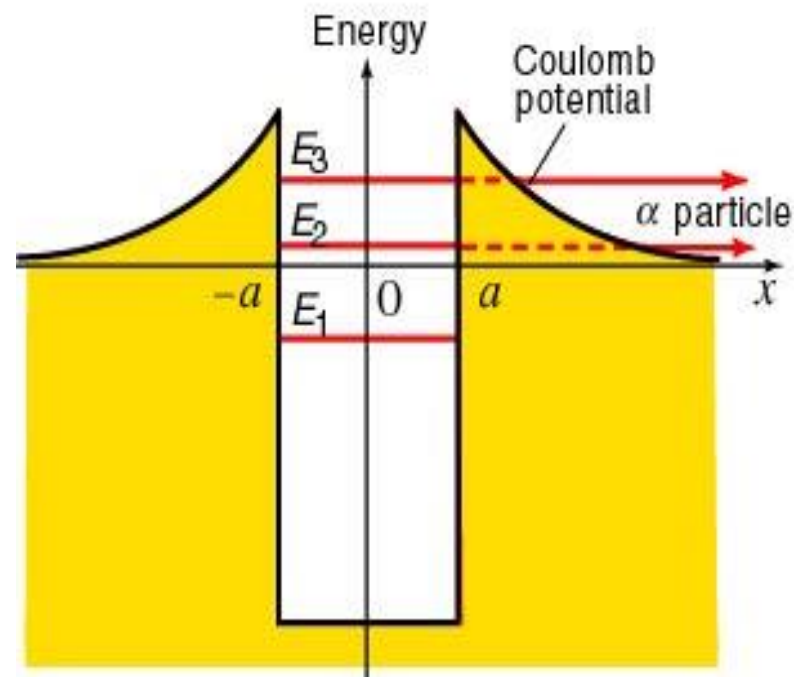
Thus, interplay between Surface and Coulomb terms is important when consider effects of deformation

Fission Barrier in 1D LDM ('Text-book' plot)

Competition between increasing Surface and decreasing Coulomb energies by increasing deformation leads to a local maximum in their difference called **Fission Barrier** (the top of the barrier is called the 'saddle point')



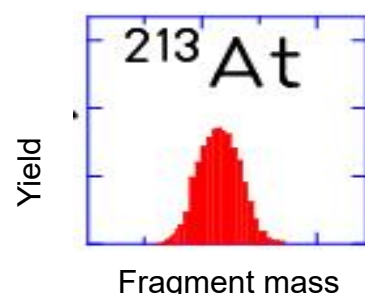
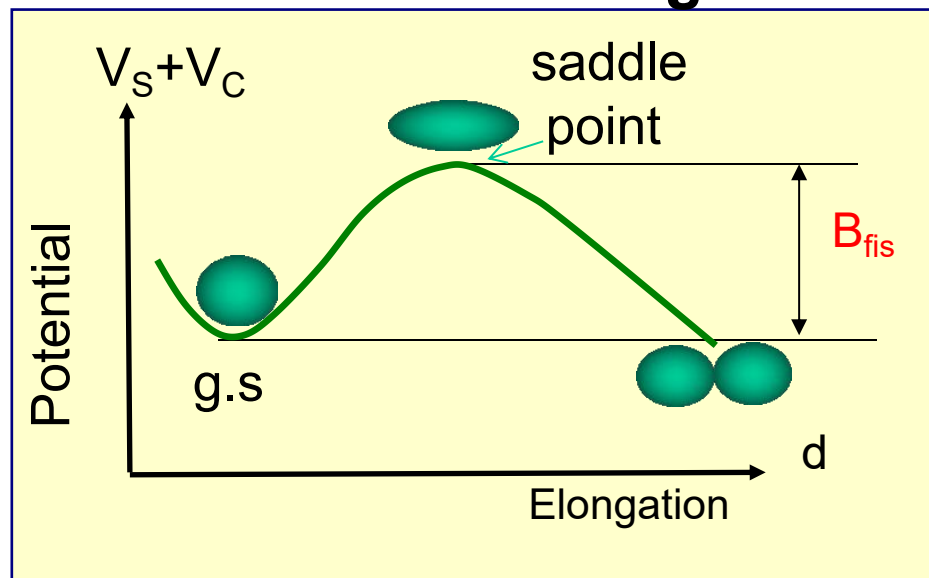
To be compared to alpha decay



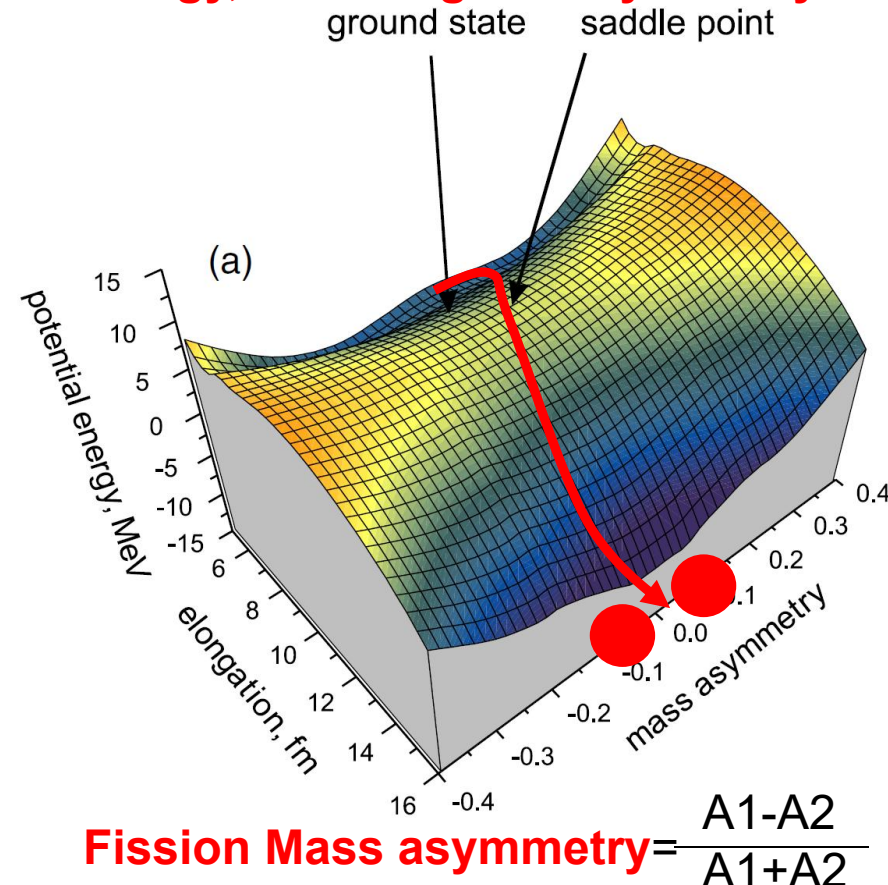
NB: in both spontaneous fission and alpha decay, fission happens **via the tunnelling**

Textbooks: Fission Barrier and Mass Distribution in "pure" LDM (no shell effects yet)

Text-book 1D figure



3D energy, including the asymmetry



$$\text{Fission Mass asymmetry} = \frac{A_1 - A_2}{A_1 + A_2}$$

Mass asymmetry=0, if $A_1=A_2$

Pure LDM (no shell corrections): **symmetric mass split ($A_1=A_2$, a single peak in the FF's mass distribution)**, fission follows the single 'symmetric valley' in the potential energy (red line on the plot). Any 'attempt' to fission asymmetrically needs higher energy.

Symmetric vs Asymmetric Fission in 3D (with shell effects included)

A.N. Andreyev, K. Nishio, K.-H. Schmidt, Reports on Progress in Physics, 1 (2018)

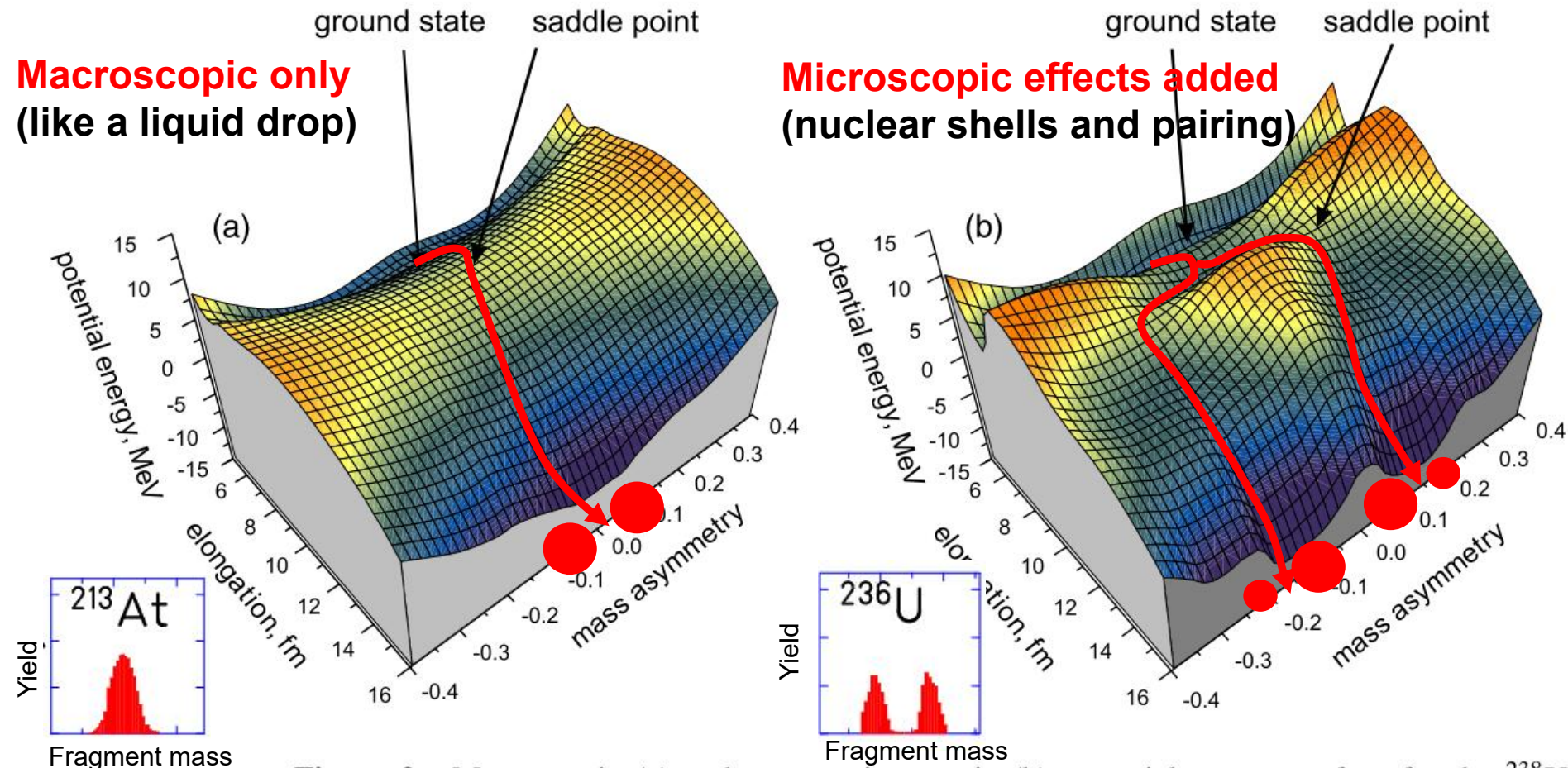
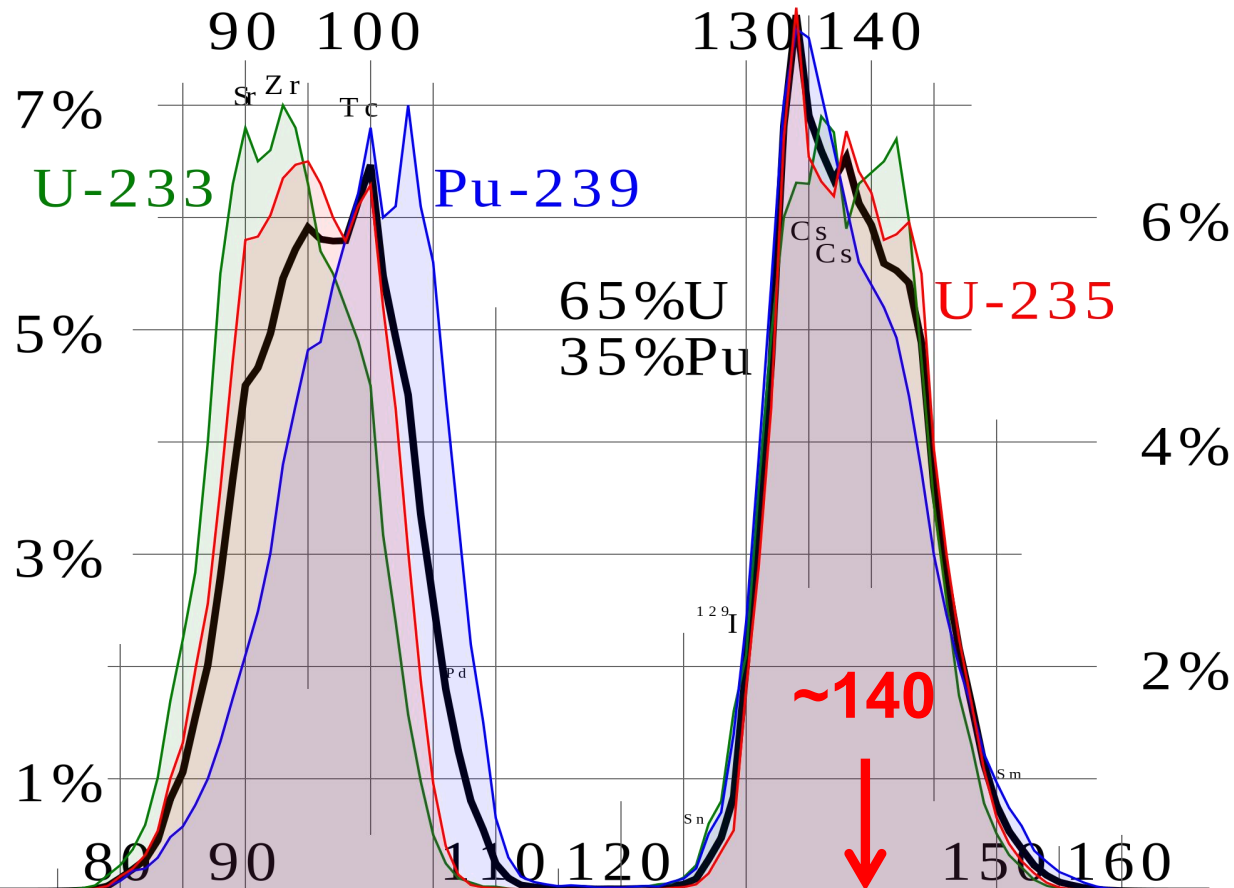


Figure 2. Macroscopic (a) and macro-microscopic (b) potential energy surface for the ^{238}U

**Symmetric Mass Split (single peak)
– if pure LDM (no shell effects)**

**Asymmetric Mass Split (two
peaks) if shell effects included**

Examples of Mass Distributions in fission of $^{233,235}\text{U}$ and ^{239}Pu



6%

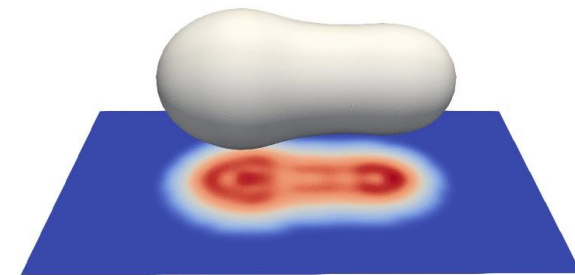
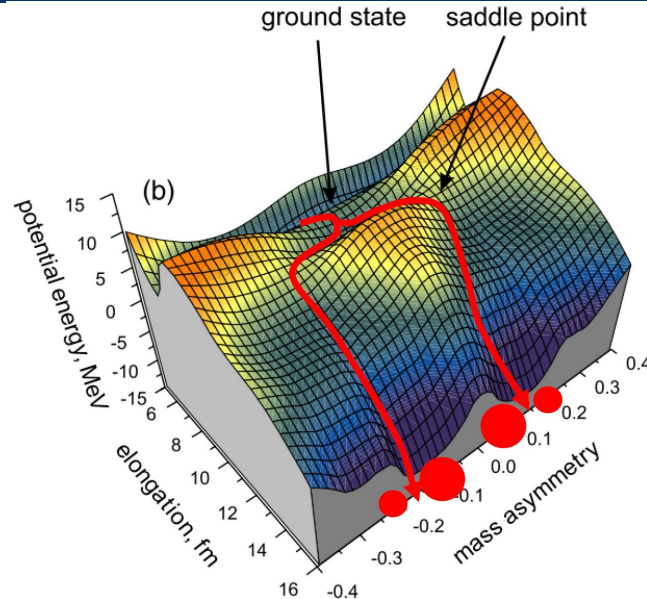
4%

2%

Proton shells in the heavy fragment around $Z=52,54$ drive the asymmetry in the heavy actinides (K.H-Schmidt et al)

- Fission product mass yields for thermal neutron fission of ^{235}U , ^{239}Pu
- ~ 400 different mass pairs (~ 800 different nuclei) are produced in fission
- Note the persistence of the heavier mass peak at $A \sim 140$
- The complementary light fission fragment mass increases as function of the compound system's mass

What are (typical) observables in fission?

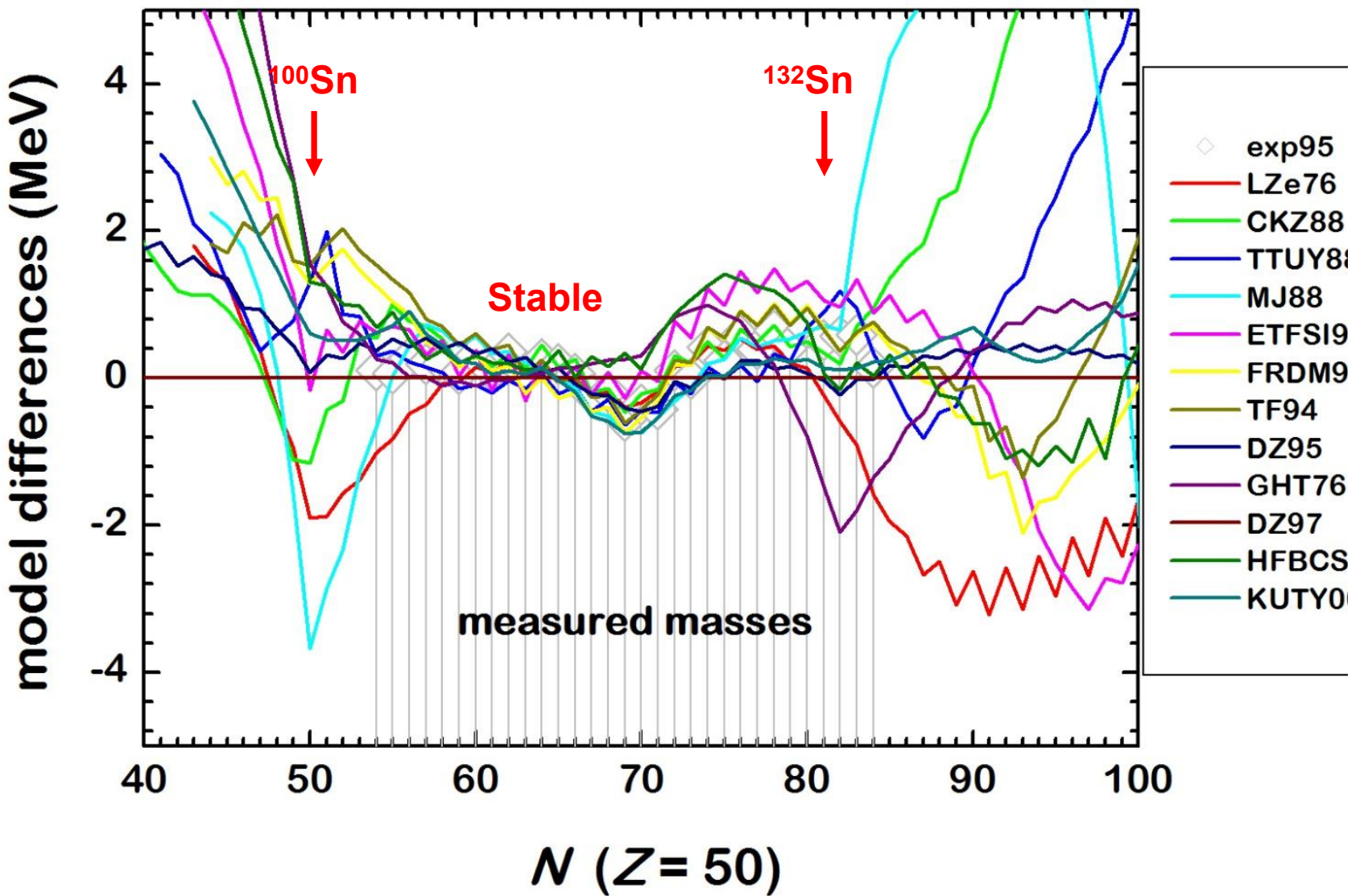


- **Half-lives** (e.g. for SF – from ms to billions of years)
- **Fission fragments mass and charge distributions** (symmetric, asymmetric, multimodal)
- **Kinetic energies of FFs**, & their sum – **Total Kinetic Energy(TKE)**
- **Prompt neutron and γ -ray multiplicities**, energies of γ 's and n's
- **Fission barrier height** (a derived value! Can't be measured directly)
- NB, **typical FFs energies in SF are ~1 AMeV**, difficult to measure with sufficient precision (can be overcome **in inverse kinematics** – the modern approach)

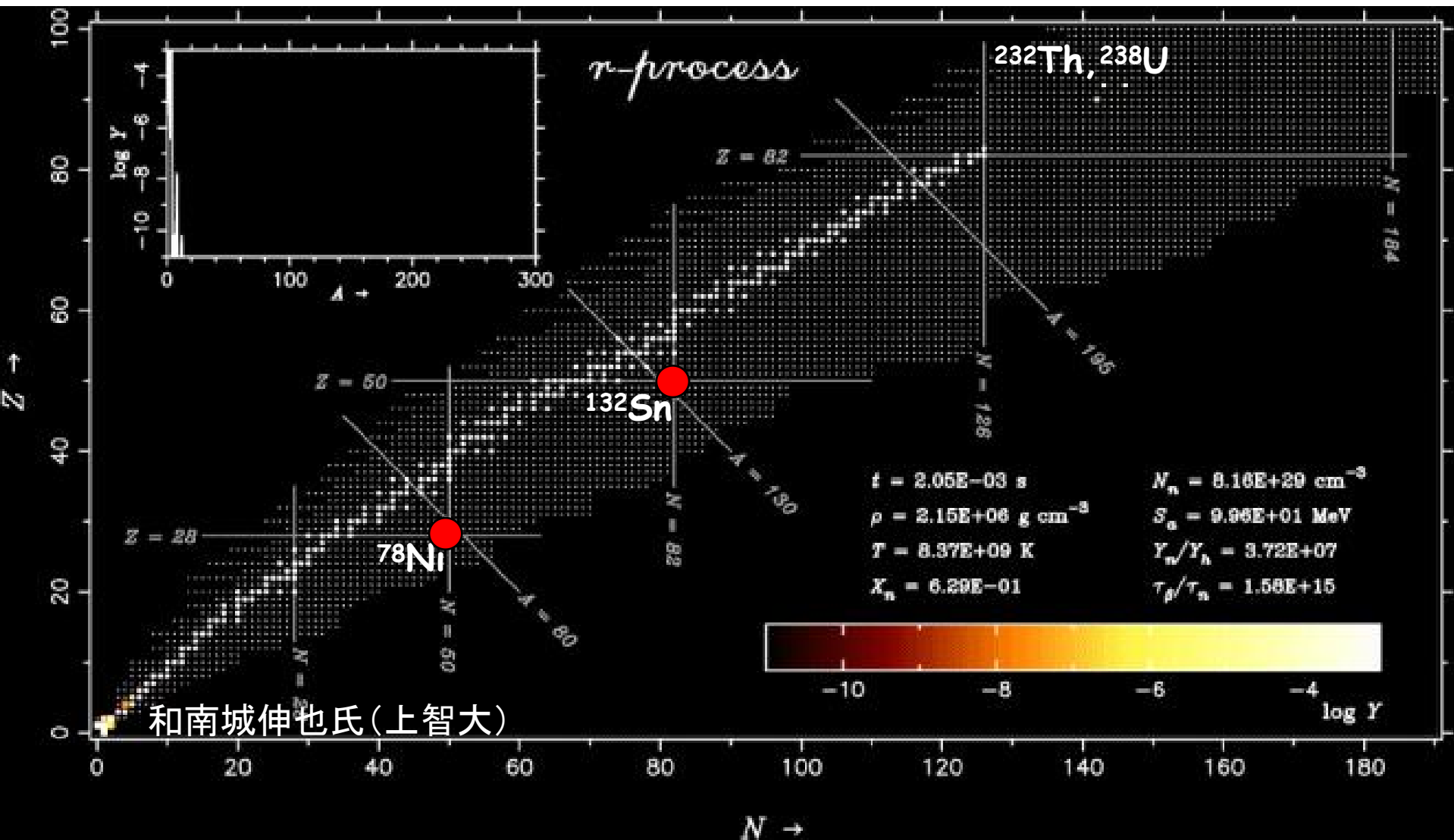
Outlook: Why 'new regions of fission'?

- Many nuclear properties change far from stability line (e.g. disappearance of traditional magic numbers, appearance of new shell gaps, halos, skins...)
- What happens to fission e.g. on the extremely neutron-rich or proton-rich sides? (isospin dependence of fission, r-process...)
- Not simple to answer, as to fission these nuclei at low excitation energy ($E^* \sim B_f$) is a very challenging task (most of them do not fissions from g.s.) - need data at low energy (SF, beta-delayed fission, n-induced fission)

Example: Calculations of mass for Sn isotopes (or why we need to go far off stability)



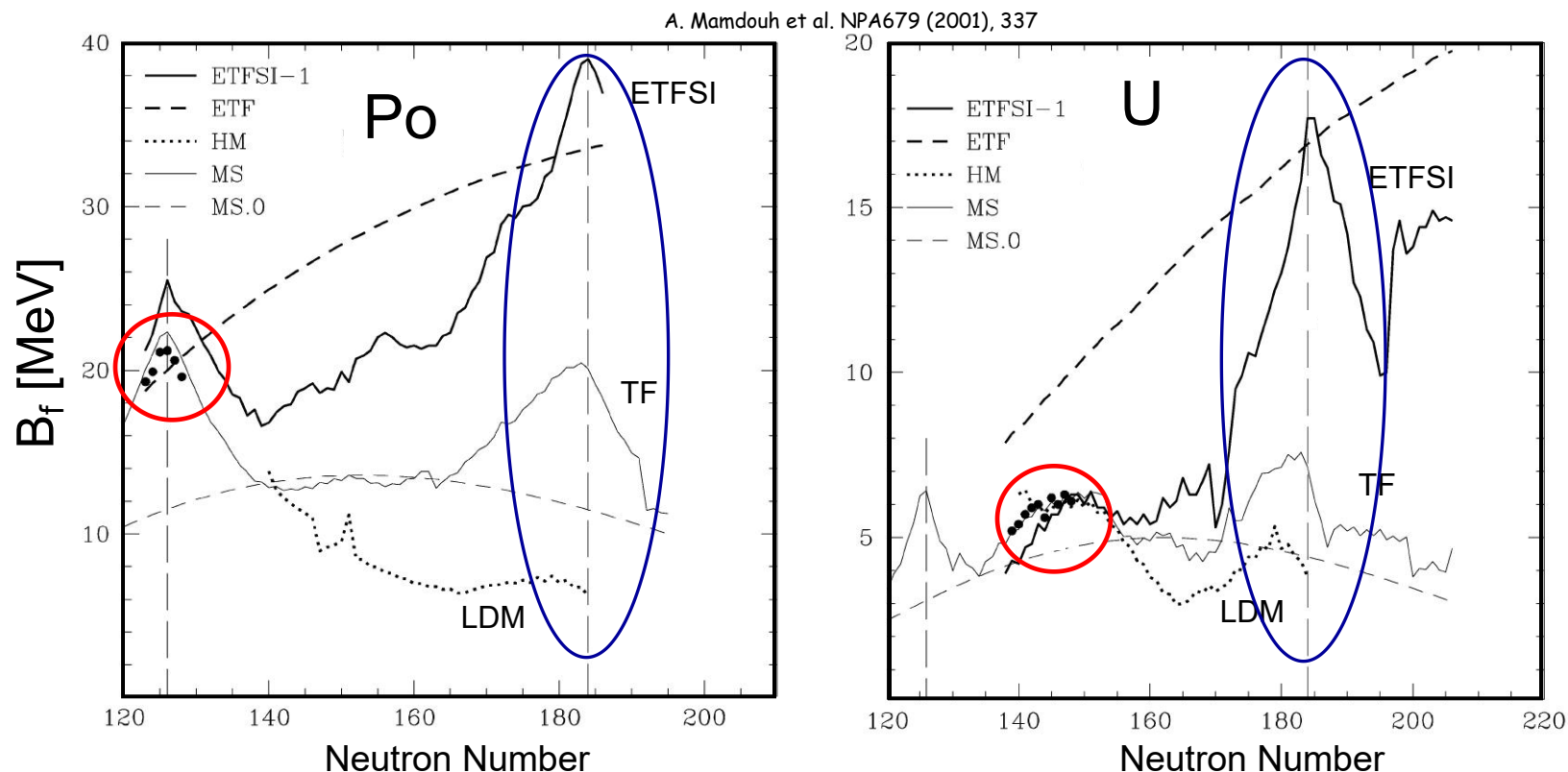
R-process network calculations



R-process termination by fission: need to know **fission barriers** and **FFs mass distributions for $Z>82$, $N>180$ nuclei!** (hardly ever achievable in the lab?)

Example: Fission Barrier Calculations for r-process nuclei

Full symbols – experimental data
Lines – calculations (LDM, TF, ETFSI)



- Good agreement between $B_{f,\text{cal}}$ and $B_{f,\text{exp}}$ for nuclei close to stability
- Large disagreement far of stability (both on n-def. and n-rich sides)
- Need **measured** fission data far of stability to 'tune' fission models

Fission re-cycling in r-process: influence of the fission fragments mass distributions modelling

THE ASTROPHYSICAL JOURNAL, 808:30 (13pp), 2015 July 20

doi:10.1088/0004-637X/808/1/30

© 2015. The American Astronomical Society. All rights reserved.

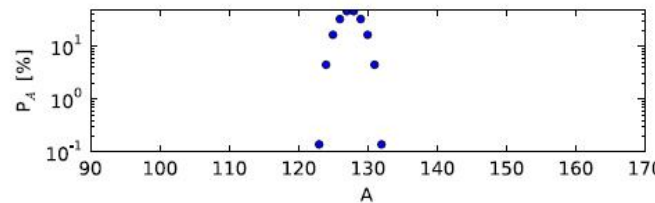
^{274}Pu

THE ROLE OF FISSION IN NEUTRON STAR MERGERS AND ITS IMPACT ON THE *r*-PROCESS PEAKS

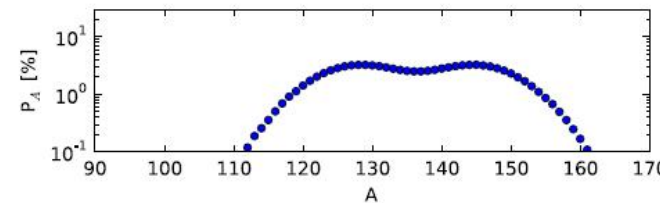
M. EICHLER¹, A. ARCONES^{2,3}, A. KELIC³, O. KOROBKIN⁴, K. LANGANKE^{2,3}, T. MARKETIN⁵, G. MARTINEZ-PINEDO^{2,3}, I. PANOV^{1,6}, T. RAUSCHER^{1,7}, S. ROSSWOG⁴, C. WINTERLER⁸, N. T. ZINNER⁹, AND F.-K. THIELEMANN¹

THE ASTROPHYSICAL JOURNAL, 808:30 (13pp), 2015 July 20

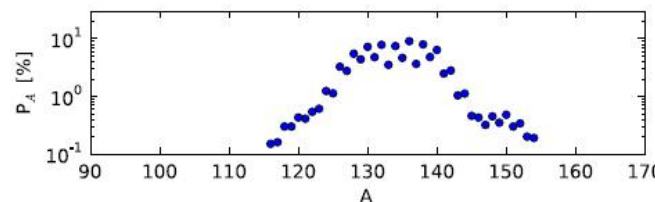
EICHLER ET AL.



(a) Panov et al. (2008)



(b) Kodama & Takahashi (1975)



(c) ABLA07

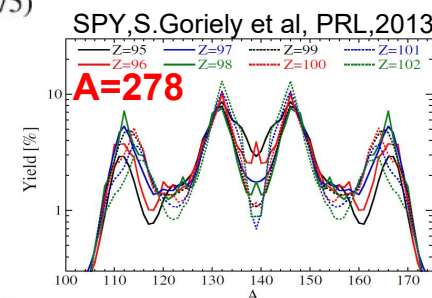


Figure 3. Fission fragment distributions for the models considered in our calculations, here for the case of neutron-induced fission of ^{274}Pu . For this reaction Panov et al. (2008) predict 19 ABLA07-released fission neutrons. Kodama & Takahashi (1975) do not predict any fission neutrons. For Panov et al. (2001) neutrons can be released if the fragments would lie beyond the neutron dripline. The distribution for Panov et al. (2001) consists only of two products with $A_1 = 130$ and $A_2 = 144$.

Recall: in r-process network calculations, we need fission data for e.g. ^{274}Pu , but so far the fission around ^{239}Pu was studied only

Fission re-cycling in r-process: competition between spontaneous, neutron-induced and beta-delayed fission

Calculations of fission rates for r-process
nuclear Physics A 747 (2005) 633–654
nucleosynthesis [★]

I.V. Panov ^{a,b,*}, E. Kolbe ^a, B. Pfeiffer ^c, T. Rauscher ^a, K.-L. Kratz ^c,
F.-K. Thielemann ^a

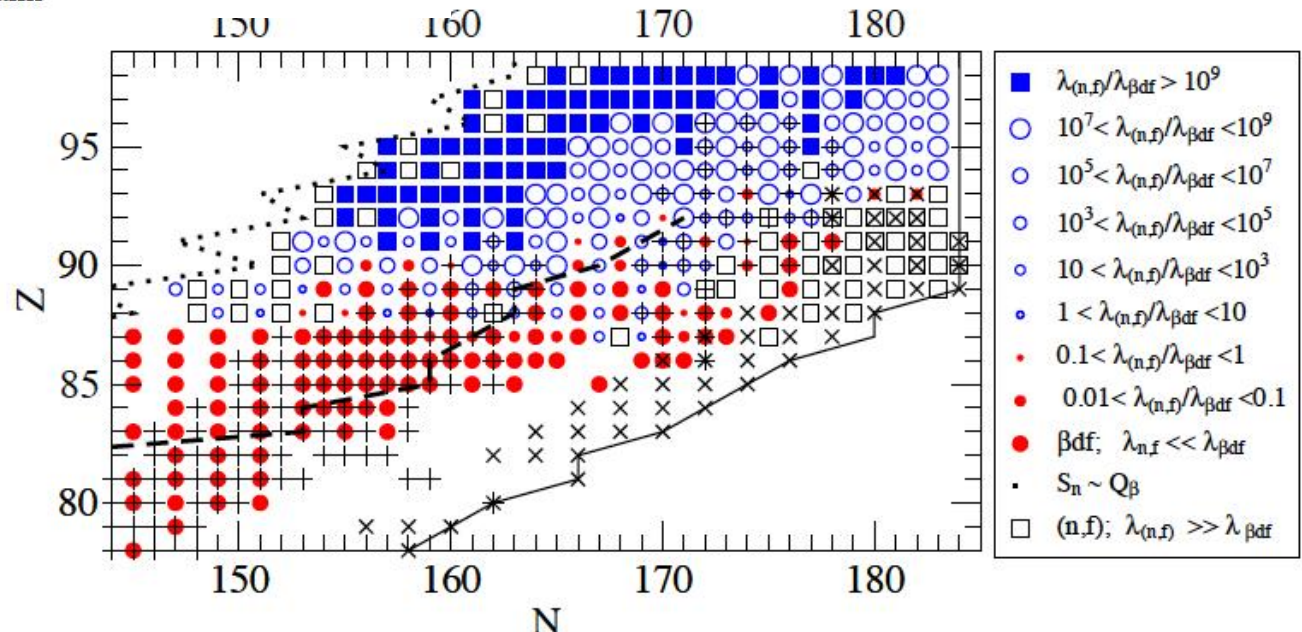
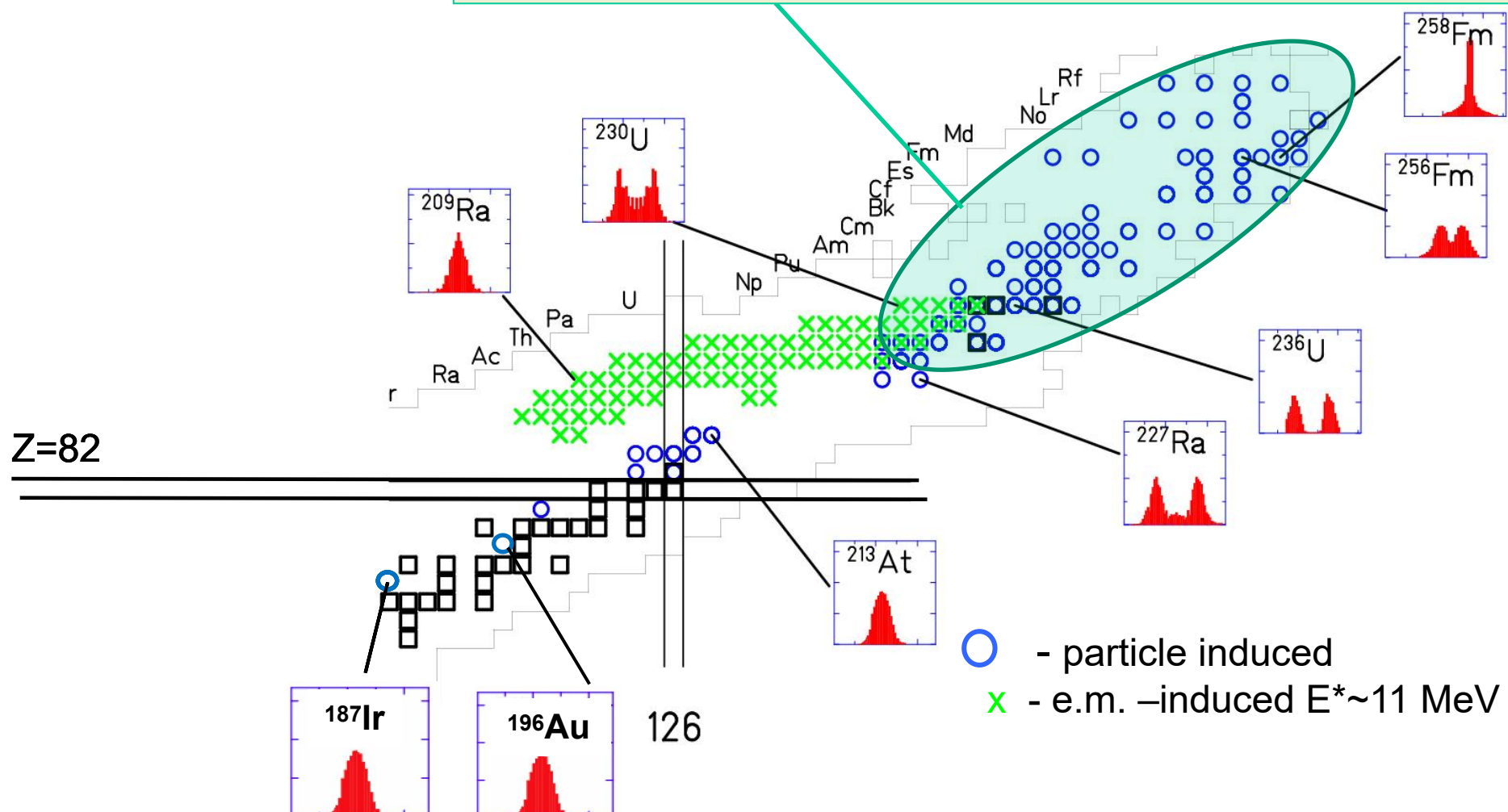


Fig. 7. The map of rates ratios $\lambda_{n,f}/\lambda_{\beta df}$ for $\rho Y_n = 1$ and $T_9 = 1$. The most abundant nuclei along the r-process path, for $n_n \approx 10^{26}$ (crosses), and $n_n \approx 10^{19}$ (pluses) are marked. The position of the neutron drip-line (full line), nuclei with neutron separation energy $S_n \approx 2$ MeV (dashed line) and nuclei with beta-decay energies $Q_\beta \sim S_n$ (dotted line) are denoted as well. These results were obtained for the mass model of Hilf et al. [22] and fission barriers by Howard and Moller [1].

Experimental information on low-energy fission Nuclei with measured charge/mass split (RIPL-2 + GSI)

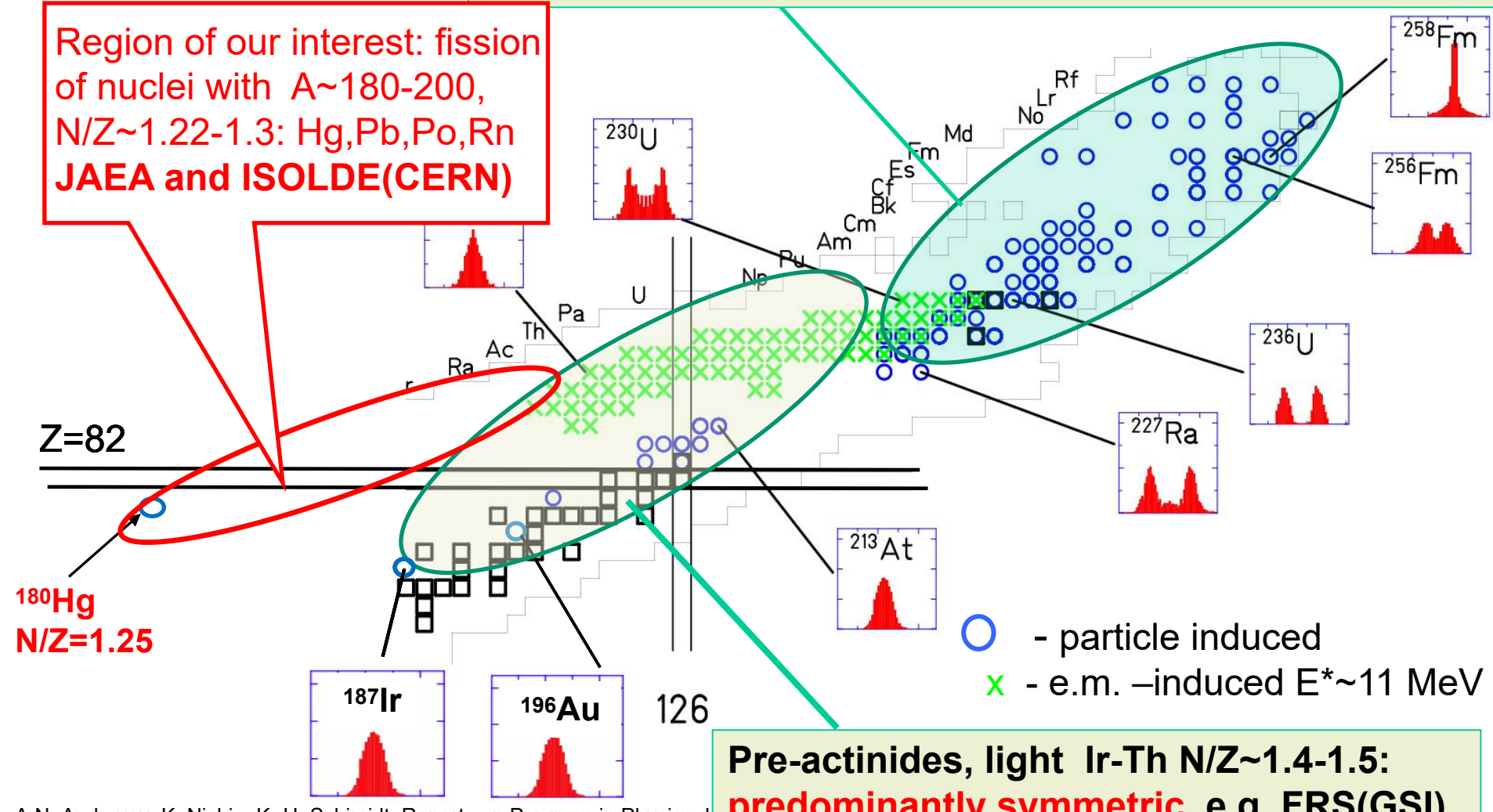
Heavy Actinides, N/Z~1.56: predominantly asymmetric; spontaneous fission, fission isomers, (bimodal)



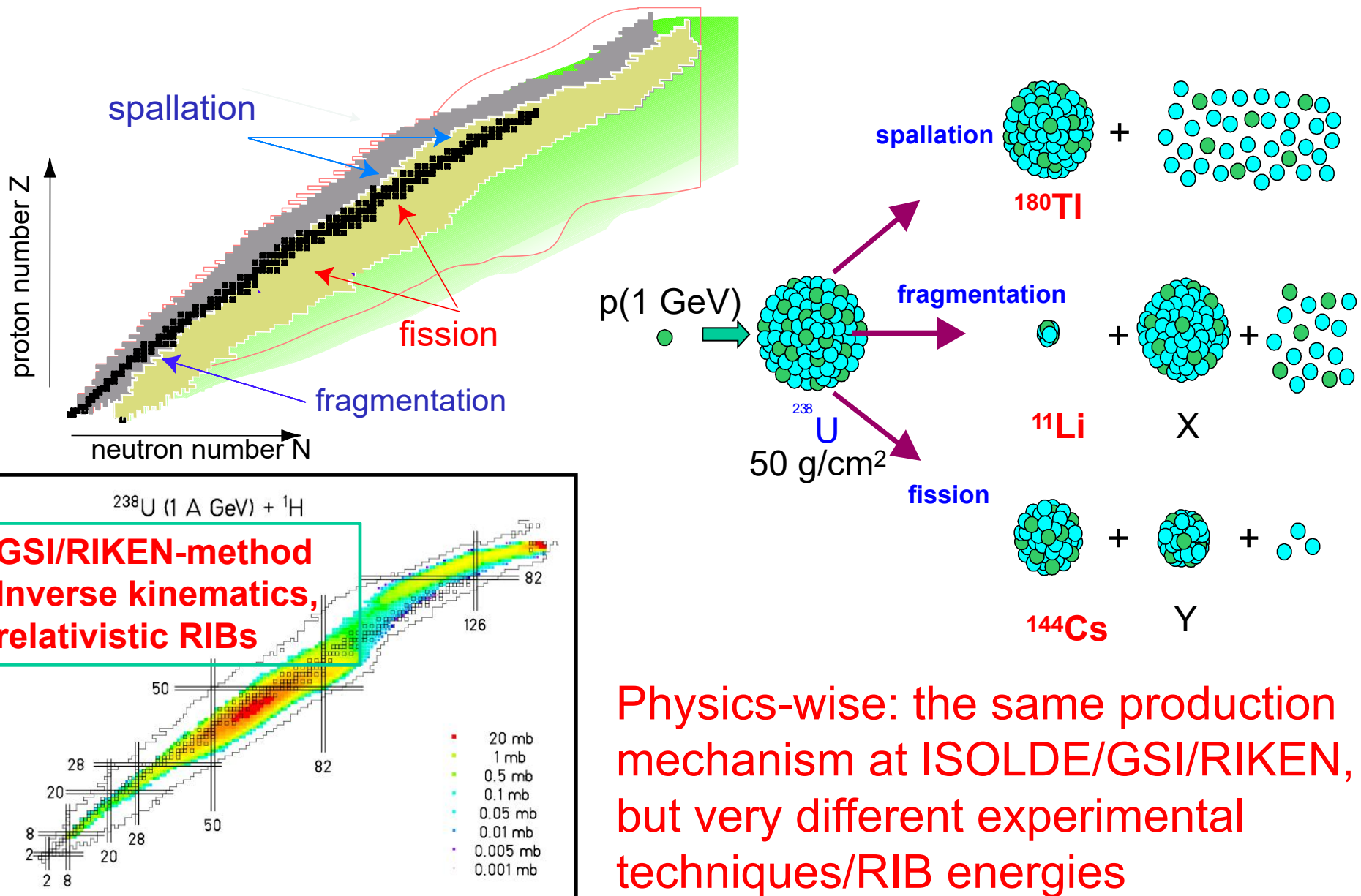
Experimental information on low-energy fission Nuclei with measured charge/mass split (RIPL-2 + GSI)

Heavy Actinides, N/Z~1.56: predominantly asymmetric; spontaneous fission, fission isomers, (bimodal)

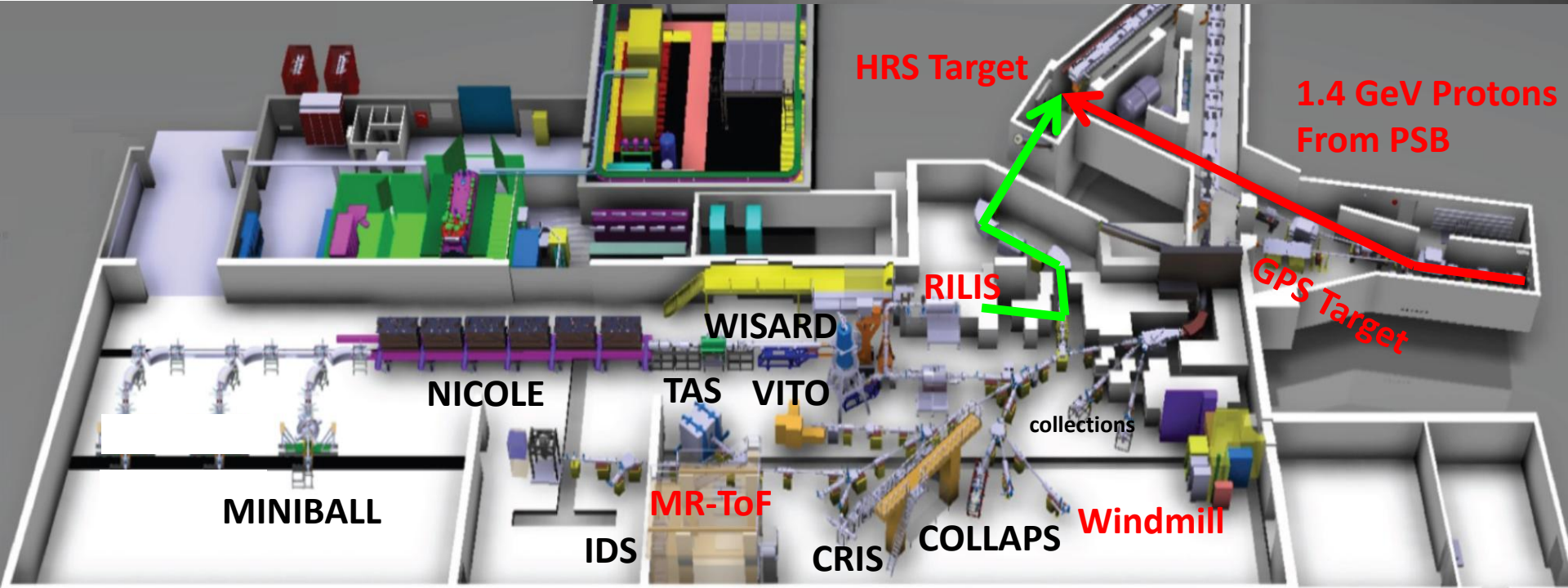
Region of our interest: fission of nuclei with A~180-200, N/Z~1.22-1.3: Hg,Pb,Po,Rn
JAEA and ISOLDE(CERN)



RIBs Production Reactions at ISOLDE (CERN) induced by p(1 GeV) with a thick Uranium Target



The ISOLDE facility at CERN



ISOLDE Facility (CERN, Geneva)

(example of a surface-ionization ion source)



ISOLDE Target Unit

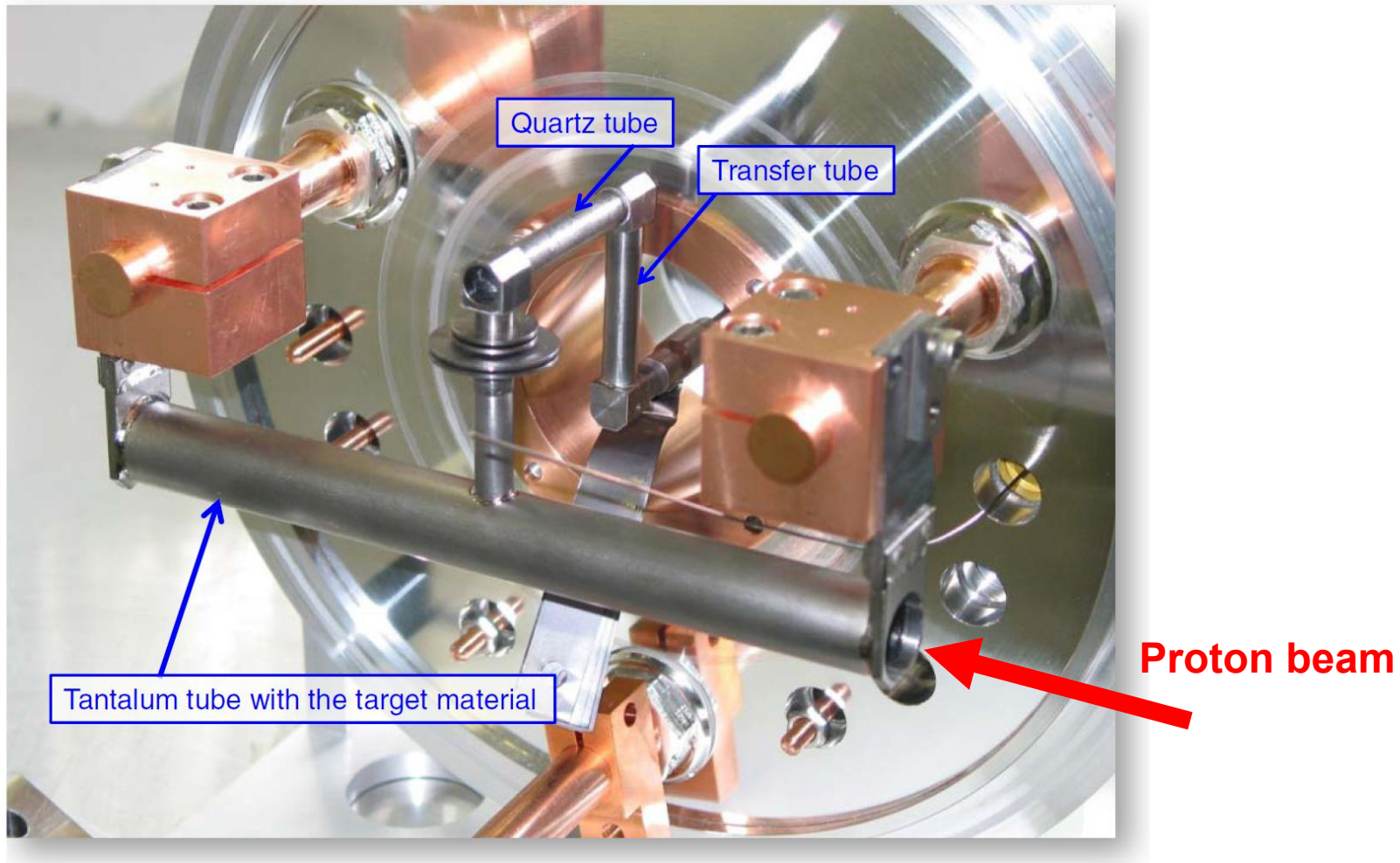
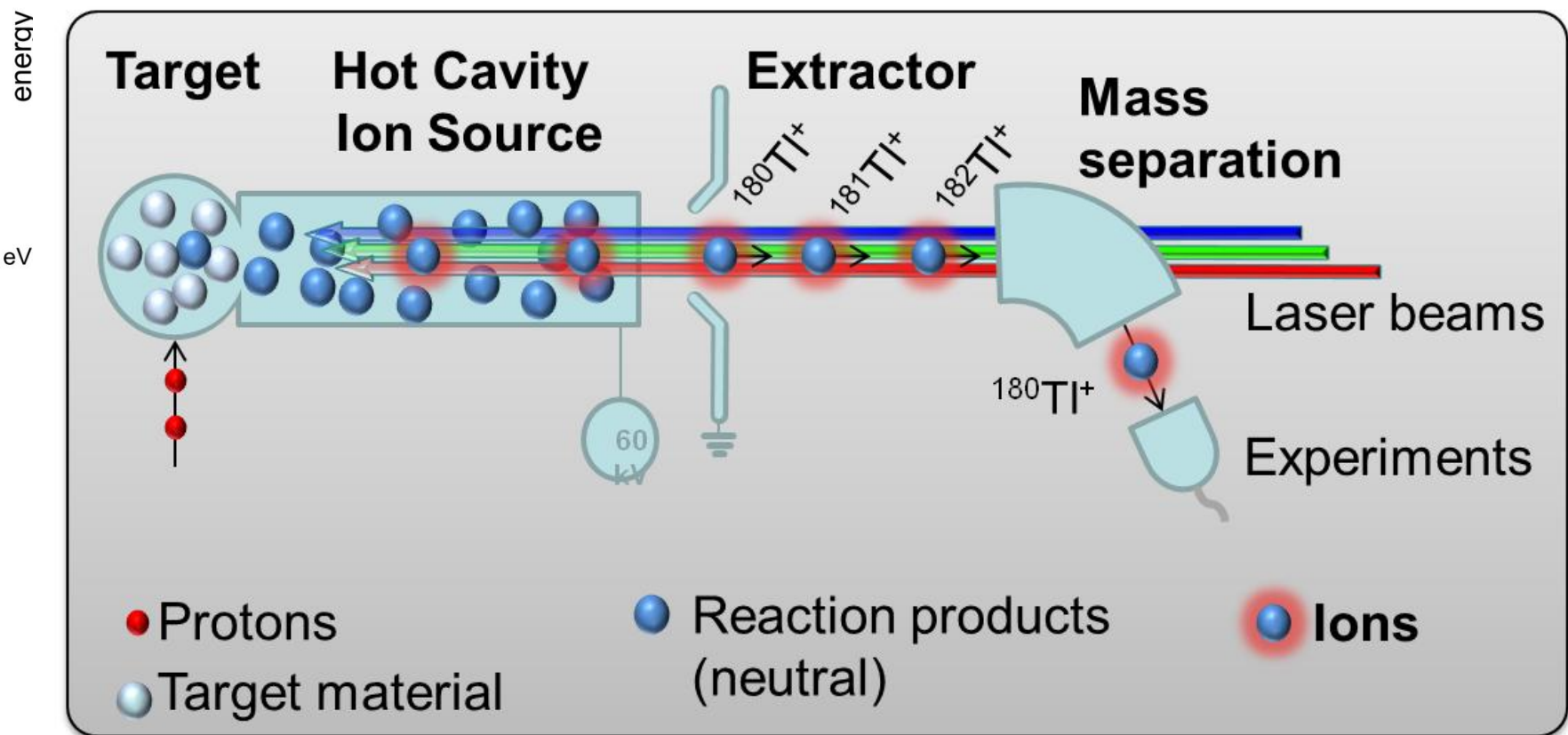
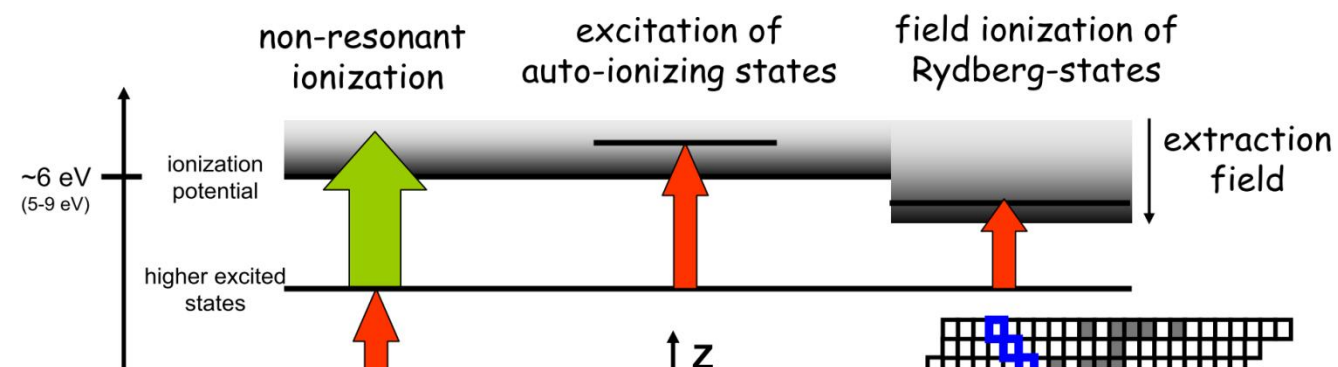
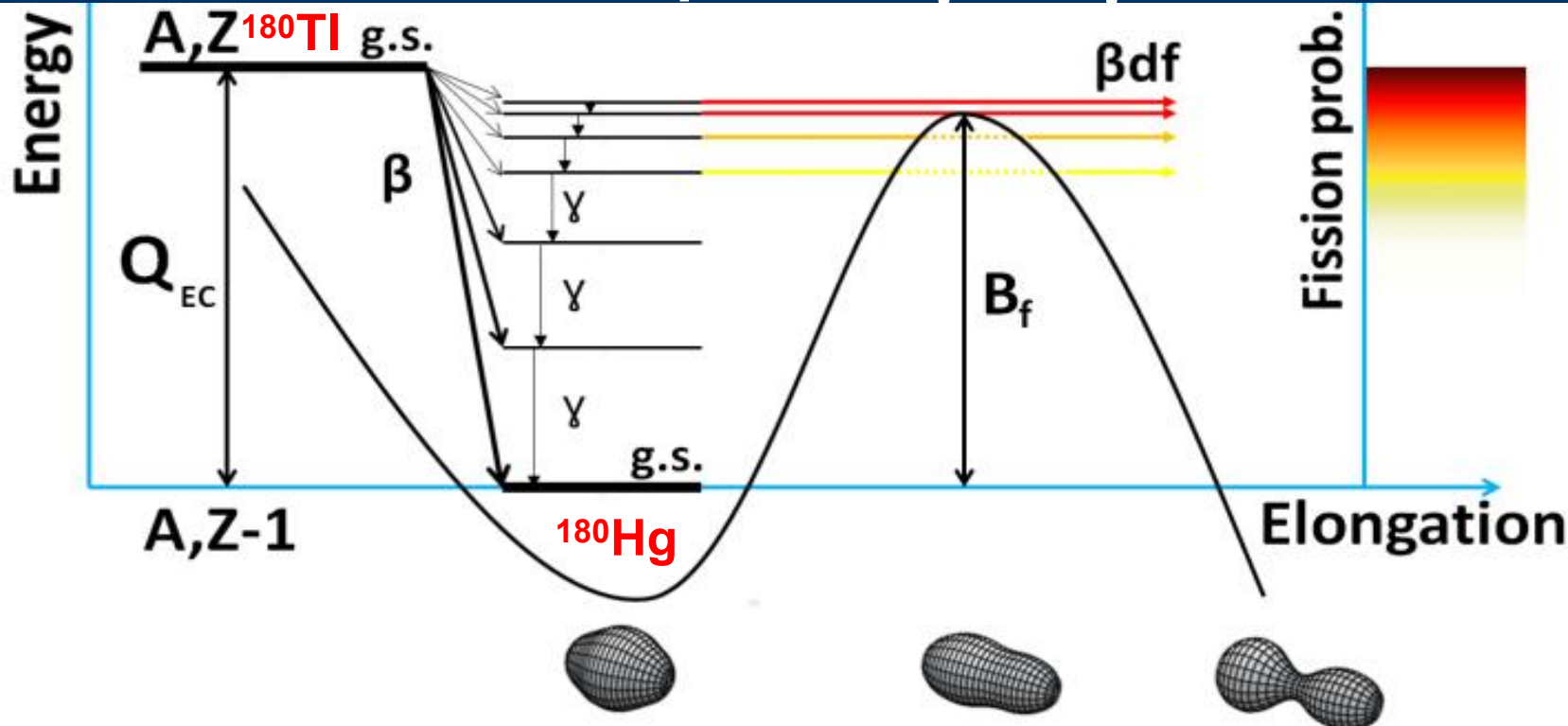


Figure 16. A photo of the ISOLDE target unit. The tantalum target container is ohmically heated. The radioactive atoms are transported to the ion source via the transfer tube. Part of the tube contains a quartz container that absorbs the rubidium atoms. This configuration was used to produce zinc beams using laser resonant ionization. Adapted from [48].

Resonance Laser Ionization of an Atom



Beta-Delayed Fission of low-energy RIBs (a sub-class of β -delayed particle decays)

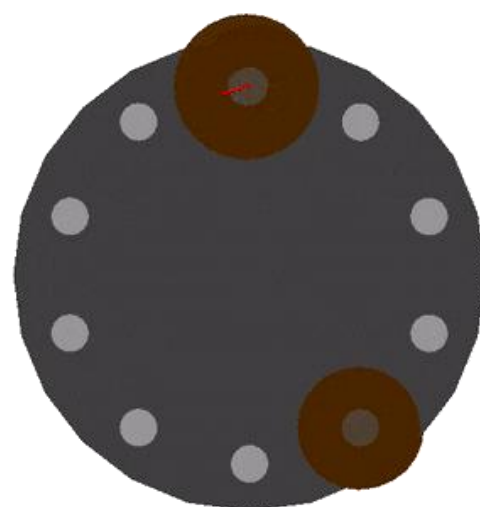
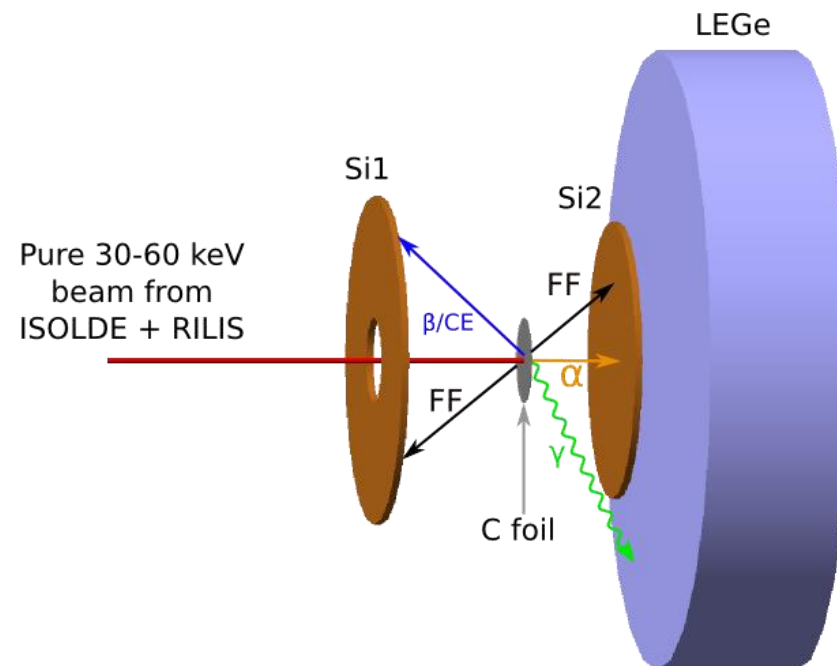
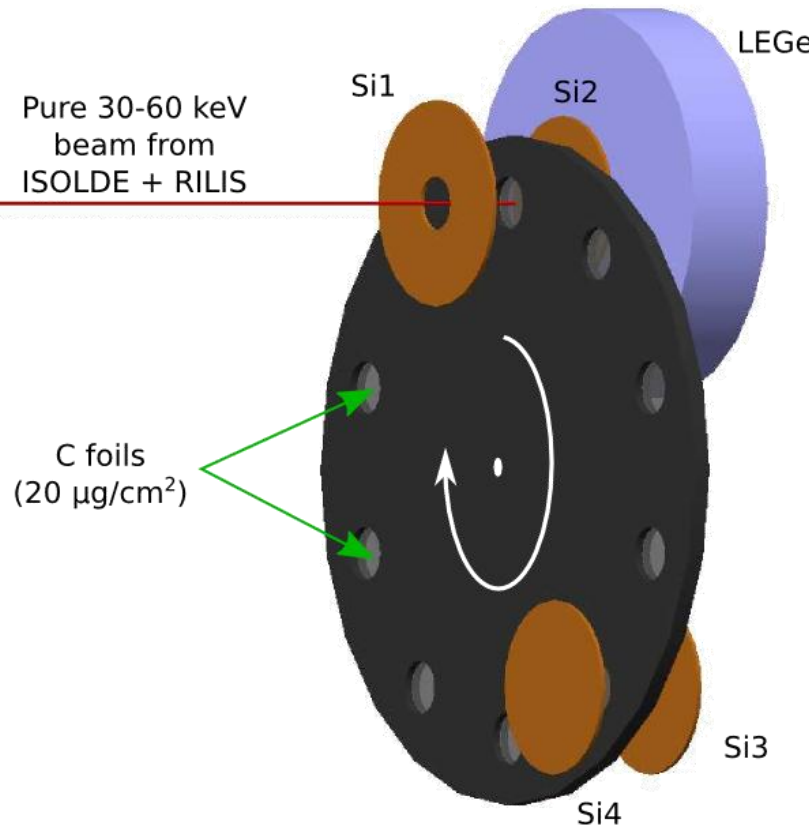


- Two step process: β decay followed by fission
- Low-energy fission ($E^* \sim 3-12$ MeV, limited by Q_{EC})
e.g. ^{180}TI : $Q_{EC}=10.4$ MeV, $B_{f,calc}=9.8$ MeV
- Low angular momentum of the state e.g. ^{180}TI : $I=4$ or 5

A.N. Andreyev, M. Huyse, P. Van Duppen, Reviews of Modern Physics, 85, 1541 (2013): ~30 cases known
J.Konki, J. Khuyagbaatar et al, $^{240}\text{Es}, ^{236}\text{Bk}$, PLB764 (2017); J. Khuyagbaatar, EPJA55(2019)
G.Wilson, AA et al, ^{230}Am , PRC96(2017)

Detection system for β DF studies at ISOLDE

A. Andreyev et al., PRL 105, 252502 (2010)

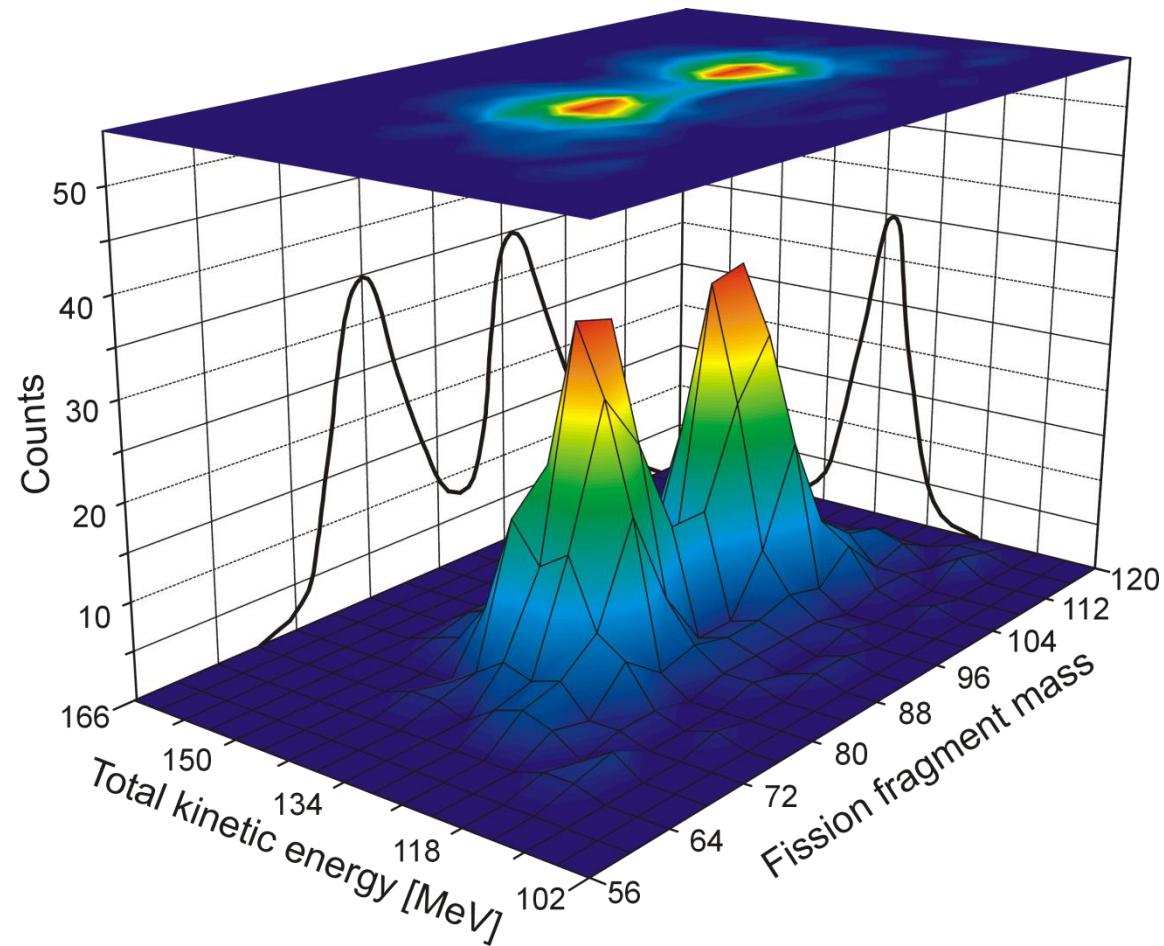
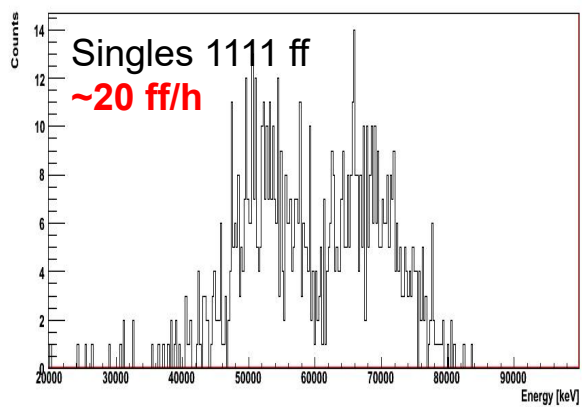
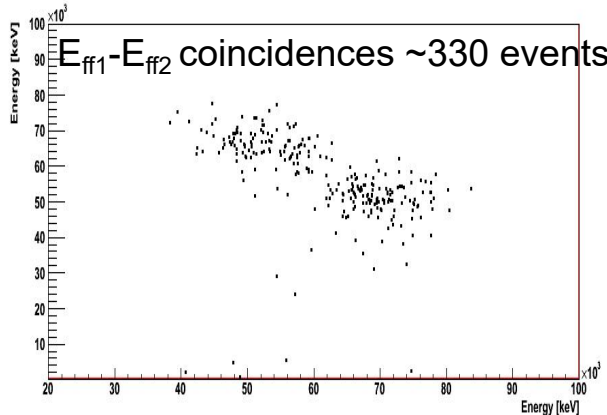


Setup: Si detectors both sides of the C-foil

- Simple setup & DAQ: 2 Surface barrier detectors (1 of them – annular) and 2 PIPS detectors.
- 34% geometrical efficiency at implantation site.
- Alpha-gamma coincidences
- Digital electronics

Mass distribution of fission fragments from β DF of ^{180}Tl (recall - it's daughter $^{180}\text{Hg}=2\times^{90}\text{Zr}$, who is actually fissionning!)

ASYMMETRIC energy split! Thus asymmetric mass split: $M_H=100(4)$ and $M_L=80(4)$



A problem: “low-energy” FF’s - 1 AMeV only, A and Z identification difficult
The most probable fission fragments are ^{100}Ru ($N=56, Z=44$) and ^{80}Kr ($N=44, Z=36$)

New Type of Asymmetric Fission in Proton-Rich Nuclei

PRL 105, 252502 (2010)

PHYSICAL REVIEW LETTERS

week ending
17 DECEMBER 2010

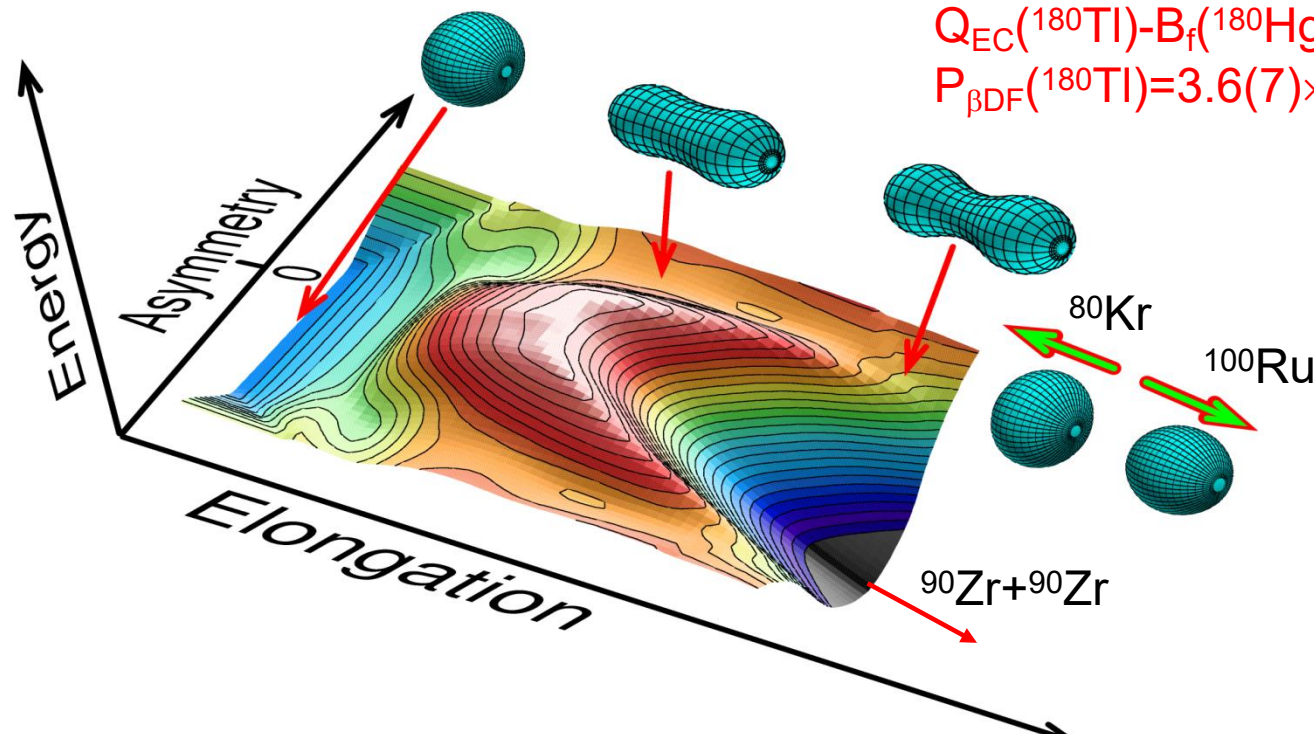


New Type of Asymmetric Fission in Proton-Rich Nuclei via β DF of ^{180}TI

A. N. Andreyev,^{1,2} J. Elseviers,¹ M. Huyse,¹ P. Van Duppen,¹ S. Antalic,³ A. Barzakh,⁴ N. Bree,¹ T. E. Cocolios,¹ V. F. Comas,⁵ J. Diriken,¹ D. Fedorov,⁴ V. Fedosseev,⁶ S. Franschoo,⁷ J. A. Heredia,⁵ O. Ivanov,¹ U. Köster,⁸ B. A. Marsh,⁶ K. Nishio,⁹ R. D. Page,¹⁰ N. Patronis,^{1,11} M. Seliverstov,^{1,4} I. Tsekhanovich,^{12,17} P. Van den Bergh,¹ J. Van De Walle,⁶ M. Venhart,^{1,3} S. Vermote,¹³ M. Veselsky,¹⁴ C. Wagemans,¹³ T. Ichikawa,¹⁵ A. Iwamoto,⁹ P. Möller,¹⁶ and A. J. Sierk¹⁶

¹Instituut voor Kern- en Stralingsfysica, K.U. Leuven, University of Leuven, B-3001 Leuven, Belgium

²School of Engineering, University of the West of Scotland,
Paisley, PA1 2BE, United Kingdom, and the Scottish Universities Physics Alliance (SUPA)



Calculations according to 5D fission model, P. Möller et al., Nature 409, 785 (2001)

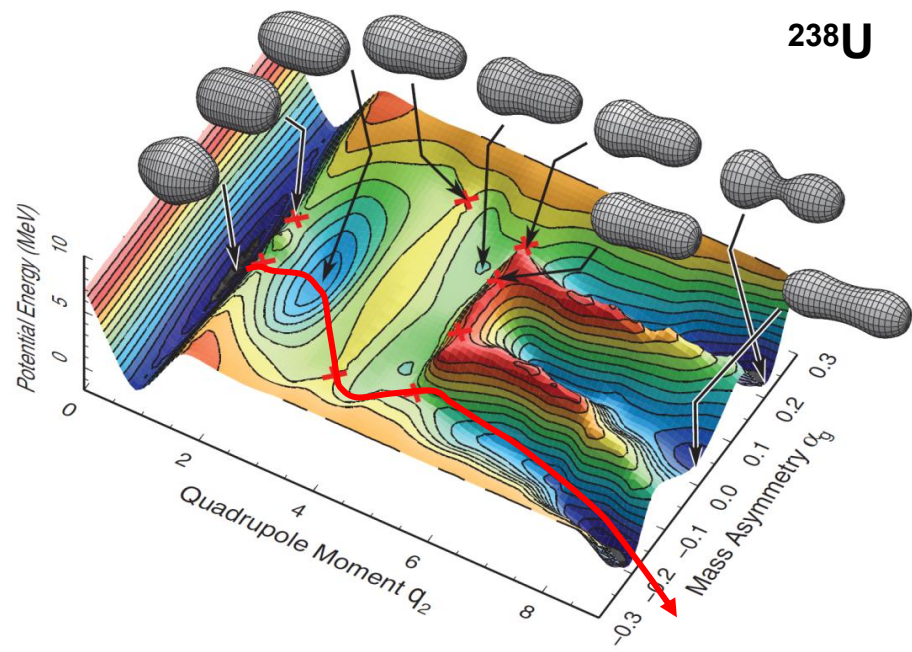
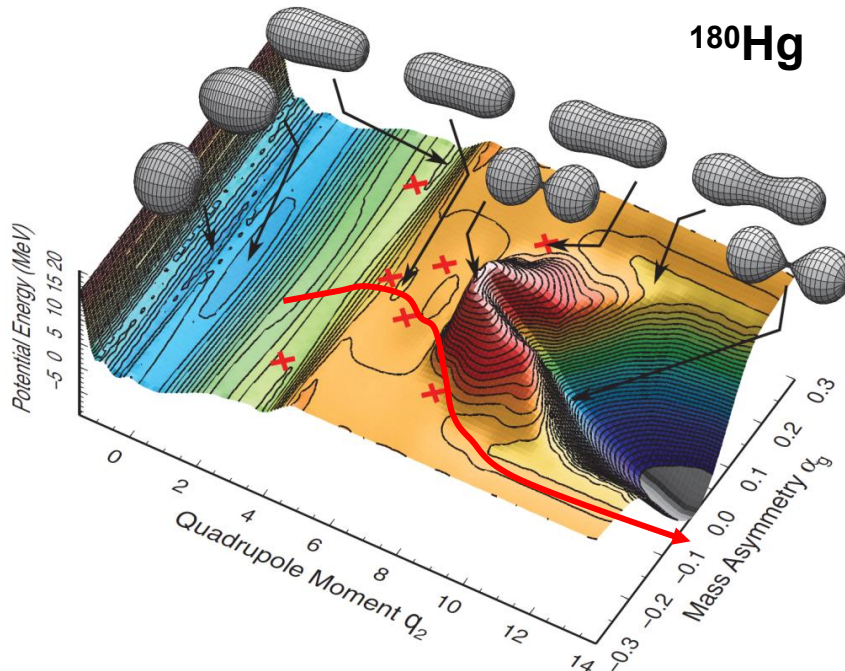
Two types of asymmetry: what's the difference?

PHYSICAL REVIEW C 86, 024610 (2012)

Contrasting fission potential-energy structure of actinides and mercury isotopes

Takatoshi Ichikawa,¹ Akira Iwamoto,² Peter Möller,³ and Arnold J. Sierk³

Conclusions: The mechanism of asymmetric fission must be very different in the lighter proton-rich mercury isotopes compared to the actinide region and is apparently unrelated to fragment shell structure. Isotopes lighter than ^{192}Hg have the saddle point shielded from a deep symmetric valley by a significant ridge. The ridge vanishes for the heavier Hg isotopes, for which we would expect a qualitatively different asymmetry of the fragments.



Asymmetry in the U-region is due to strong shell effects of fission fragments around ^{132}Sn
Asymmetry in the neutron-deficient Pb-region – due to shell effects of CN (but, octupoles?)

Brownian Metropolis Shape Motion

based on J. Randrup and P. Möller, PRL 106, 132503 (2011)

Phys. Rev. C 85, 024306 (2012)

Calculated fission yields of neutron-deficient mercury isotopes

Peter Möller^{1,*}, Jørgen Randrup², and Arnold J. Sierk¹

¹ Theoretical Division, Los Alamos National Laboratory, Los Alamos, New Mexico 87545, USA

² Nuclear Science Division, Lawrence Berkeley National Laboratory, Berkeley, California 94720, USA

(Dated: November 21, 2011)

The recent unexpected discovery of asymmetric fission of ^{180}Hg following the electron-capture decay of ^{180}Tl has led to intense interest in experimentally mapping the fission-yield properties over more extended regions of the nuclear chart and compound-system energies. We present here a first calculation of fission-fragment yields for neutron-deficient Hg isotopes, using the recently developed Brownian Metropolis shape motion treatment. The results for ^{180}Hg are in approximate agreement with the experimental data. For ^{174}Hg the symmetric yield increases strongly with decreasing energy, an unusual feature, which would be interesting to verify experimentally.

PACS numbers: 25.85.-w, 24.10.Lx, 24.75.+i

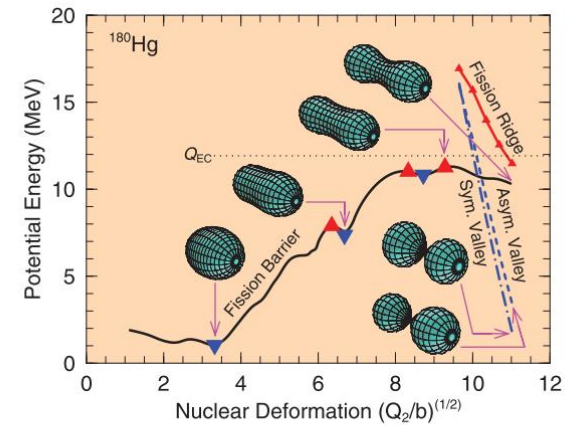
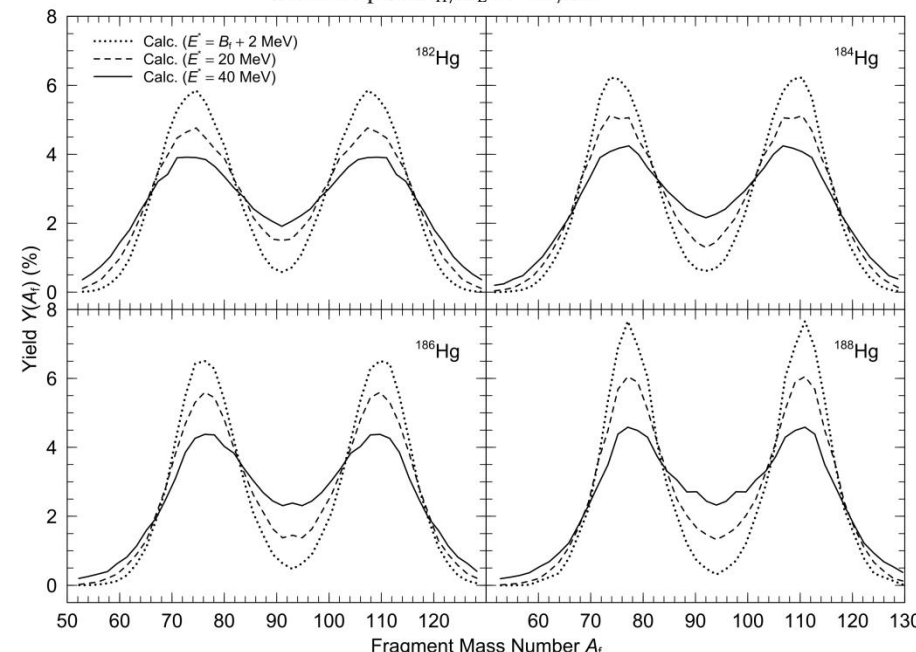
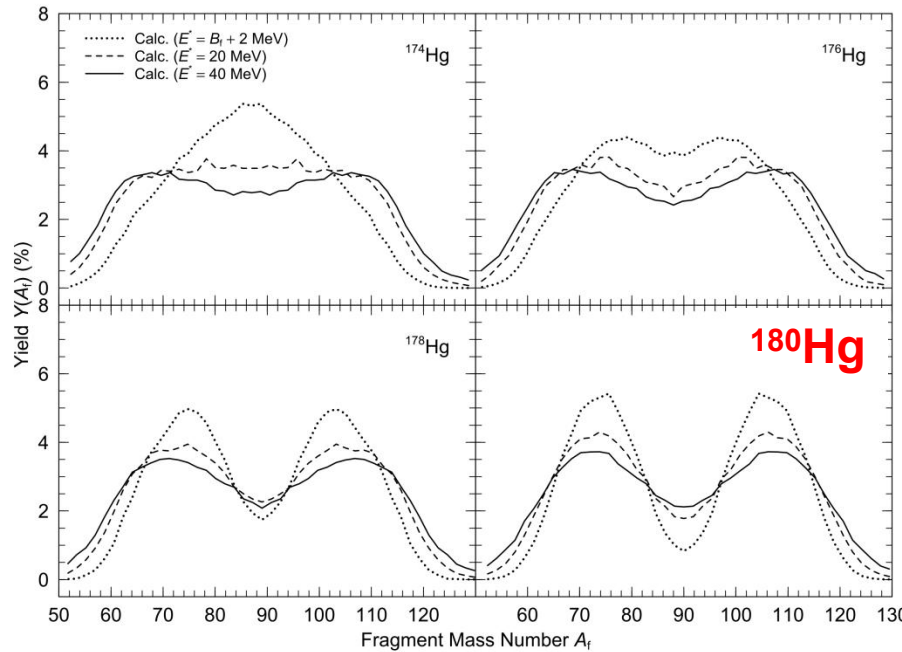


FIG. 4. (Color online) Minima, saddles, major valleys, and ridges in the 5D potential-energy surface of ^{180}Hg (see text). At the last plotted point on the fission barrier, $(Q_2/b)^{(1/2)} \approx 11$, the asymmetry of the shape is $A_H/A_L = 108/72$.

'Improved' Scission-Point Model

PHYSICAL REVIEW C 86, 044315 (2012)

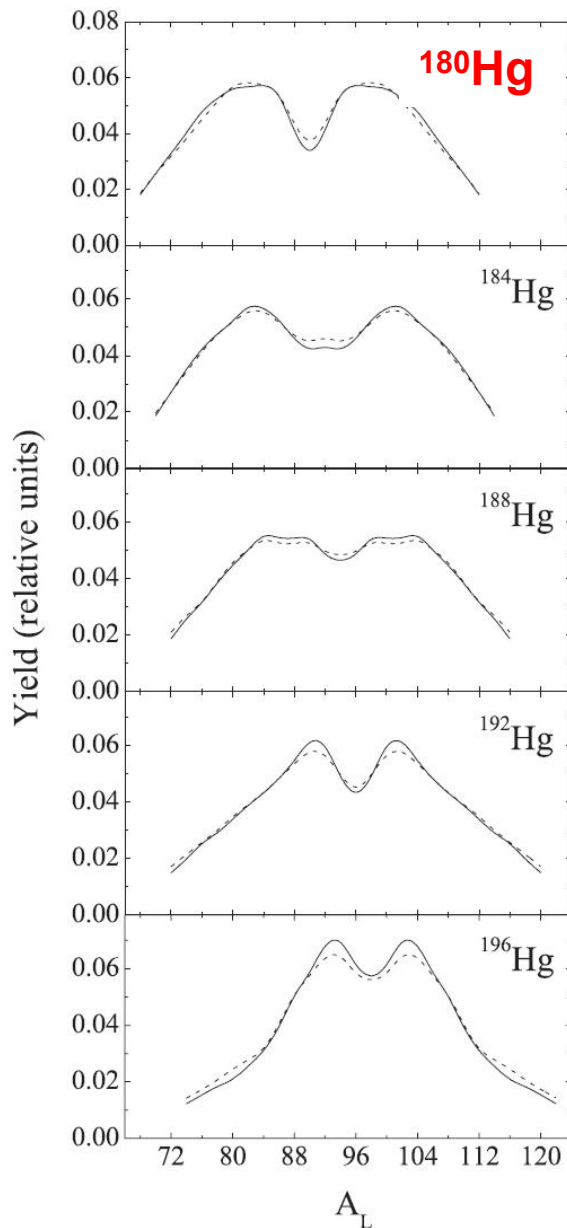
Mass distributions for induced fission of different Hg isotopes

A. V. Andreev, G. G. Adamian, and N. V. Antonenko

Joint Institute for Nuclear Research, 141980 Dubna, Russia

(Received 20 June 2012; revised manuscript received 6 September 2012; published 11 October 2012)

With the improved scission-point model mass distributions are calculated for induced fission of different Hg isotopes with even mass numbers $A = 180, 184, 188, 192, 196$, and 198 . The calculated mass distribution and mean total kinetic energy of fission fragments are in good agreement with the existing experimental data. The asymmetric mass distribution of fission fragments of ^{180}Hg observed in the recent experiment is explained. The change in the shape of the mass distribution from asymmetric to more symmetric is revealed with increasing A of the fissioning ^AHg nucleus, and reactions are proposed to verify this prediction experimentally.



- Inter-fragment distance is not fixed and calculated.
- values of ~ 0.5 - 1 fm result (Wilkins – fixed at 1.4 fm)
- Mass symmetry/asymmetry doesn't change as a function of E^* (up to $E^* \sim 60$ MeV) – good for future experiments

SPY self-consistent Scission-Point Model

PHYSICAL REVIEW C **86**, 064601 (2012)

Role of deformed shell effects on the mass asymmetry in nuclear fission of mercury isotopes

Stefano Panebianco, Jean-Luc Sida, Hélène Goutte, and Jean-François Lemaître
 IRFU/Service de Physique Nucléaire, CEA Centre de Saclay, F-91191 Gif-sur-Yvette, France

Noël Dubray and Stéphane Hilaire
 CEA, DAM, DIF, F-91297, Arpajon, France
 (Received 9 October 2012; published 3 December 2012)

$$\begin{aligned} E_{\text{av}}(Z_{1,2}, N_{1,2}, \beta_{1,2}, d) \\ = E_{\text{tot}} - E_{\text{HFB}}(Z_1, N_1, \beta_1) - E_{\text{HFB}}(Z_2, N_2, \beta_2) \\ - E_{\text{nucl}}(Z_{1,2}, N_{1,2}, \beta_{1,2}, d) - E_{\text{Coul}}(Z_{1,2}, N_{1,2}, \beta_{1,2}, d). \end{aligned}$$

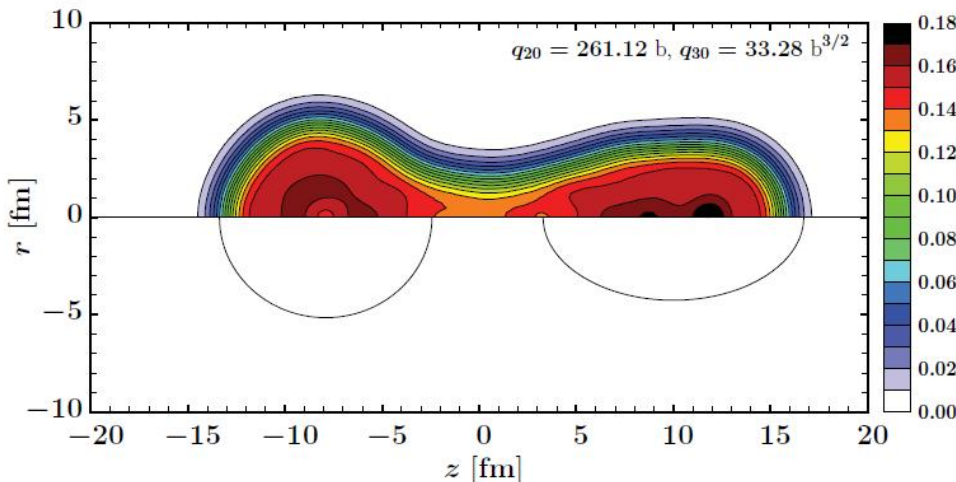


FIG. 4. (Color online) Total nuclear density for the most energetically favorable scission configuration in ^{180}Hg fission, extracted from a self-consistent HFB calculation. In the lower part of the figure, two

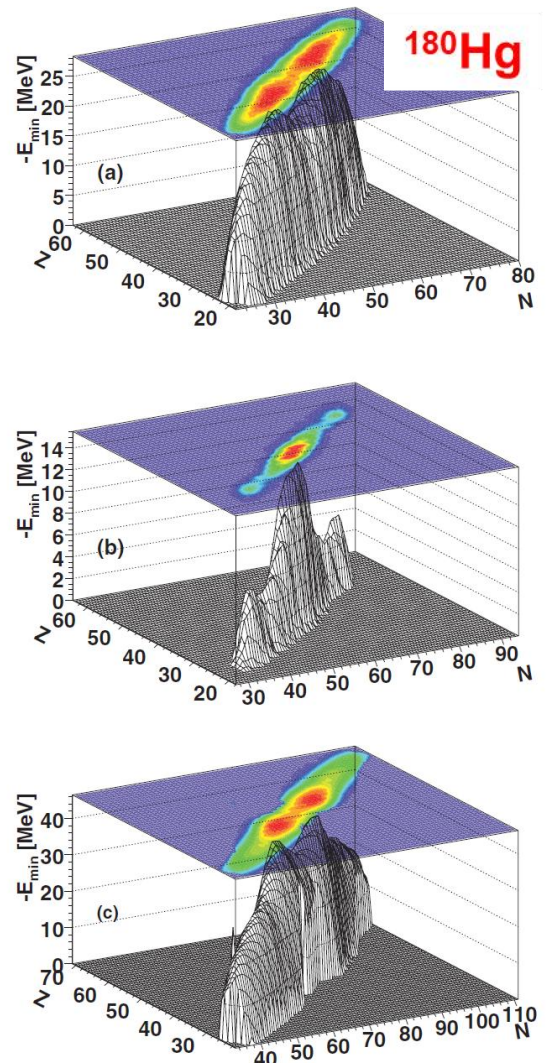


FIG. 2. (Color online) Minimum absolute available energy at scission calculated for all possible fragmentations in (a) ^{180}Hg and (b) ^{198}Hg fission at 10 MeV and in (c) the thermal n -induced fission of ^{235}U .

Mean-field HFB+Gogny D1S/SkM*

PHYSICAL REVIEW C 86, 024601 (2012)

Fission modes of mercury isotopes

M. Warda,¹ A. Staszczak,^{1,2,3} and W. Nazarewicz^{2,3,4}

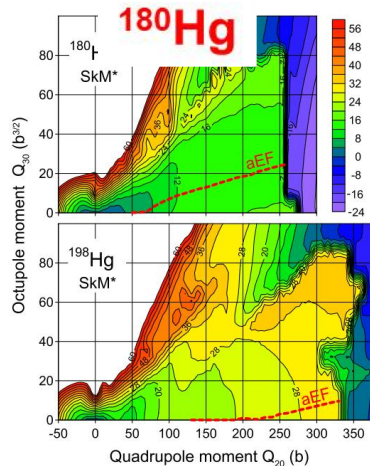


FIG. 2. (Color online) PES for ^{180}Hg (top) and ^{198}Hg (bottom) in the plane of collective coordinates $Q_{20} - Q_{30}$ in HFB-SkM*. The aEF fission pathway corresponding to asymmetric elongated fragments is marked. The difference between contour lines is 4 MeV. The effects due to triaxiality, known to impact inner fission barriers in the actinides, are negligible here.

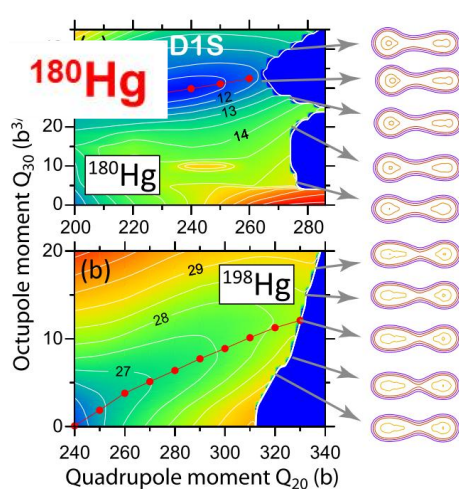
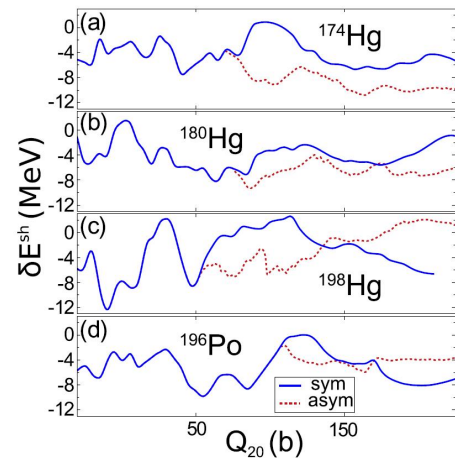
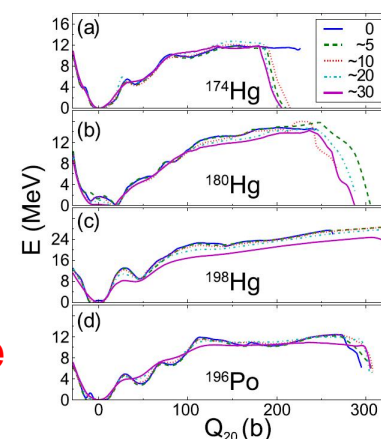
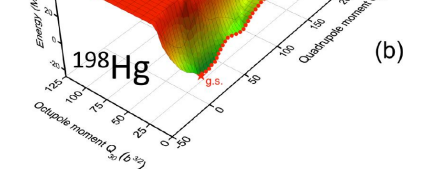
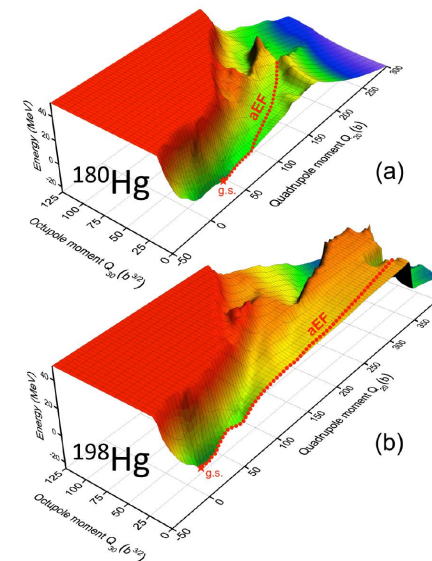


FIG. 3. (Color online) PES in HFB-D1S for ^{180}Hg (top) and ^{198}Hg (bottom) in the (Q_{20}, Q_{30}) plane in the pre-scission region of aEF valley. The symmetric limit corresponds to $Q_{30} = 0$. The aEF valley and density profiles for pre-scission configurations are indicated. The difference between contour lines is 0.5 MeV. Note different Q_{30} -scales in ^{180}Hg and ^{198}Hg plots.

PHYSICAL REVIEW C 90, 021302(R) (2014)

Excitation-energy dependence of fission in the mercury region

J. D. McDonnell,^{1,2} W. Nazarewicz,^{2,3,4} J. A. Sheikh,^{2,3,5} A. Staszczak,^{2,6} and M. Warda⁶



Important: Fission allows to study shell effects at extreme deformations, even close to scission!

Octupole shapes of fission fragments as a culprit for mass-asymmetry?

PHYSICAL REVIEW C **100**, 041602(R) (2019)

Rapid Communications

Effect of shell structure on the fission of sub-lead nuclei

Guillaume Scamps^{⊗*}

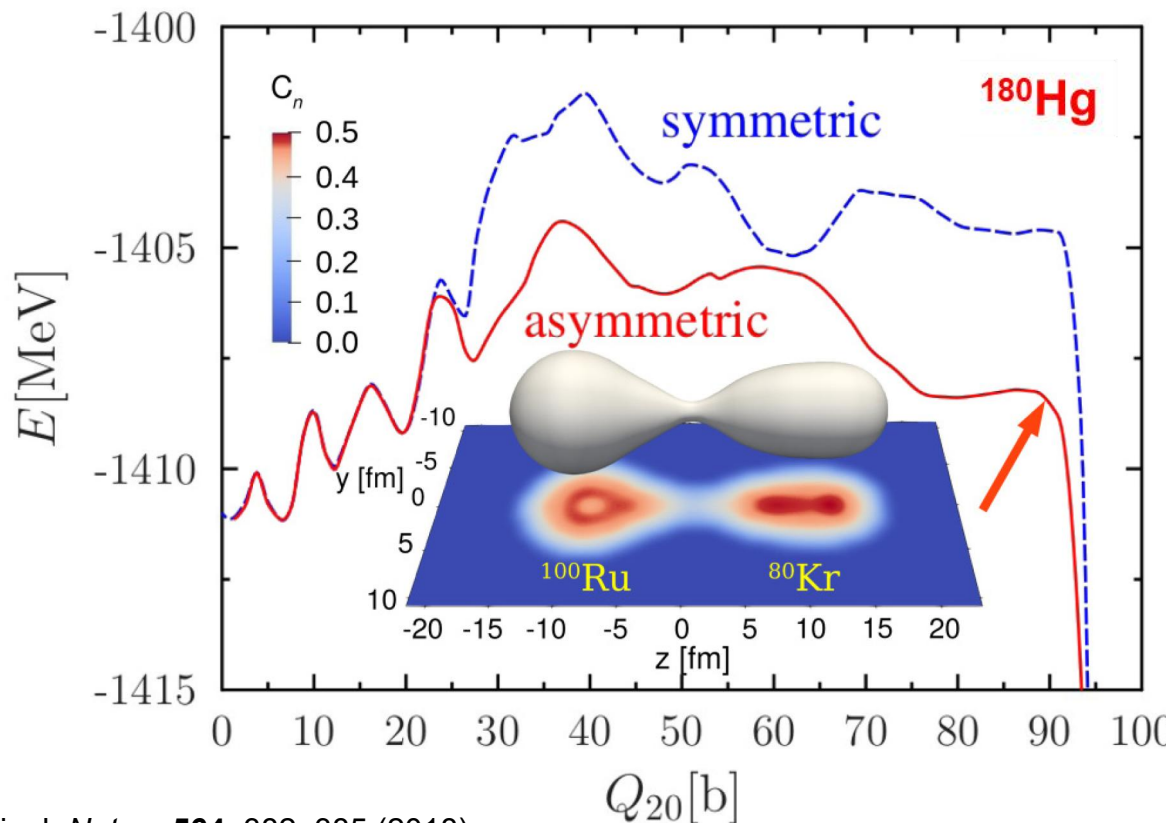
Center for Computational Sciences, University of Tsukuba, Tsukuba 305-8571, Japan

and Institut d'Astronomie et d'Astrophysique, Université Libre de Bruxelles, Campus de la Plaine CP 226, BE-1050 Brussels, Belgium

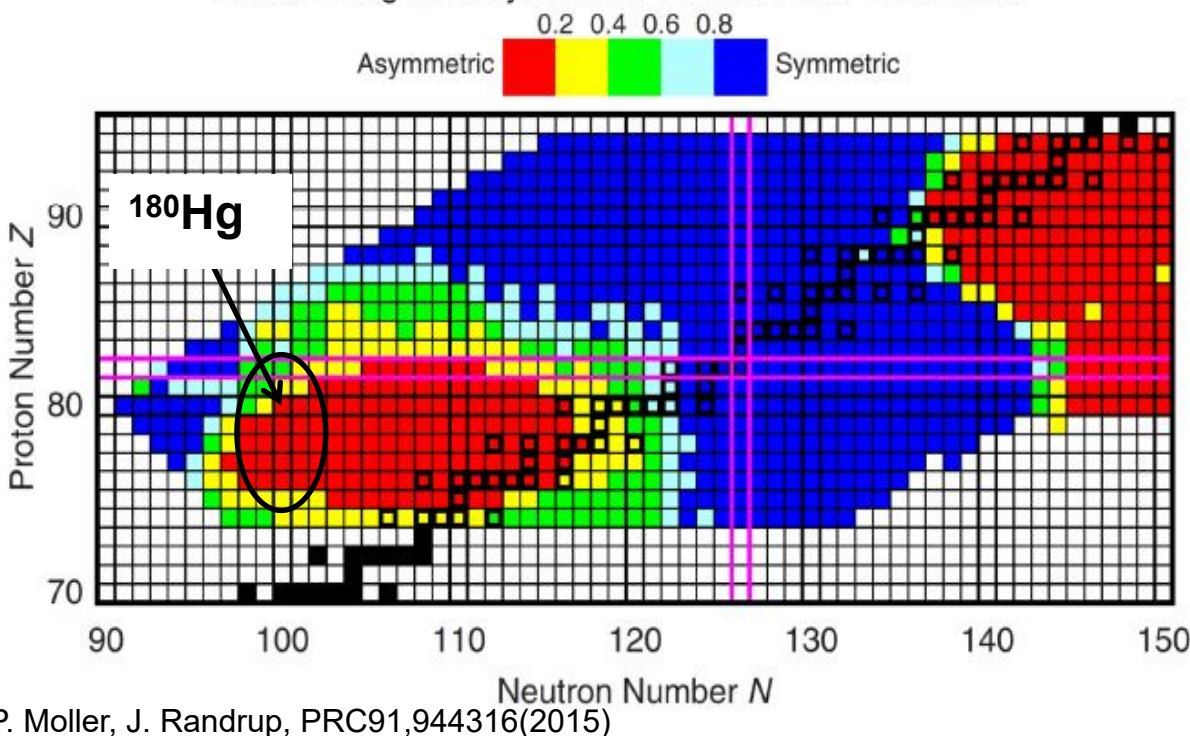
Cédric Semenel[†]

Department of Theoretical Physics and Department of Nuclear Physics, Research School of Physics and Engineering,

Australian National University, Canberra, Australian Capital Territory 2601, Australia



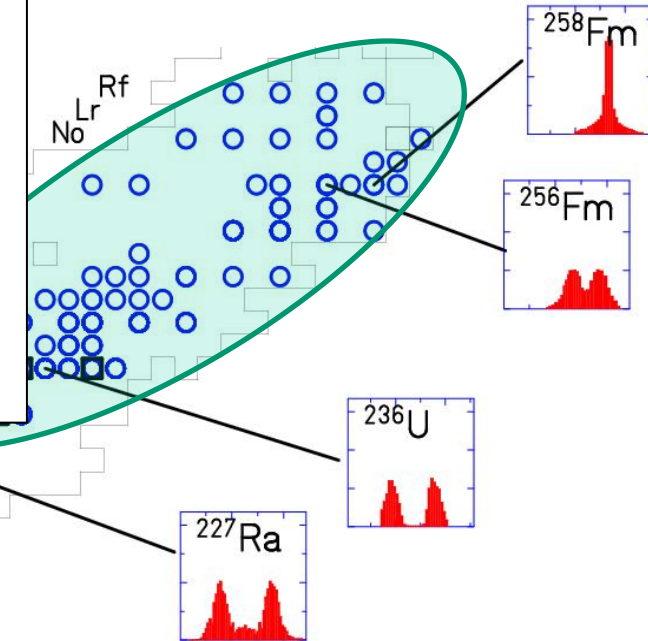
Fission-Fragment Symmetric-Yield to Peak-Yield Ratio



P. Moller, J. Randrup, PRC91,944316(2015)

Symmetry

**predominantly asymmetric;
isomers**



ISOLDE

A.N. Andreyev, K. Nishio, K.-H. Schmidt, Reports on Progress in Fission, 1,

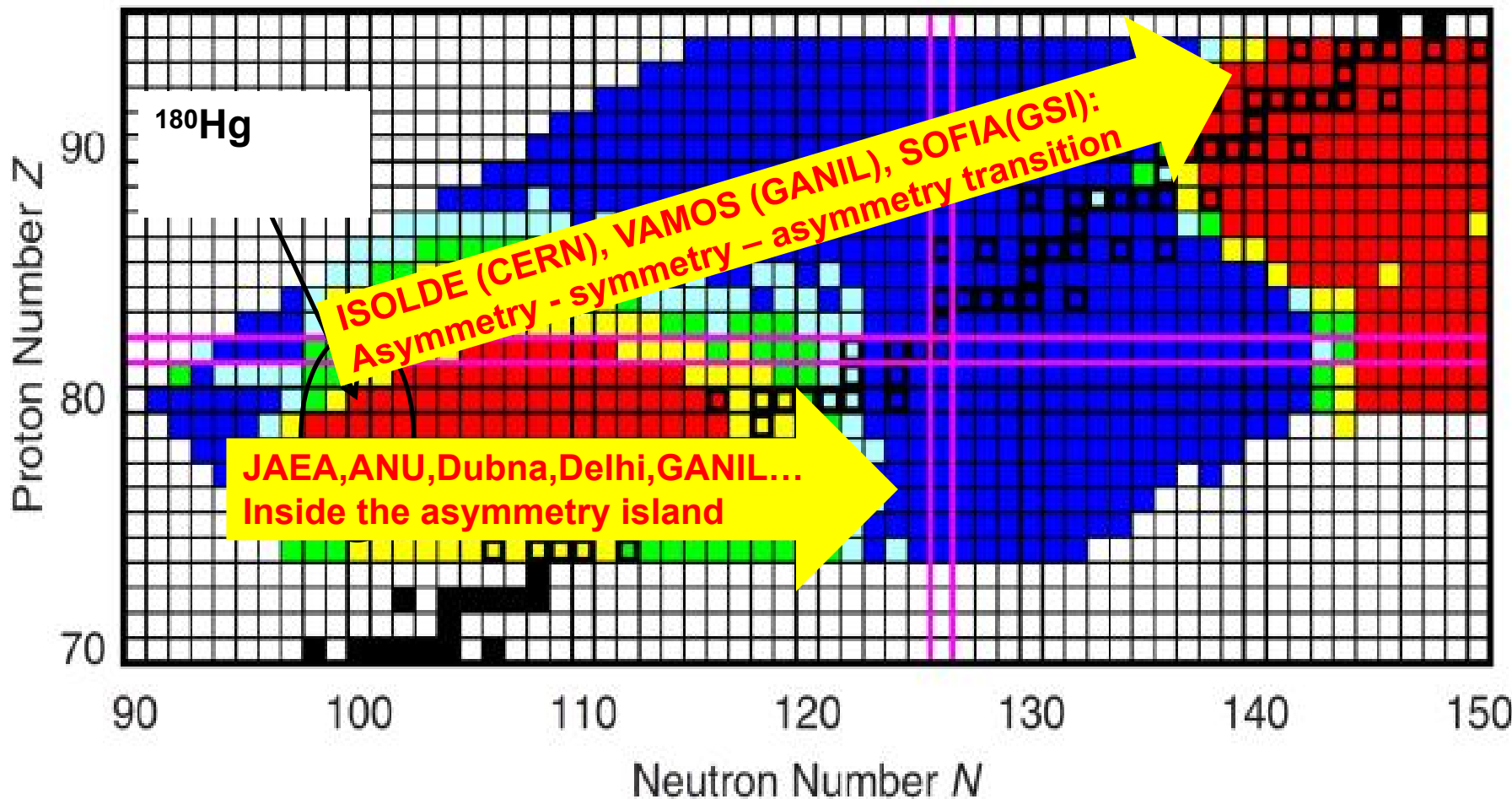
- particle induced
- e.m. -induced $E^* \sim 11$ MeV

**Pre-actinides, light Ir-Th $N/Z \sim 1.4-1.5$:
predominantly symmetric, e.g. FRS(GSI)**

From Asymmetry to Symmetry

(what effect is responsible for asymmetry in the lead region?)

Fission-Fragment Symmetric-Yield to Peak-Yield Ratio



Dominance of proton shell effects in low-energy fission

Physics Letters B 825 (2022) 136859

Contents lists available at ScienceDirect

Physics Letters B

www.elsevier.com/locate/physletb



Evidence for the general dominance of proton shells in low-energy fission

K. Mahata ^{a,b,*}, C. Schmitt ^{c,*}, Shilpi Gupta ^{a,b}, A. Srivastava ^{a,b}, G. Scamps ^d,
K.-H. Schmidt ^e

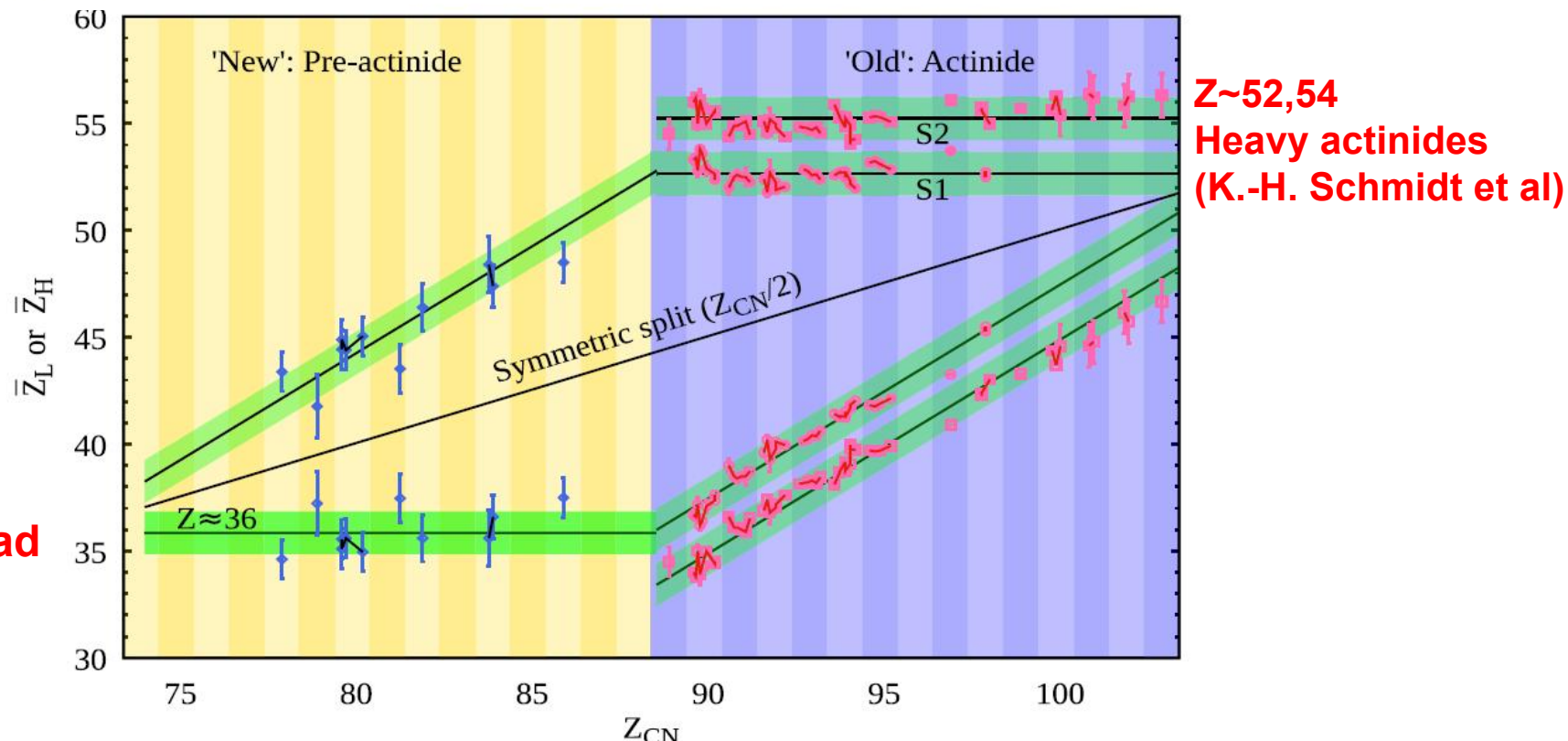


Fig. 4. Evolution of the average $\bar{Z}_{L(H)}$ positions for the asymmetric fission channel as a function of Z_{CN} from above rare-earth to very-heavy and super-heavy elements. For clarity, isotopes of a same element are connected by a black segment and shifted according to the difference between their masses. The points are from

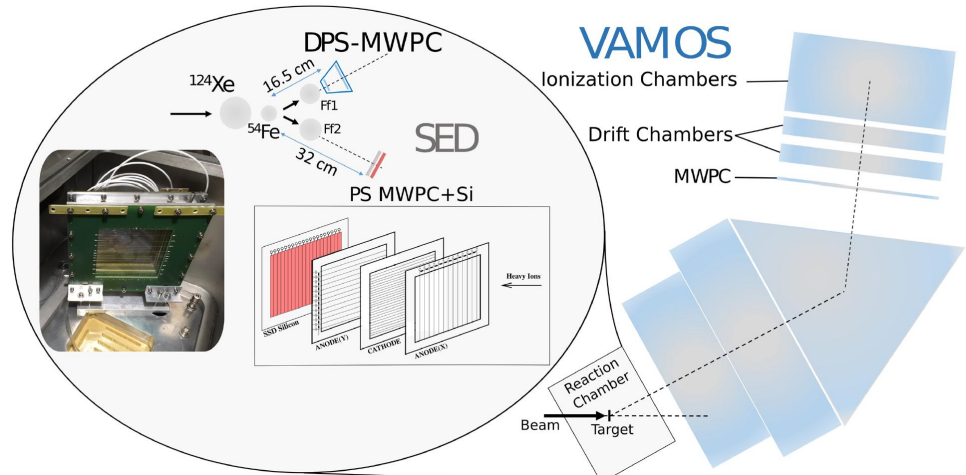
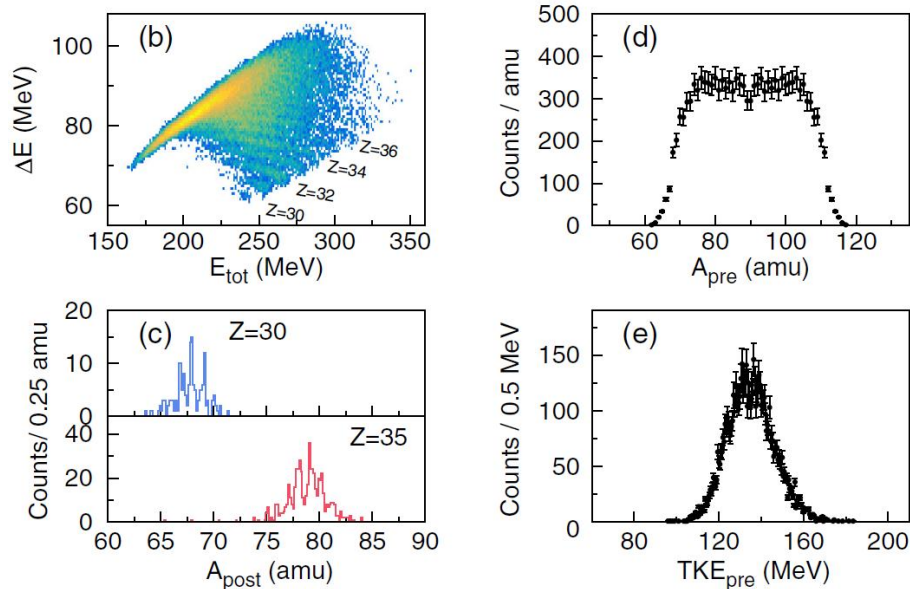
$^{178}\text{Hg}^*$ fission in inverse kinematics at VAMOS

$^{124}\text{Xe}(4.3 \text{ AMeV}) + ^{54}\text{Fe} \rightarrow ^{178}\text{Hg}^*, E^* = 34 \text{ MeV}$

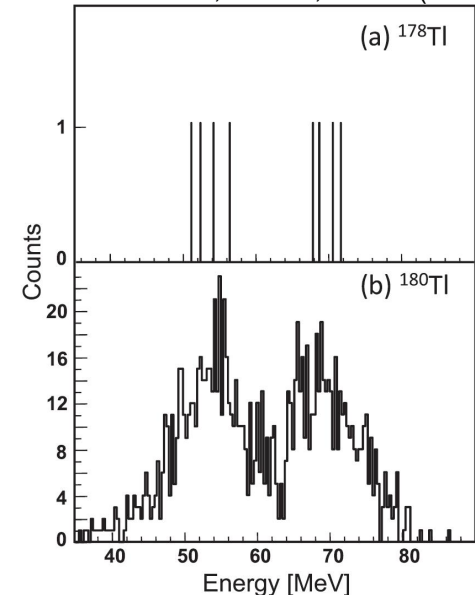
PHYSICAL REVIEW LETTERS 126, 132502 (2021)

Experimental Evidence for Common Driving Effects in Low-Energy Fission from Sublead to Actinides

C. Schmitt^{1,*}, A. Lemasson², K.-H. Schmidt³, A. Jhingan,⁴ S. Biswas,² Y. H. Kim⁵, D. Ramos⁶, A. N. Andreyev^{6,7,8}, D. Curien¹, M. Ciemala⁹, E. Clément,² O. Dorvaux,¹ B. De Canditiis,¹ F. Didierjean,¹ G. Duchêne,¹ J. Dudouet^{10,11}, J. Frankland², B. Jacquot², C. Raison,⁶ D. Ralet,² B.-M. Retalieu,² L. Stuttgé,¹ and I. Tsekhanovich¹²



bdf of ^{178}Ti , ISOLDE, $E^* \sim 10 \text{ MeV}$
V. Liberati et al, PRC88,044322 (2013)



- Coulomb barrier energies, inverse kinematics: high FF's energies, allows Z-identification.
- Confirmed asymmetric mass split of ^{178}Hg , even at a higher E^*
- First direct confirmation of importance of Z=36!

Universality of shell effects in low-energy fission

Phys. Lett. B 865 (2025) 139459



Contents lists available at ScienceDirect

Physics Letters B

journal homepage: www.elsevier.com/locate/physletb

Letter

Universality of shell effects in fusion-fission mass distributions

J. Buete^{a,b,*}, B.M.A. Swinton-Bland^{a,3}, D.J. Hinde^a, K.J. Cook^{a,b}, M. Dasgupta^a, A.C. Berriman^a, D.Y. Jeung^a, K. Banerjee^{a,1}, L.T. Bezzina^a, I.P. Carter^a, C. Sengupta^{a,2}, C. Simenel^{a,c}, E.C. Simpson^a

^a Department of Nuclear Physics and Accelerator Applications, Research School of Physics, Australian National University, Canberra, ACT 2601, Australia

^b Facility for Rare Isotope Beams, Michigan State University, MI 48824, USA

^c Department of Fundamental and Theoretical Physics, Research School of Physics, Australian National University, Canberra, ACT 2601, Australia

J. Buete, B.M.A. Swinton-Bland, D.J. Hinde et al.

Physics Letters B 865 (2025) 139459

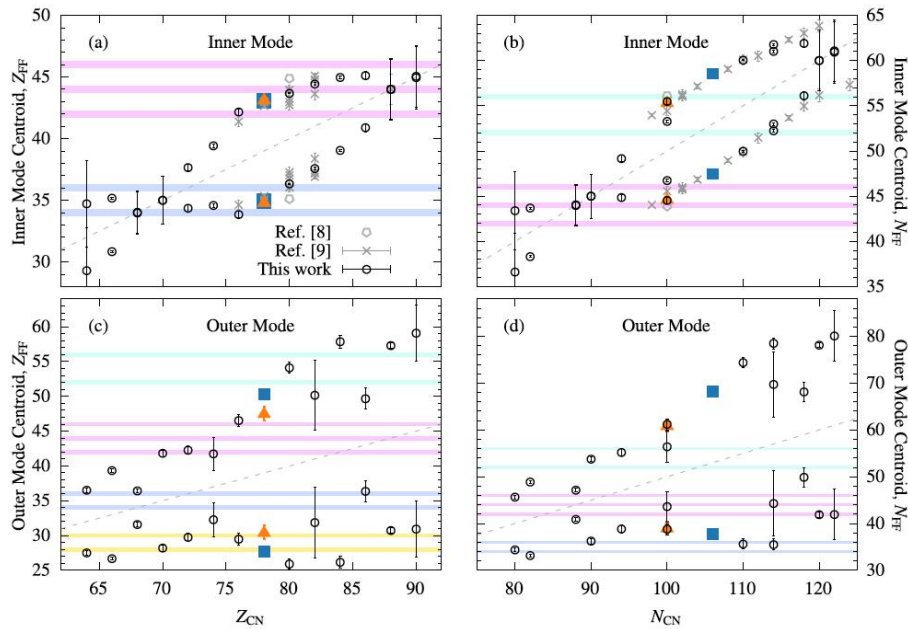


Fig. 4. The proton Z (left) and neutron N (right) numbers for the shell-driven fission modes determined via a two-dimensional fit to the mass-RTKE distribution

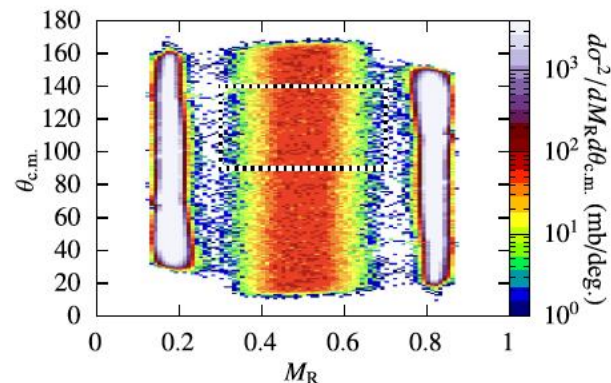


Fig. 1. The mass-angle distribution for ^{176}Os . The vertical high intensity bands

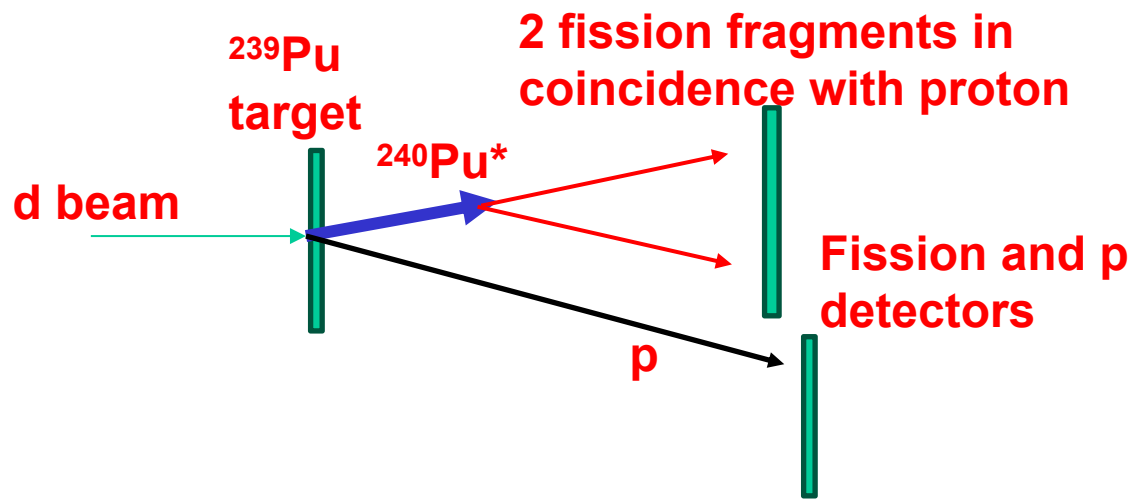
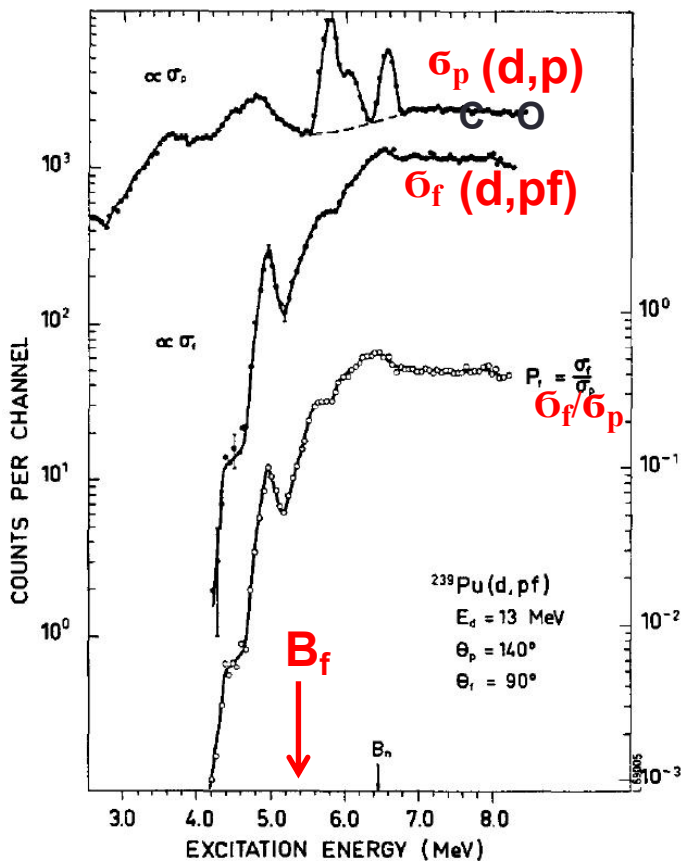
Reaction	CN	Z_{CN}	$E_{\text{c.m.}}$ (MeV)	E_{gs}^* (MeV)	E_{sp}^* (MeV)
$^{32}\text{S} + ^{112}\text{Cd}$	^{144}Gd	64	114.6	69.8	38.0
$^{32}\text{S} + ^{116}\text{Sn}$	^{148}Dy	66	115.3	65.6	36.7
$^{32}\text{S} + ^{124}\text{Te}$	^{156}Er	68	117.4	65.1	37.1
$^{16}\text{O} + ^{144}\text{Sm}$	^{160}Yb	70	89.84	61.4	36.3
$^{32}\text{S} + ^{134}\text{Ba}$	^{166}Hf	72	119.4	58.3	35.3
$^{32}\text{S} + ^{142}\text{Ce}$	^{174}W	74	120.3	60.0	39.0
$^{32}\text{S} + ^{144}\text{Nd}$	^{176}Os	76	117.6	49.9	32.5
$^{34}\text{S} + ^{144}\text{Sm}$	^{178}Pt	78	117.6	37.7	23.8
$^{32}\text{S} + ^{152}\text{Sm}$	^{184}Pt	78	118.9	55.4	39.5
$^{32}\text{S} + ^{158}\text{Gd}$	^{190}Hg	80	119.4	54.1	40.4
$^{32}\text{S} + ^{164}\text{Dy}$	^{196}Pb	82	120.5	53.8	42.0
$^{32}\text{S} + ^{166}\text{Er}$	^{198}Po	84	120.6	45.1	35.7
$^{32}\text{S} + ^{172}\text{Yb}$	^{204}Rn	86	120.2	42.9	34.9
$^{32}\text{S} + ^{176}\text{Hf}$	^{208}Ra	88	125.1	42.8	36.4
$^{32}\text{S} + ^{180}\text{W}$	^{212}Th	90	128.9	41.1	36.1

Back to classics: 1970'ies - Fission in d, pf
approach with stable/long-lived targets

Modern version - inverse kinematics
with post-accelerated RIBs at Coulomb
energies impinging on a deuterated
target (e.g. ISOLDE)

1970'ies: Classical fission studies in d,pf approach: determination of fission modes and fission barriers

Fission probability as a function of E^* : **direct nucleon transfer, e.g.**
(d,pf) reactions with stable/long-lived targets.

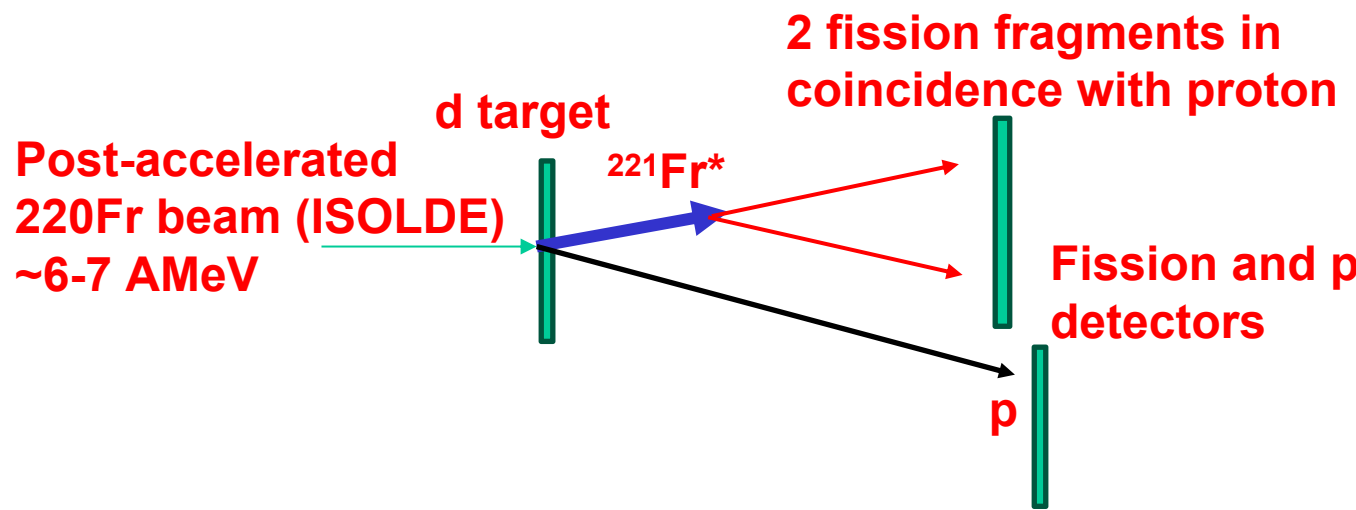


Allows to deduce e.g. the fission barrier height (with some assumptions)

$$P_{\text{fis}}(E^*) = \frac{P_0}{1 + \exp\left(\frac{2\pi(B_f - E^*)}{\hbar\omega}\right)}$$

Modern approach: the same reaction mechanism, but
in **inverse kinematics**, with post-accelerated RIB's

Example: ^{220}Fr (27 s)+d \rightarrow $^{221}\text{Fr}^*$ + p \rightarrow 2FF+p



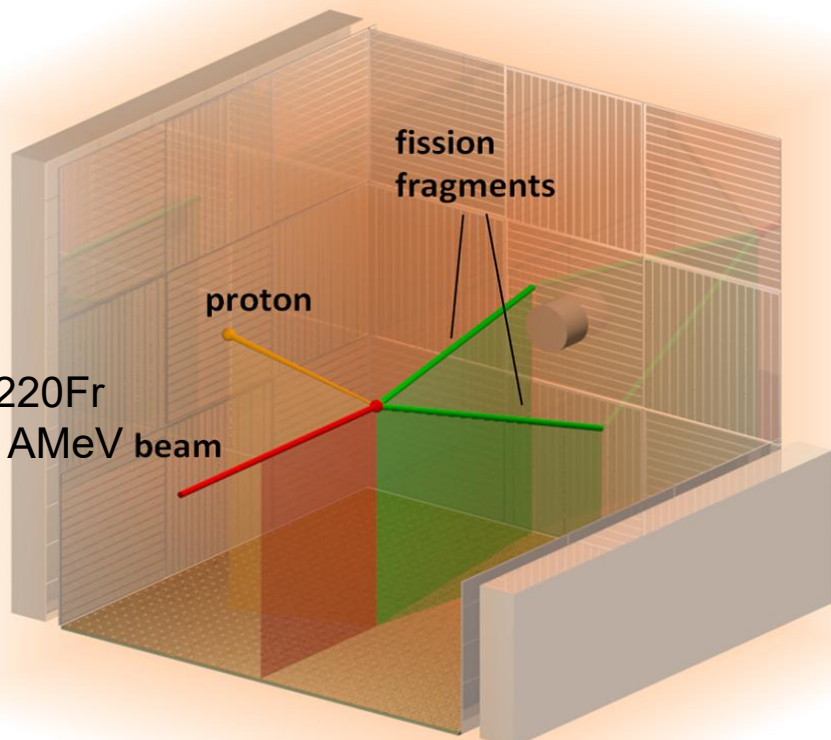
Main advantages in comparison to 'old' direct kinematics

1. Allows to study fission of ("any") RIB's, even very short-lived
2. Higher fission fragment energies (easier identification of energy, mass, charge)
3. Kinematical focusing due to inverse reaction (easier identification)

Example 1: d,pf fission studies with post-accelerated RIBs in inverse kinematics and active (time projection) gas target

(see posters by J.R.Ma on cylindrical AT-TPC from MSU and by L.Li on cubic AT TPC from IMP)

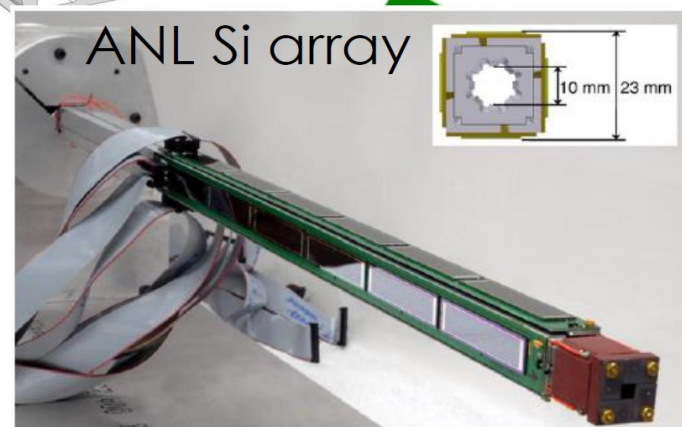
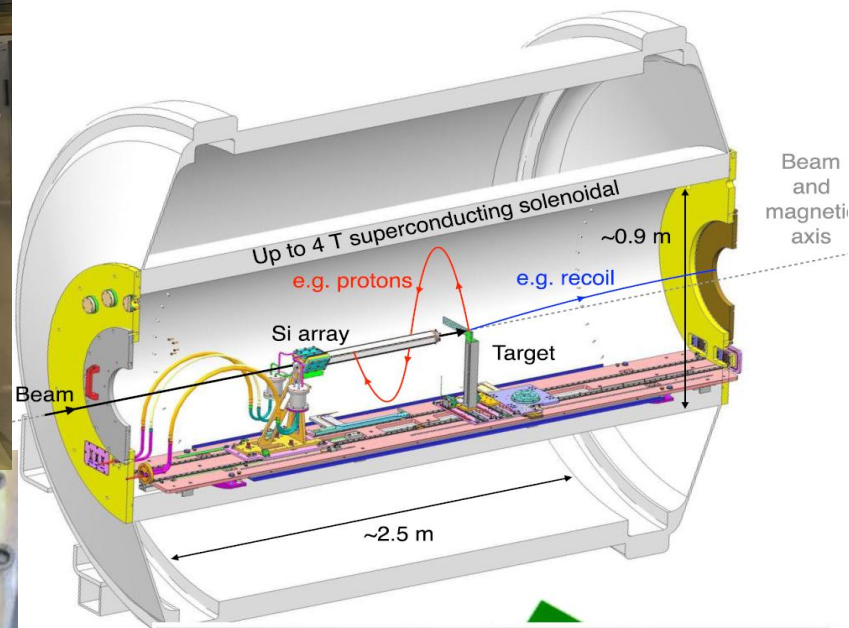
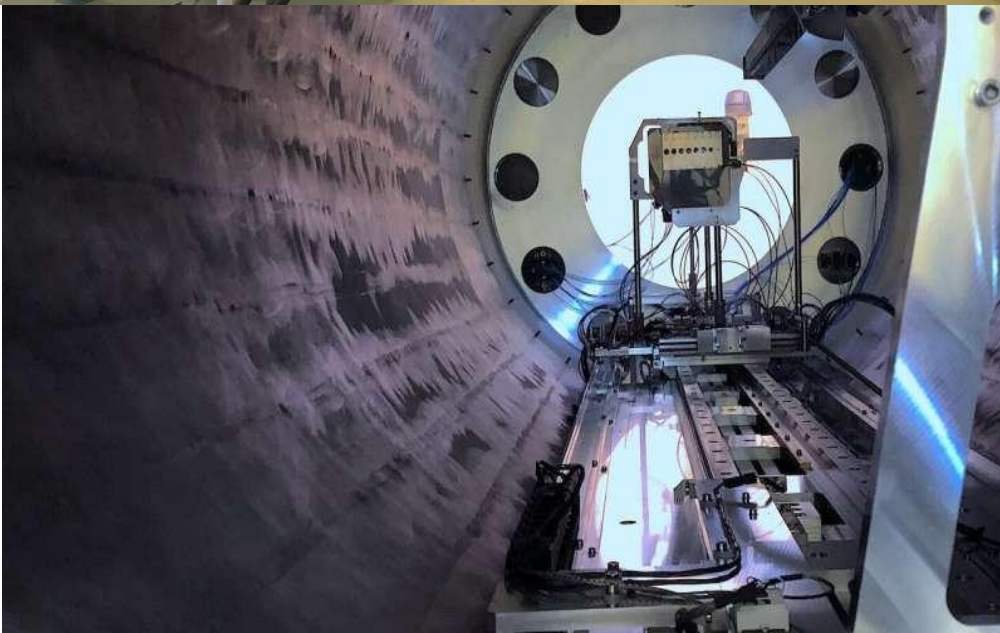
RIB,
e.g. 220Fr
5-10 AMeV beam



- A **low-energy** (30-60 keV) RIB is produced via usual ISOLDE method (mass-separated, also possibly laser-selected), e.g. 220Fr
- Then, **RIB post-acceleration** up to Coulomb energies with HIE-ISOLDE (a few AMeV)
- The RIB is sent to **ACTAR active target** (gas=target) for d,pf measurements, $220\text{Fr} + \text{d} \rightarrow 221\text{Fr}^* + \text{p} \rightarrow 2\text{FF} + \text{p}$
- **Proton-FFs coincidence measurements in ACTAR**
- **FFs energy boost, better energy/mass resolution**

Figure 2: Configuration of ACTAR TPC for the measurement of the transfer-induced fission events. The two fission fragments are detected in the forward-placed silicon array; the proton from the transfer is either stopped in the volume (as shown) or detected in the Si-CsI telescope arrays surrounding the active volume (only partly shown).

Example 2: d,pf transfer-induced fission of post-accelerated RIBs in inverse kinematics with ISOLDE Solenoid (ISS-ISOLDE)



HELIOS@ANL-ISS(ISOLDE) Collaboration

(a proof-of-principles experiment)

PRL, 2023

Direct Determination of Fission-Barrier Heights using Light-Ion Transfer in Inverse Kinematics

S. A. Bennett,¹ K. Garrett,¹ D. K. Sharp,^{1,*} S. J. Freeman,^{1,2} A. G. Smith,¹ T. J. Wright,¹ B. P. Kay,³ T. L. Tang,^{3,†} I. A. Tolstukhin,³ Y. Ayyad,⁴ J. Chen,³ P. J. Davies,⁵ A. Dolan,⁶ L. P. Gaffney,⁶ A. Heinz,⁷ C. R. Hoffman,³ C. Müller-Gatermann,³ R. D. Page,⁶ and G. L. Wilson^{8,3}

¹Department of Physics and Astronomy, University of Manchester, Manchester M13 9PL, United Kingdom

²CERN, CH-1211 Geneva 23, Switzerland

³Physics Division, Argonne National Laboratory, Lemont, Illinois 60439, USA

⁴IGFAE, Universidad de Santiago de Compostela, E-15782 Santiago de Compostela, Spain

⁵School of Physics, Engineering and Technology,

University of York, Heslington, York YO10 5DD, United Kingdom

⁶Oliver Lodge Laboratory, University of Liverpool, Liverpool L69 7ZE, United Kingdom

⁷Chalmers University of Technology, SE-41296 Göteborg, Sweden

⁸Louisiana State University, Baton Rouge, Louisiana 70803, USA

(Dated: February 28, 2023)

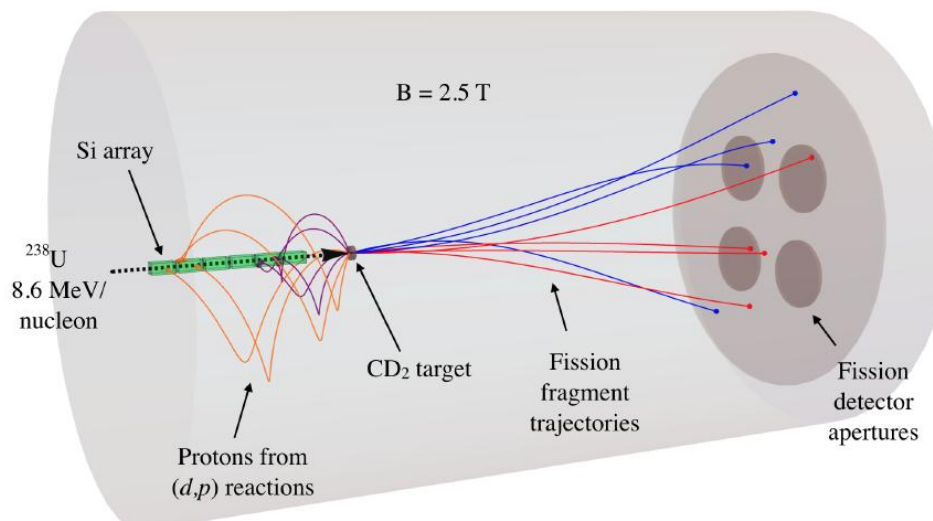
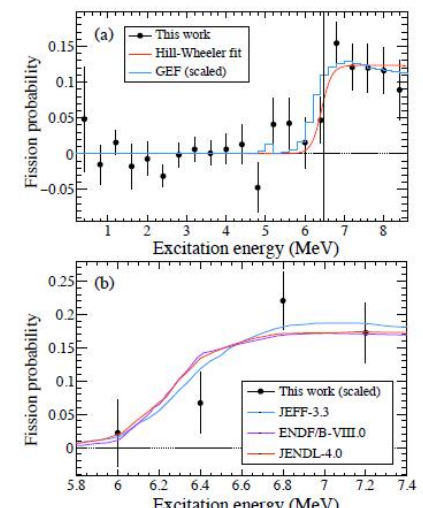
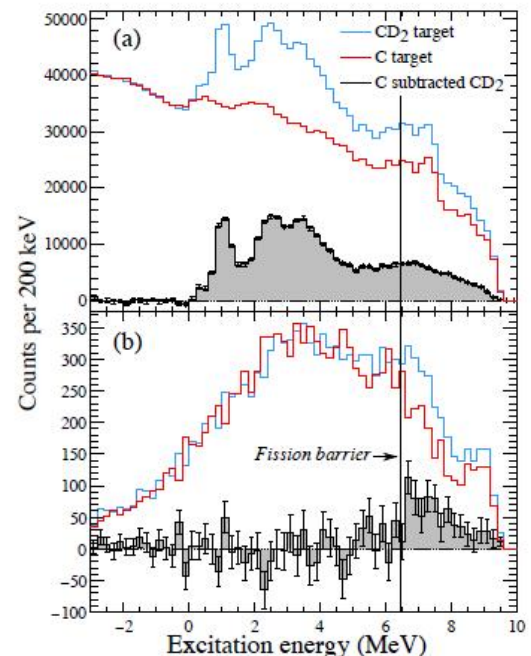


FIG. 1. To-scale schematic of the experimental setup with example particle trajectories for $^{238}\text{U}(d,pf)$ events. Example proton trajectories for reactions populating the ground state in ^{239}U (orange curves) and states at 7 MeV close to the fission barrier (purple curves) are shown for a range of c.m. proton angles. Example fission fragment trajectories are also shown for fragments with $A = 138$ (red curves) and $A = 100$ (blue curves), for a range of emission angles. The equally spaced circular detector apertures have radius 8 cm, and are centred 18 cm from the beam axis. The axial distance between the target and detector apertures is 70 cm.



Low-Energy Fission of Relativistic RIBs
in inverse kinematics at SOFIA@GSI
and SAMURAI@RIKEN
(Coulex-induced and p,2pf reactions)

Two-step RIBs production at SOFIA@GSI

- Primary beam of ^{238}U , 1 A GeV
- Fragmentation reaction on a light target, e.g. Be produces **secondary beam of fissile ions at ~ 700 AMeV (from Mercury up to Neptunium)**, sorted through FRS
- Selected secondary ions from **FRS** sent to Cave C for the fission experiment
- **Fission induced in-flight by Coulomb excitation on a heavy secondary Pb target ($E^* \sim 12$ MeV)**
- Both fission fragments identified simultaneously, both in mass and in charge (**FF's are at ~ 600 AMeV!**)

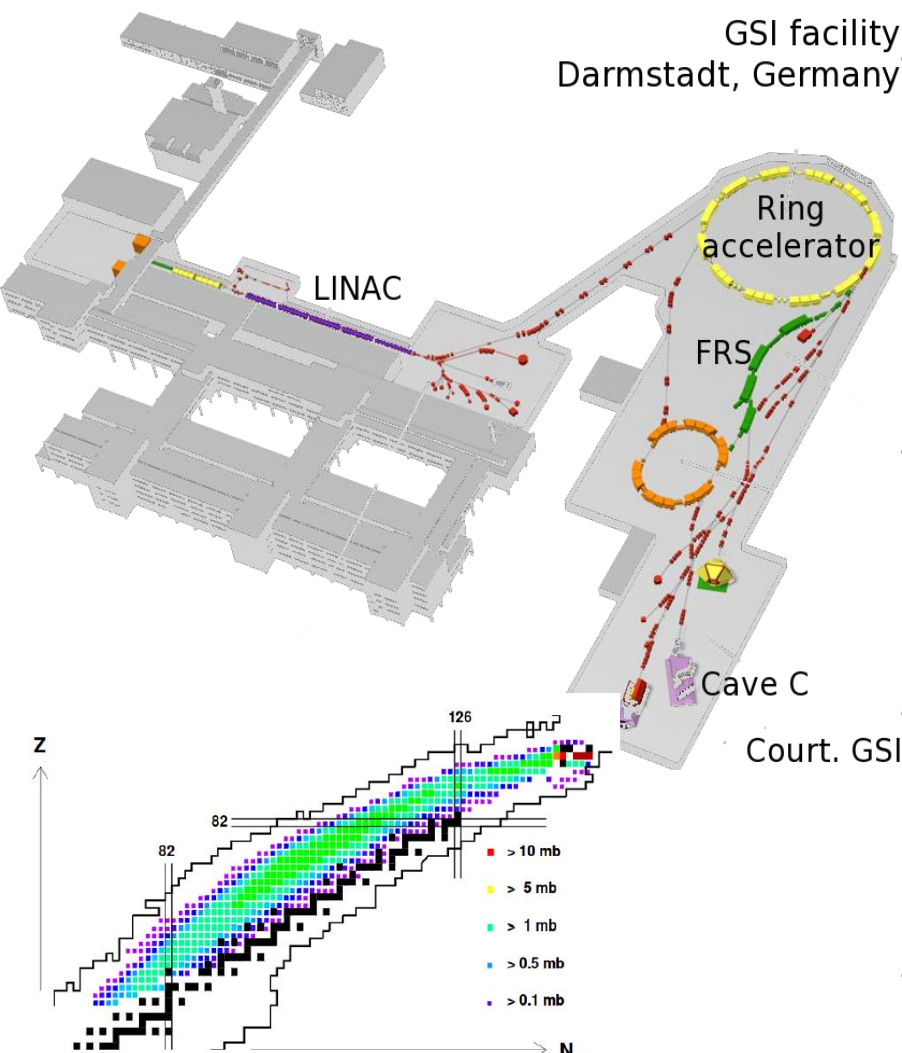


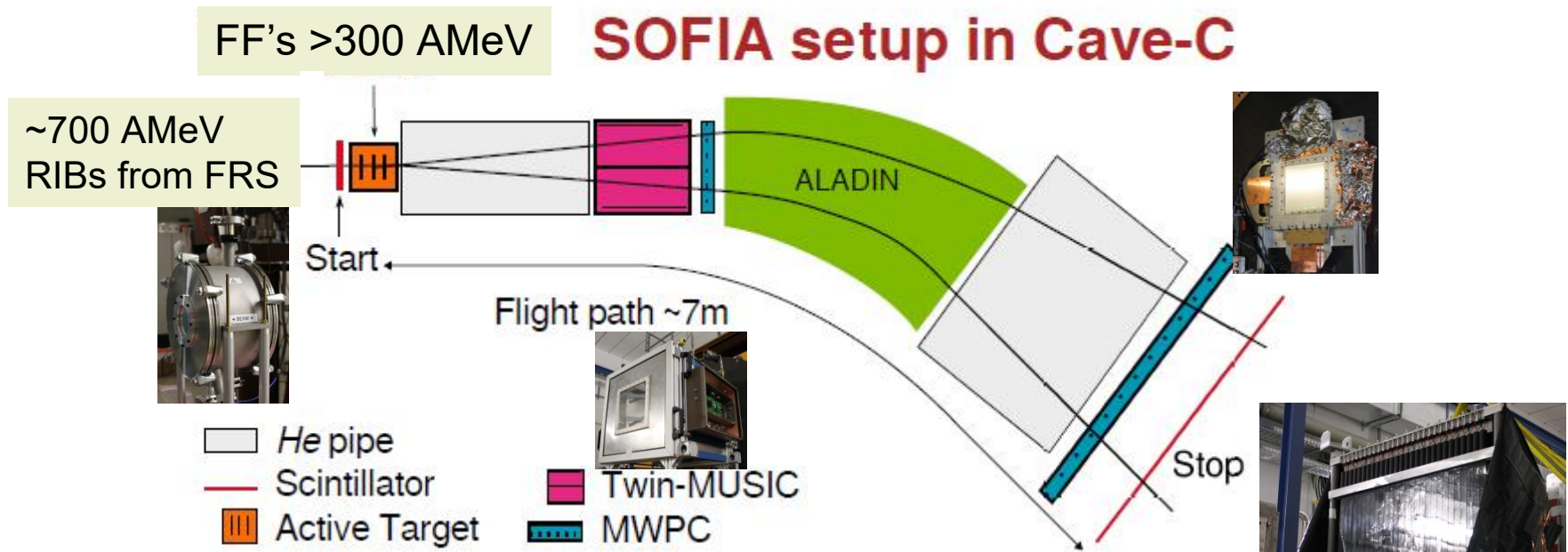
Figure 15. Measured formation cross sections of spallation residues, produced in the reaction ^{238}U (1 A GeV) + ^2H , are

Two-step production at SOFIA@GSI

Some of the Main advantages:

- fission fragments are at much higher energies (~200-600 AMeV), thus much easier to identify their A and Z.
- Emission of neutrons (neutron multiplicity) is easier to study (due to their kinematic focusing)

BUT: Needs a much more complex production method and detection system (e.g. R3B, SAMURAI)



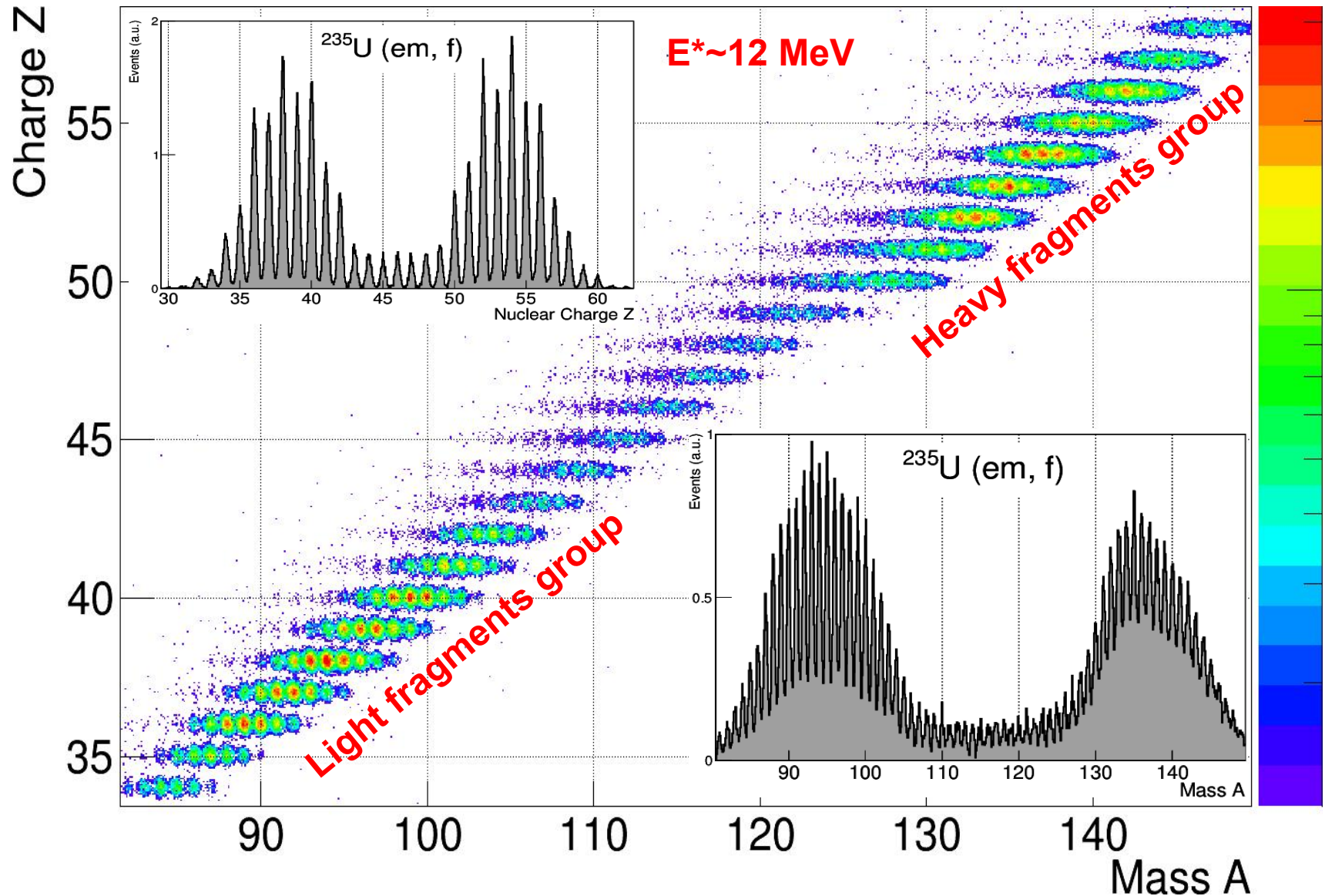
Active Target
Twin-MUSIC
MWPCs
ToF
ALADIN

Fission
Charges
Positions
Velocity
Dipole

Z
 ρ
 γv
 B

$$(B\rho, Z, \gamma v) \rightarrow A$$

Some examples ... (note fantastic A and Z resolution, hardly achievable by other techniques)



Recent Fission of secondary beams after the EM excitation: Detailed studies of multi-modal fission

INFLUENCE OF PROTON AND NEUTRON DEFORMED ...

PHYSICAL REVIEW C 106, 024618 (2022)

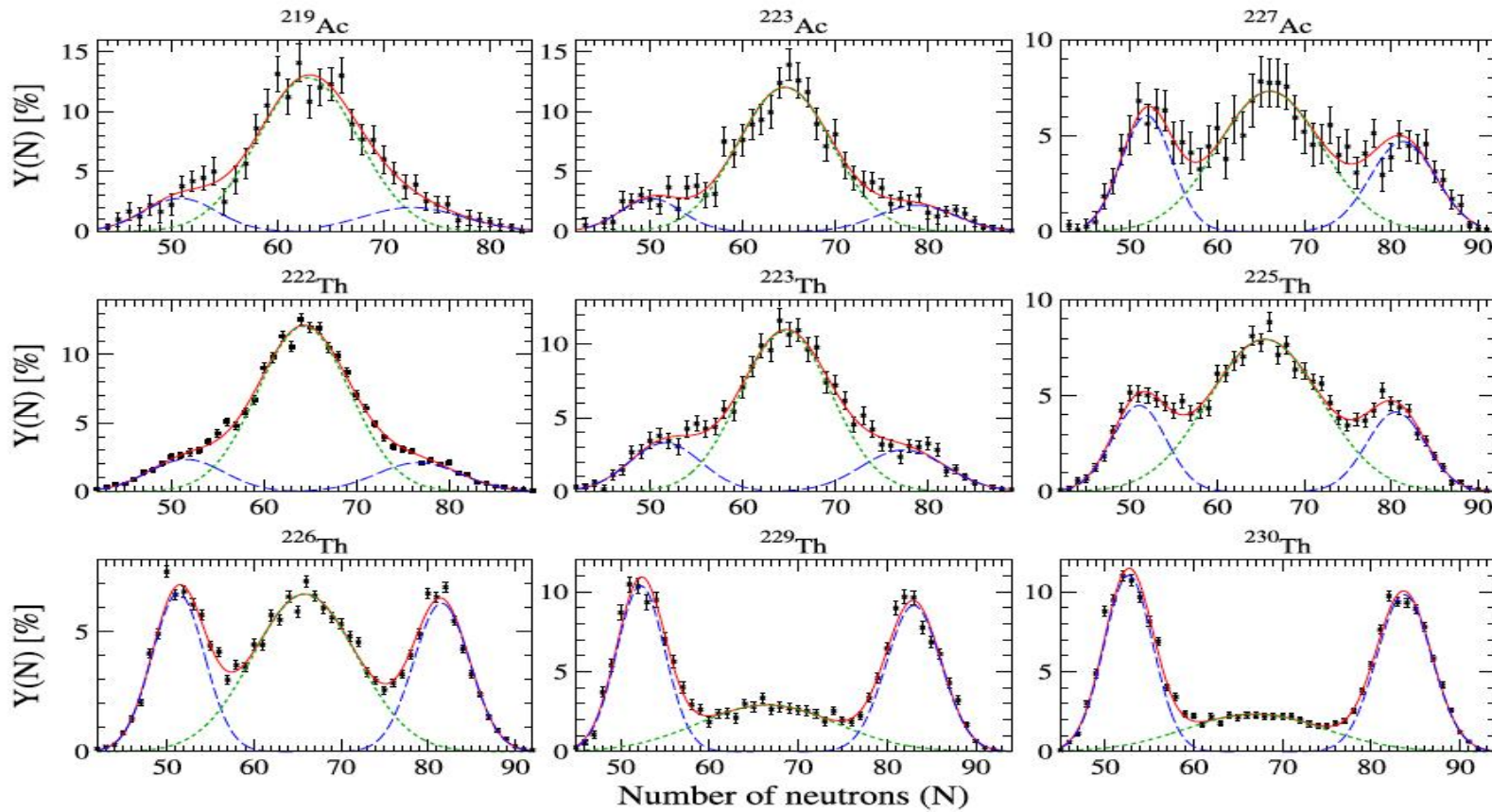


FIG. 1. Isotonic yields after prompt-neutron emission for each of the actinium and thorium isotopes fitted by a 3-Gaussian function. The data measured from the R3B/SOFIA experiments are in black. The error bars represent the statistical uncertainties. The total fit (full red lines) is decomposed into one symmetric (dotted green lines) and two asymmetric (dashed blue lines) components.

A. Chatillon et al. Phys. Rev. Lett. 124, 202502 (2020)

A. Chatillon et al., PHYSICAL REVIEW C 106, 024618 (2022)

Recent Fission of secondary beams after the EM excitation: Z=54 dominance in heavy nuclei

INFLUENCE OF PROTON AND NEUTRON DEFORMED ...

PHYSICAL REVIEW C 106, 024618 (2022)

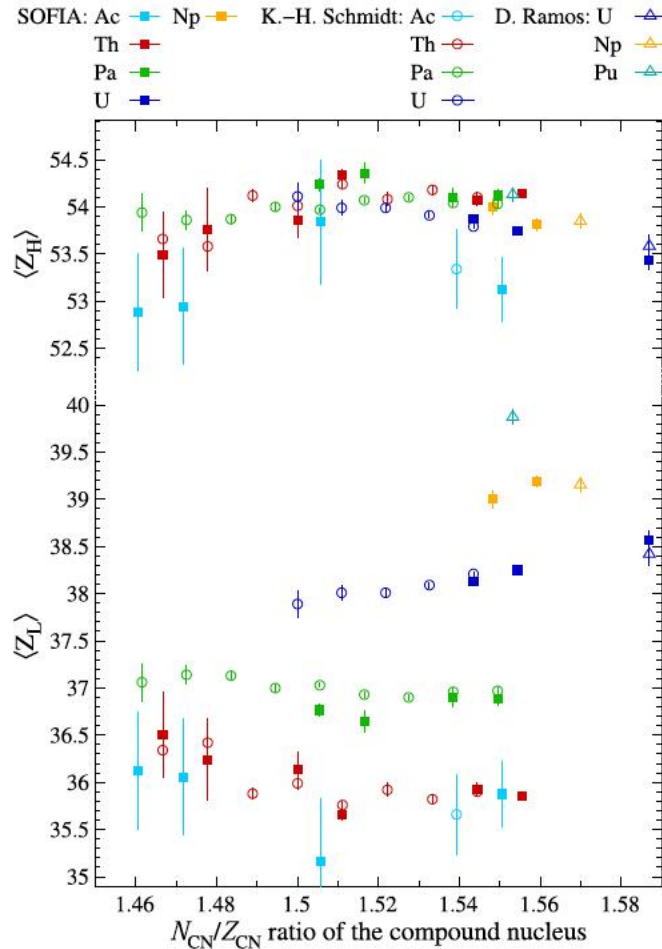


FIG. 4. The average value of the atomic number of the light and heavy fission fragments measured at R3B/SOFIA (full squares) are compared with data from Refs. [18,19] (open circles) and [24] (open triangles).

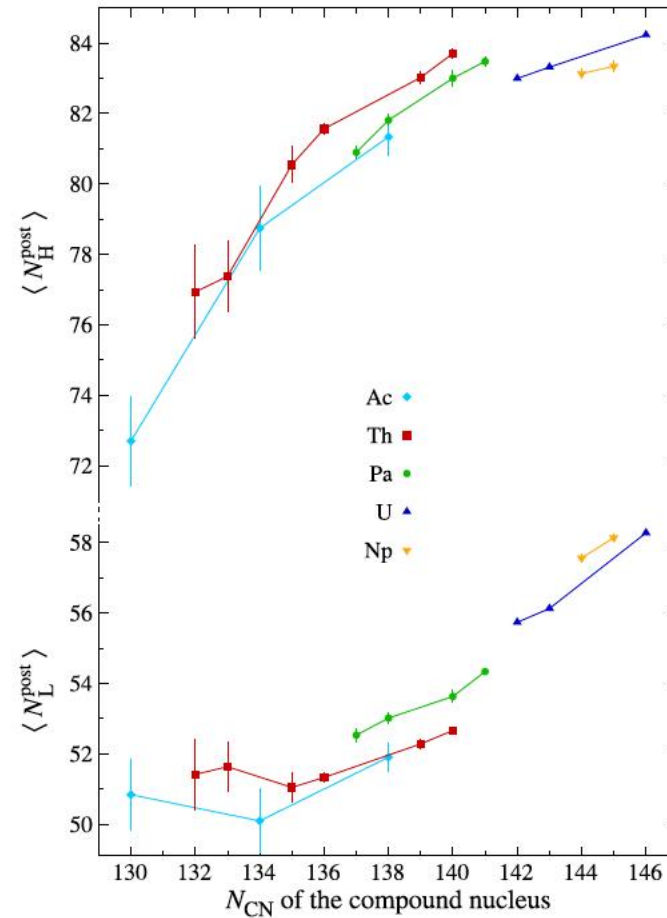


FIG. 5. Centroid positions of the light and heavy peaks of the isotonic yields measured after the prompt-neutron evaporation phase.

SOFIA 2025: An asymmetric fission island driven by shell effects in light fragments

Article

Nature, 641, 339 (2025)

An asymmetric fission island driven by shell effects in light fragments

<https://doi.org/10.1038/s41586-025-08882-7> P. Morfouace^{1,2}, J. Taleb^{1,2}, A. Chatillon^{1,2}, L. Audouin³, G. Blanchon^{1,2}, R. N. Bernard⁴,

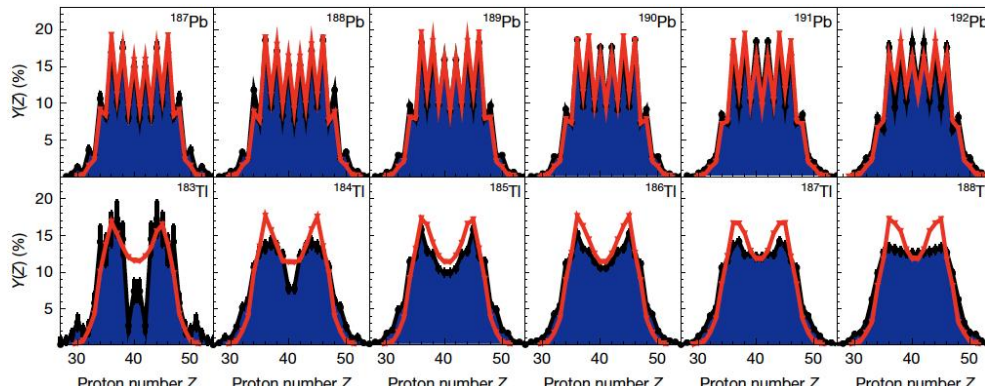


Fig. 3 | Charge yields of thallium and lead isotopes. Measured charge yields corresponding to statistical uncertainties are visible if not smaller than the

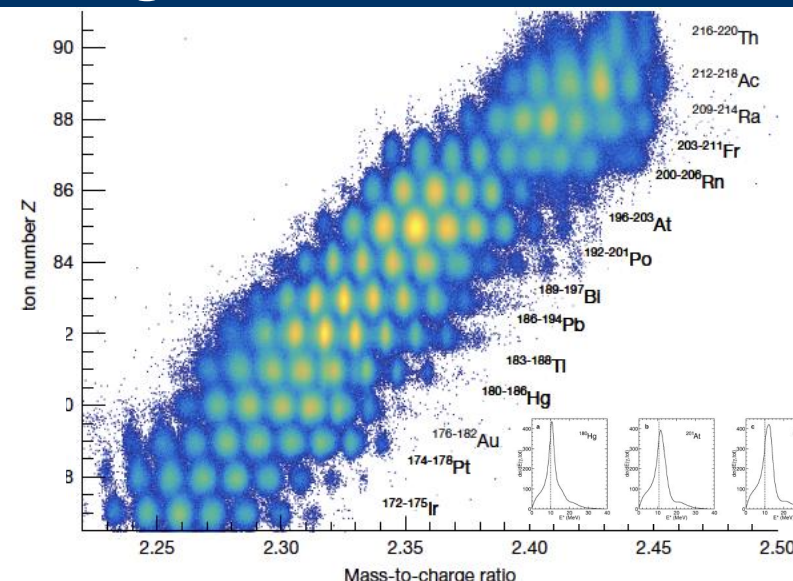


Fig. 4 | Particle identification plot of the secondary beam. Particle

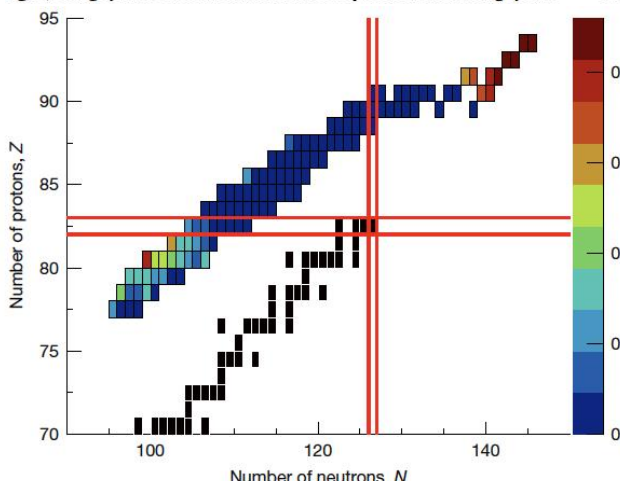
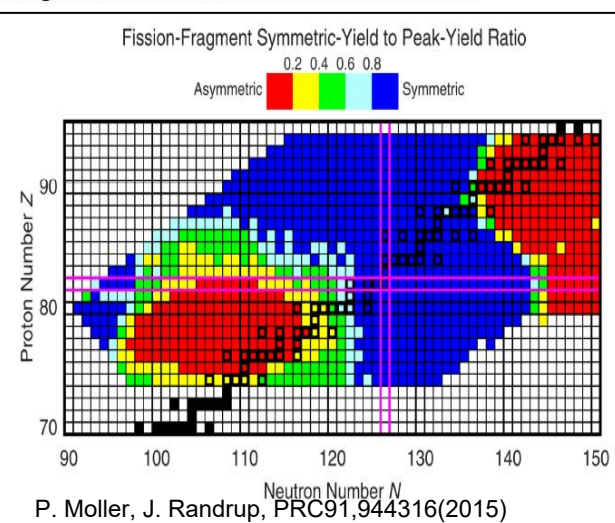


Fig. 2 | Map of the evolution of asymmetric fission. Experimental asymmetry



P. Moller, J. Randrup, PRC91, 944316(2015)

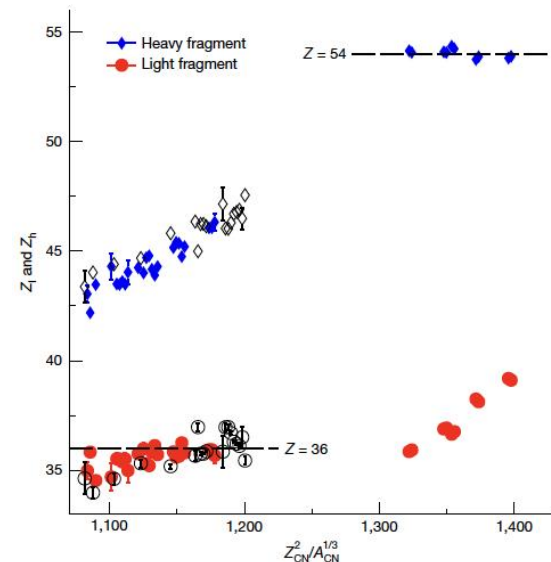


Fig. 4 | Evidence of $Z = 36$ stabilization of the light fragments. Light (red)

Dominance of proton shell effects in low-energy fission

K. Mahata et al, PLB825, 136859 (2022)

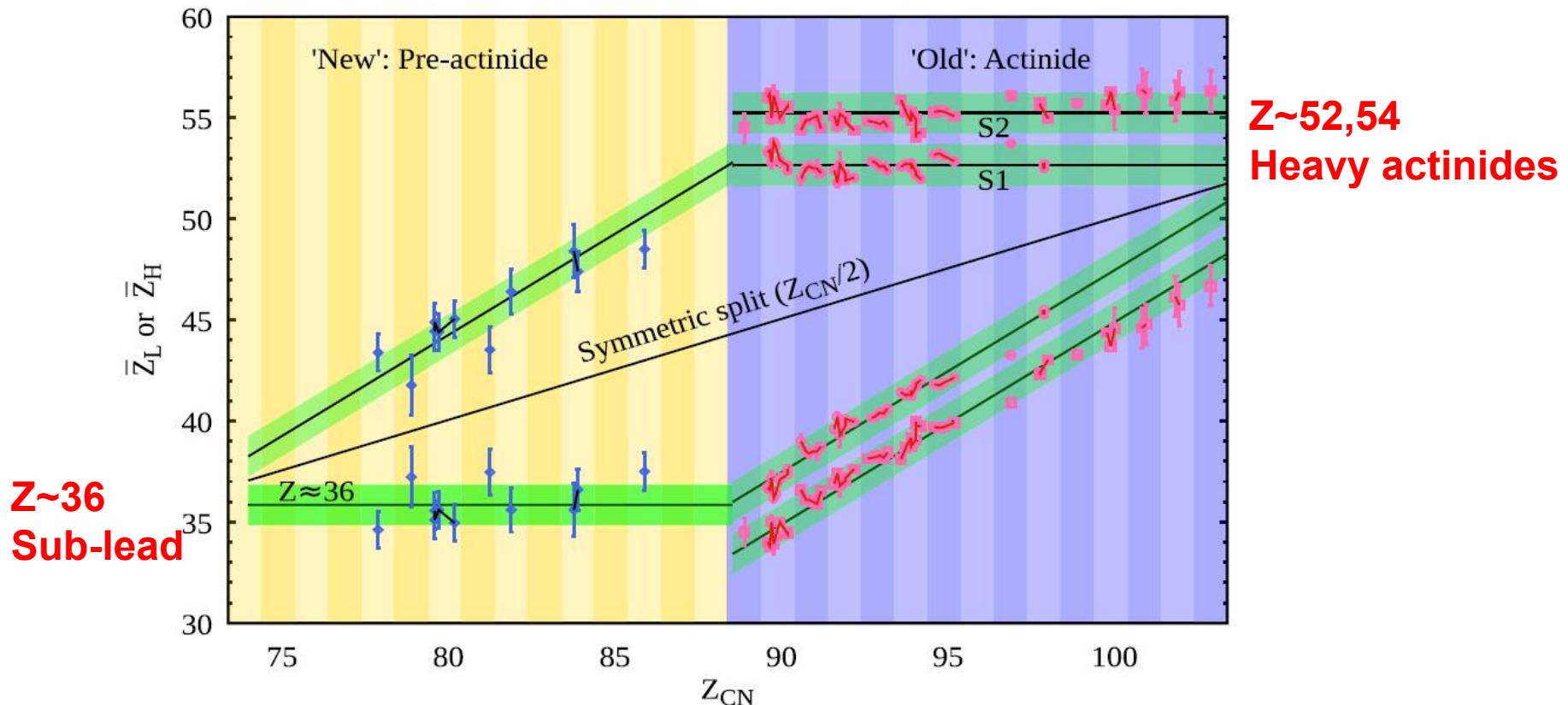
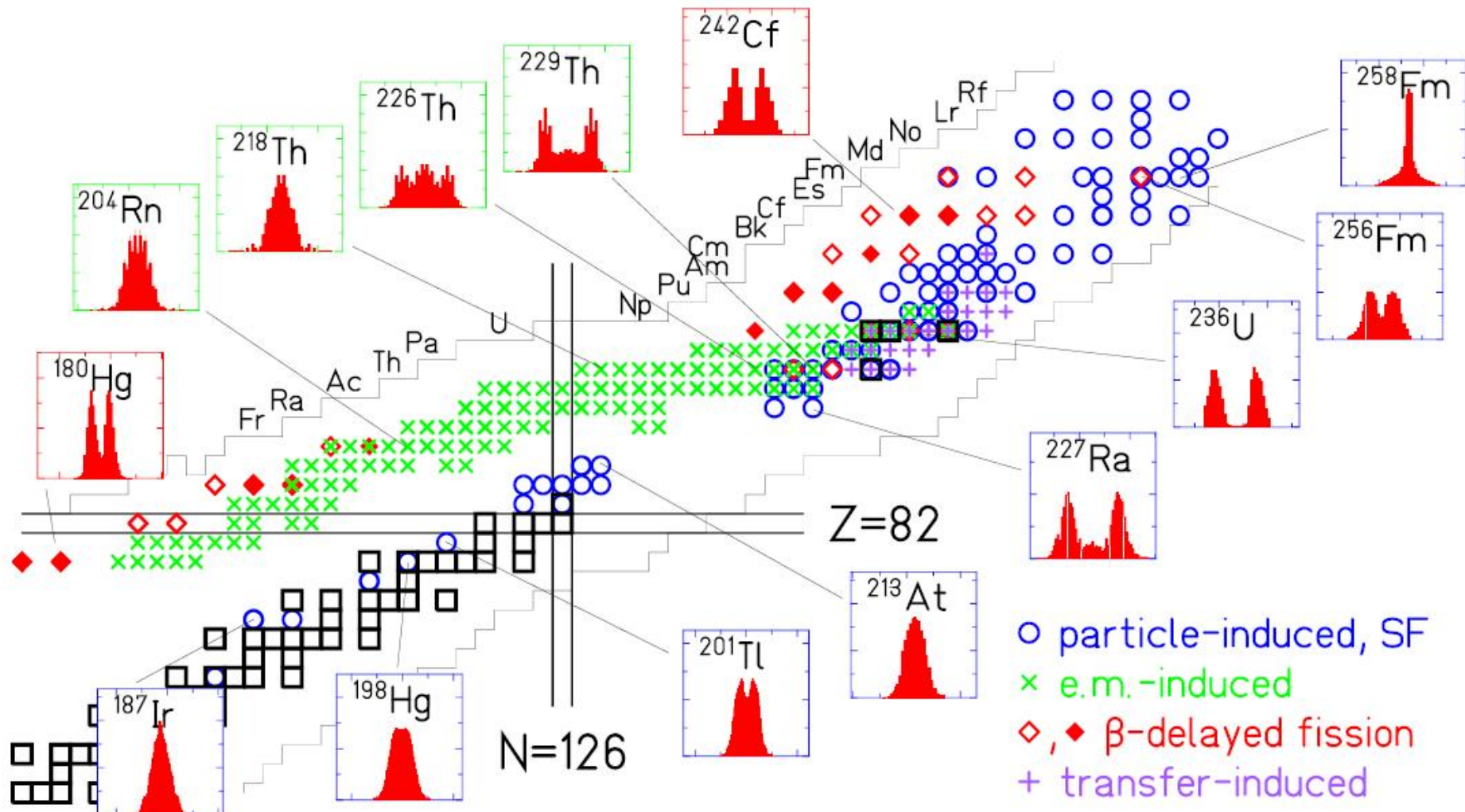


Fig. 4. Evolution of the average $\bar{Z}_{L(H)}$ positions for the asymmetric fission channel as a function of Z_{CN} from above rare-earth to very-heavy and super-heavy elements. For clarity, isotopes of a same element are connected by a black segment and shifted according to the difference between their masses. The points are from

Summary: Present Status of Fission Mass/Charge distribution measurements



Fission in 21st Century: Some of the topics covered

- Beta Delayed Fission (β DF) at ISOLDE at 60 keV
- Transfer -induced fission with ACTAR/ISS at HIE-ISOLDE
- Coulex-induced fission with SOFIA@GSI at 1 AGeV
- p,2pf at RIBF@RIKEN
- Fusion-fission with heavy ions at Coulomb energies (Dubna, ANU, India..)
- Transfer-induced fission at Coulomb energies (VAMOS@GANIL, JAEA)
- n_ToF, n-induced fission experiments (ILL,n_ToF, LANSCE,J-PARC....)
- Future fission facilities: RIBF@RIKEN, RIBF@J-PARC, RIBF@GSI, RIBF@CERN, RIBF@RIKEN?
- Future fission facilities: RIBF@RIKEN, RIBF@J-PARC, RIBF@GSI, RIBF@CERN, RIBF@RIKEN?

Thank You for your Attention!

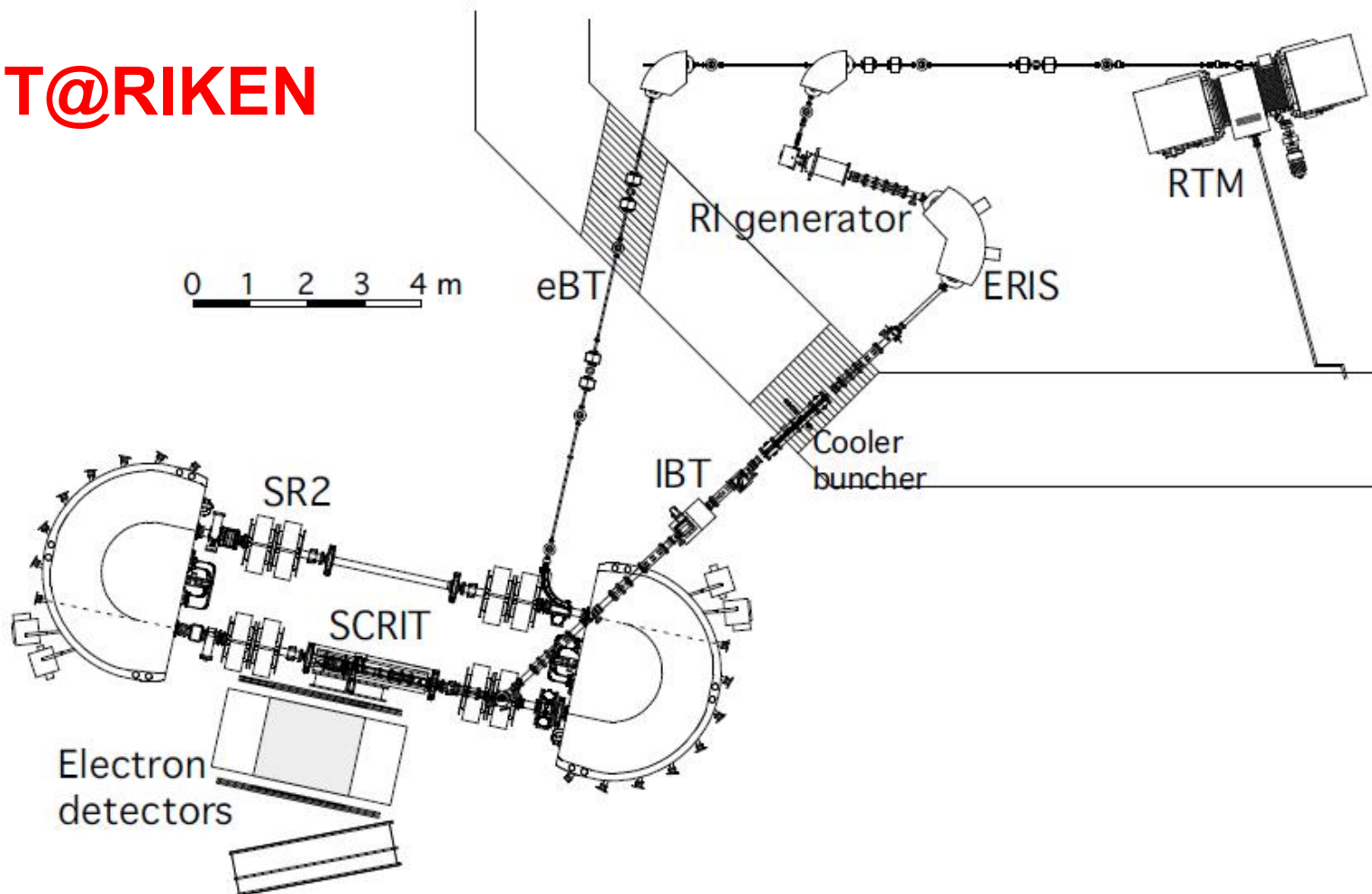
- Bright future for fission studies with RIBs
- Access to both proton- and neutron- rich nuclei
- Un-precedented precision in Z,A determination!
- Control of excitation energy event-by-event!
- However, still the 'classical' methods work and allow to study both the isospin and excitation dependence of fission in the 'new' regions of Chart of Nuclides

Future(?): Fission via Electron scattering from unstable nuclei

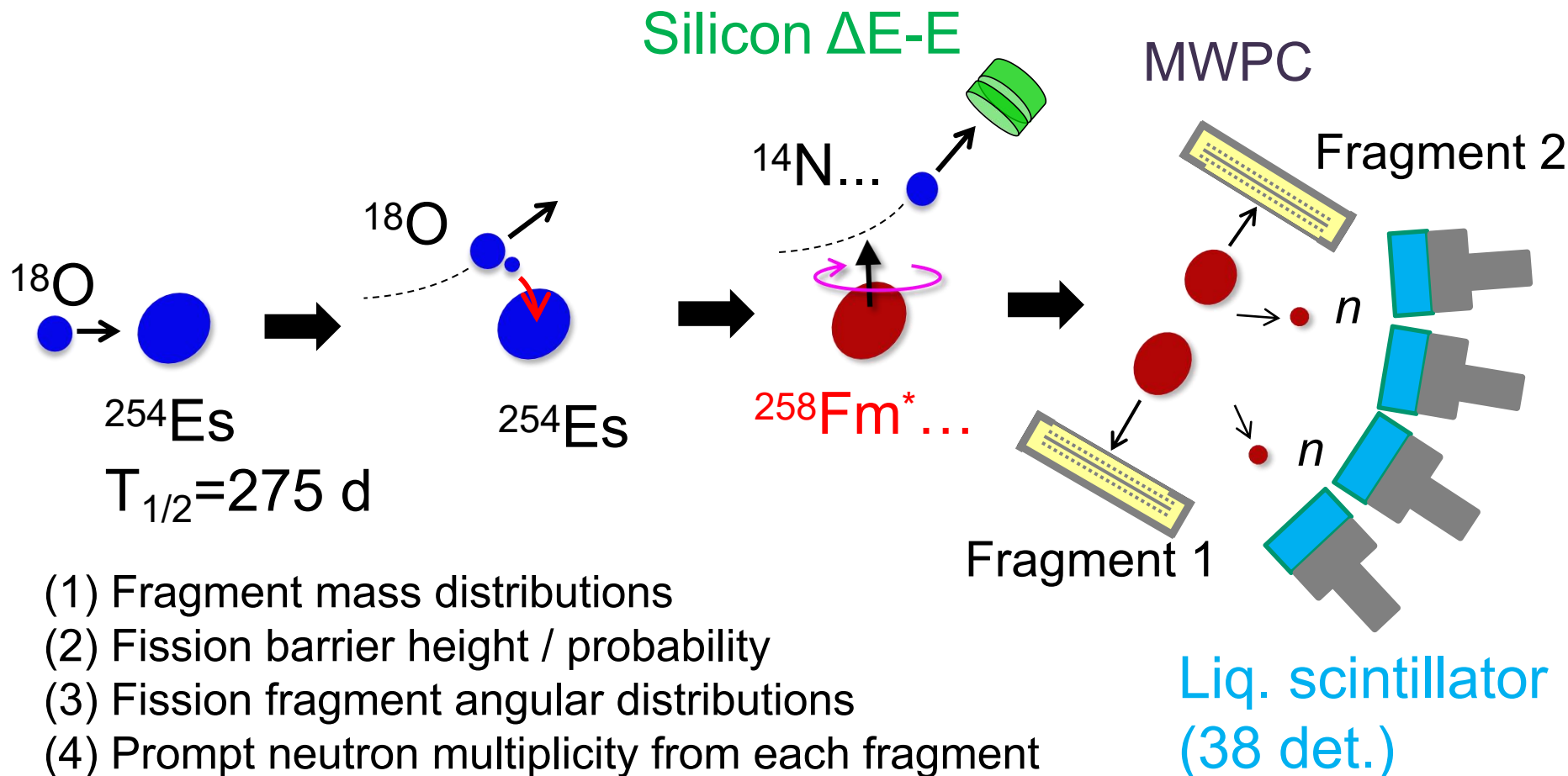
e.g. electron scattering from unstable nuclei (colliding accelerated electrons and low-energy radioactive ions!)

SCRIT at RIKEN (Japan) and ELISe at GSI (Darmstadt, Germany)

SCRIT@RIKEN

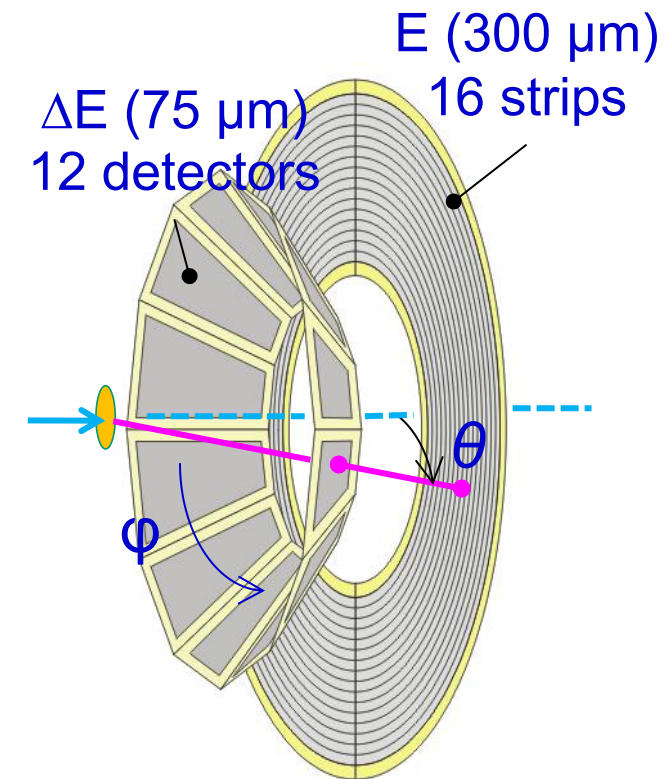
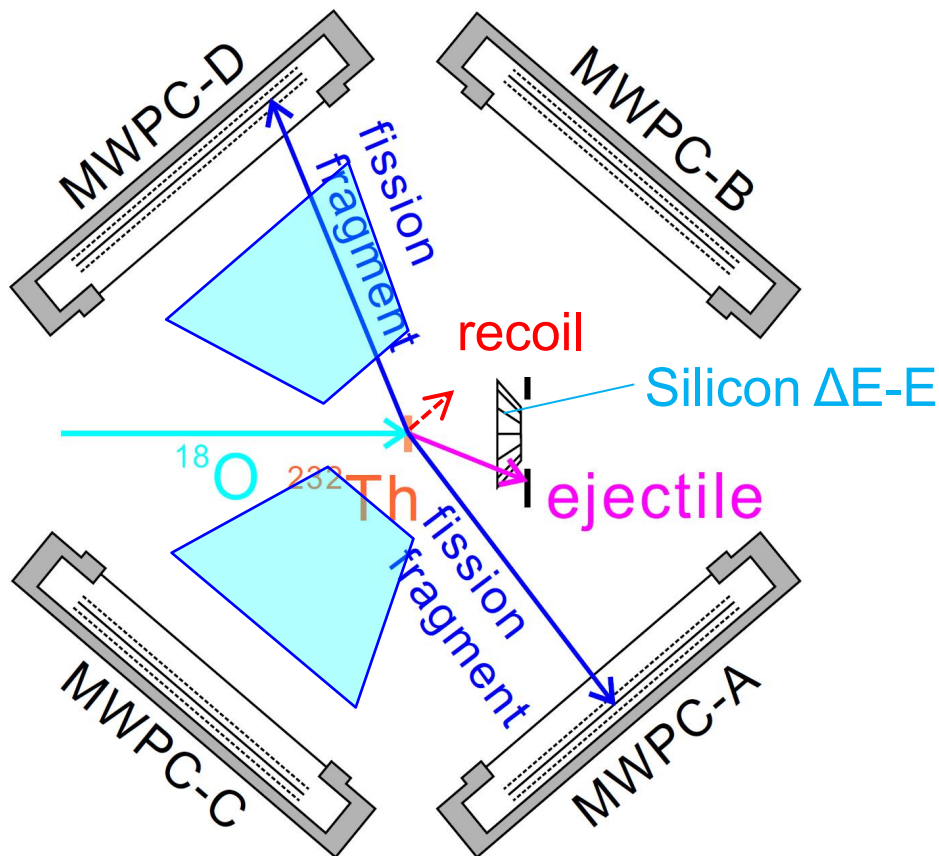


Multi-nucleon transfer (MNT) fission at JAEA(Tokai)



Measured and Planned experiments using ^{18}O beam and targets of ^{232}Th , ^{238}U , ^{248}Cm , ^{237}Np , ^{249}Cf , ^{243}Am , ^{231}Pa , ^{226}Ra , ^{254}Es

Experimental setup



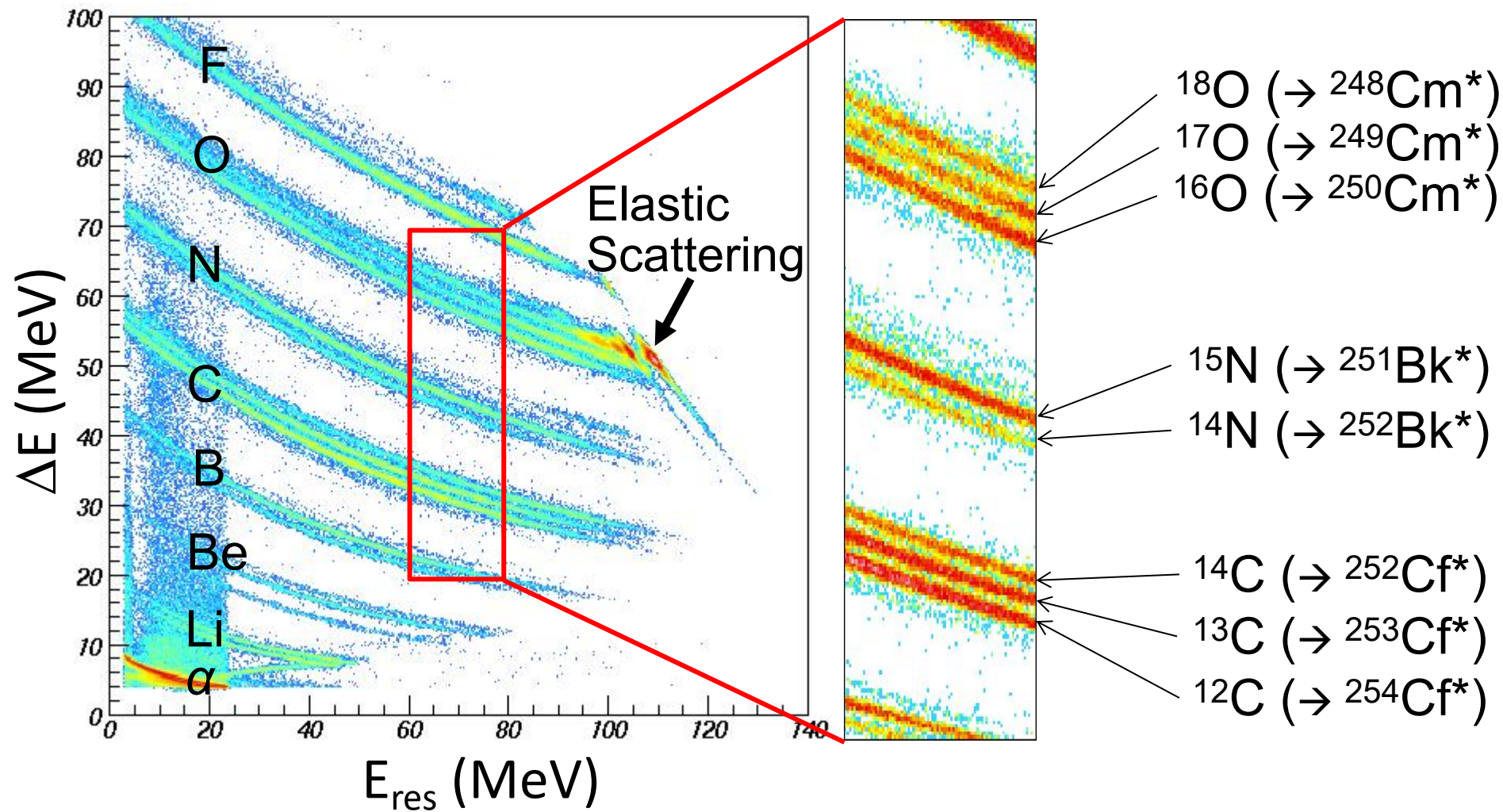
MCPs are added (T. Tanaka @ Kyushu univ./RIKEN)

START detector for the fragments.

→ TKE will also be obtained.

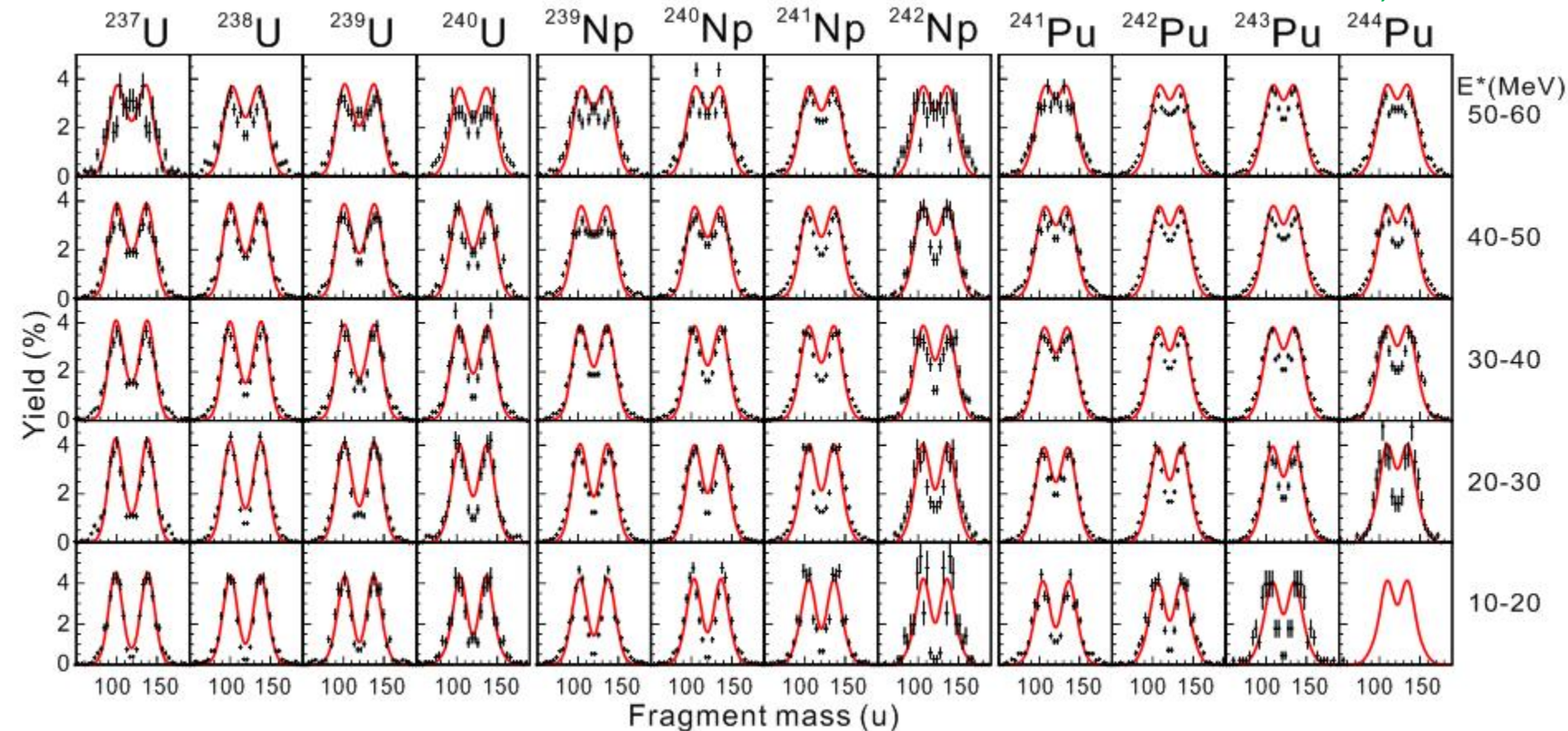
DE-E spectrum

$^{18}\text{O} + ^{248}\text{Cm}$ ($E_{\text{beam}} = 162\text{MeV}$)



Exp. and Calc. ($^{18}\text{O} + ^{238}\text{U}$)

Hirose et al. PRL, Nov 2017



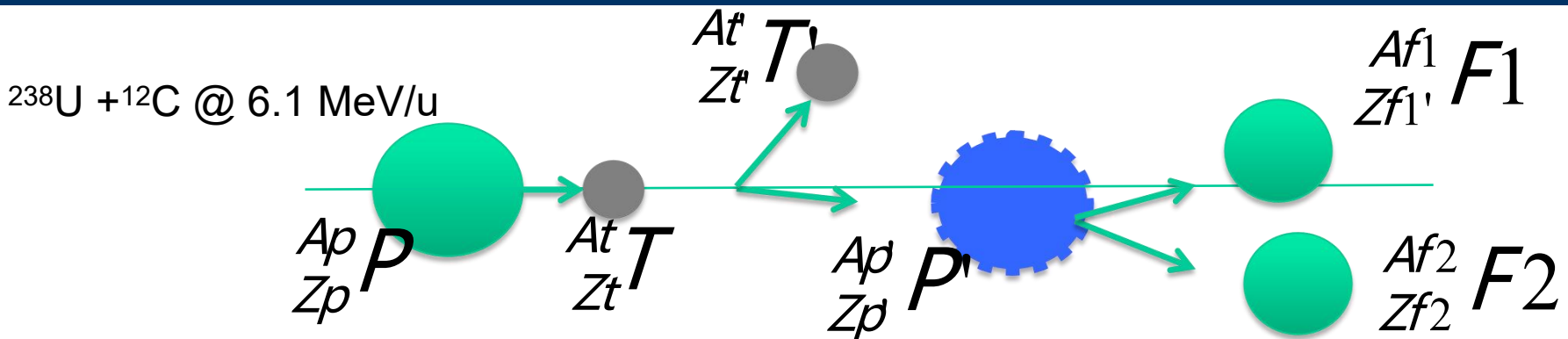
With multi-chance fission

The calculation well reproduces the experimental FFMD!

The asymmetric fissions observed in higher Ex is due to the multi-chance fission.

Note again the relatively poor FFs mass resolution (~ 3 u)

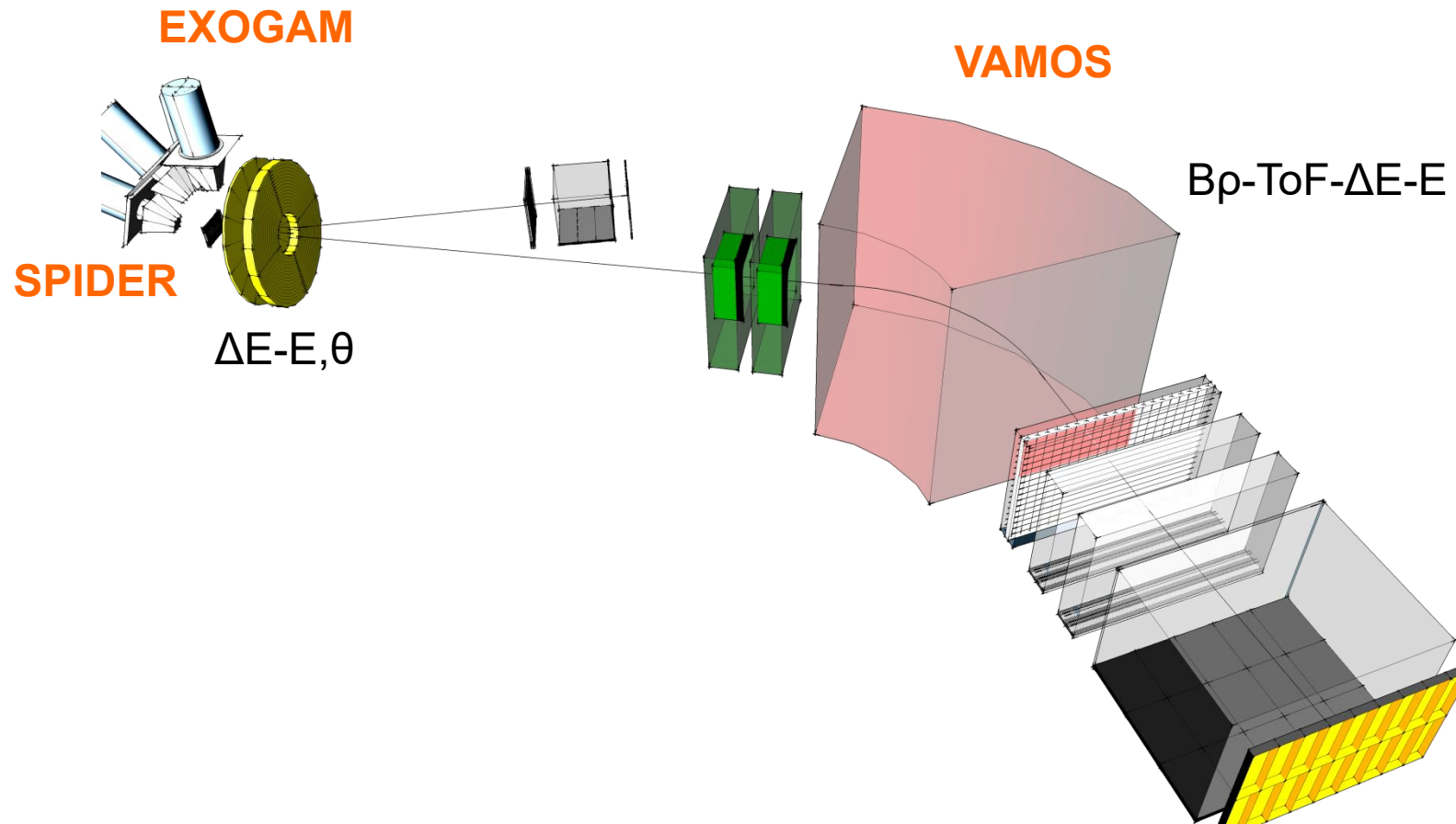
Transfer-induced fission with ^{238}U beam in inverse kinematics at Coulomb energies with VAMOS@GANIL



^{242}Cf	^{243}Cf	^{244}Cf	^{245}Cf	^{246}Cf	^{247}Cf	^{248}Cf	^{249}Cf	^{250}Cf	^{251}Cf	^{252}Cf
^{241}Bk	^{242}Bk	^{243}Bk	^{244}Bk	^{245}Bk	^{246}Bk	^{247}Bk	^{248}Bk	^{249}Bk	^{250}Bk	^{251}Bk
^{240}Cm	^{241}Cm	^{242}Cm	^{243}Cm	^{244}Cm	^{245}Cm	^{246}Cm	^{247}Cm	^{248}Cm	^{249}Cm	^{250}Cm
^{239}Am	^{240}Am	^{241}Am	^{242}Am	^{243}Am	^{244}Am	^{245}Am	^{246}Am	^{247}Am	^{248}Am	^{249}Am
^{238}Pu	^{239}Pu	^{240}Pu	^{241}Pu	^{242}Pu	^{243}Pu	^{244}Pu	^{245}Pu	^{246}Pu	^{247}Pu	
^{237}Np	^{238}Np	^{239}Np	^{240}Np	^{241}Np	^{242}Np	^{243}Np	^{244}Np			
^{236}U	^{237}U	^{238}U	^{239}U	^{240}U	^{241}U	^{242}U				

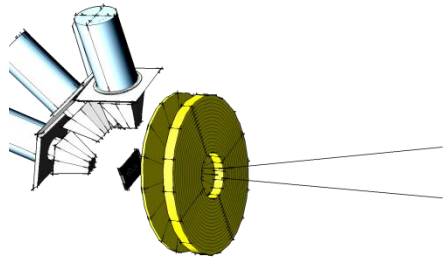
- 10 actinides produced
- E^* distribution
- Full resolution in (Z,A) of fragments
- TKE

Transfer-induced fission in inverse kinematics with VAMOS@GANIL



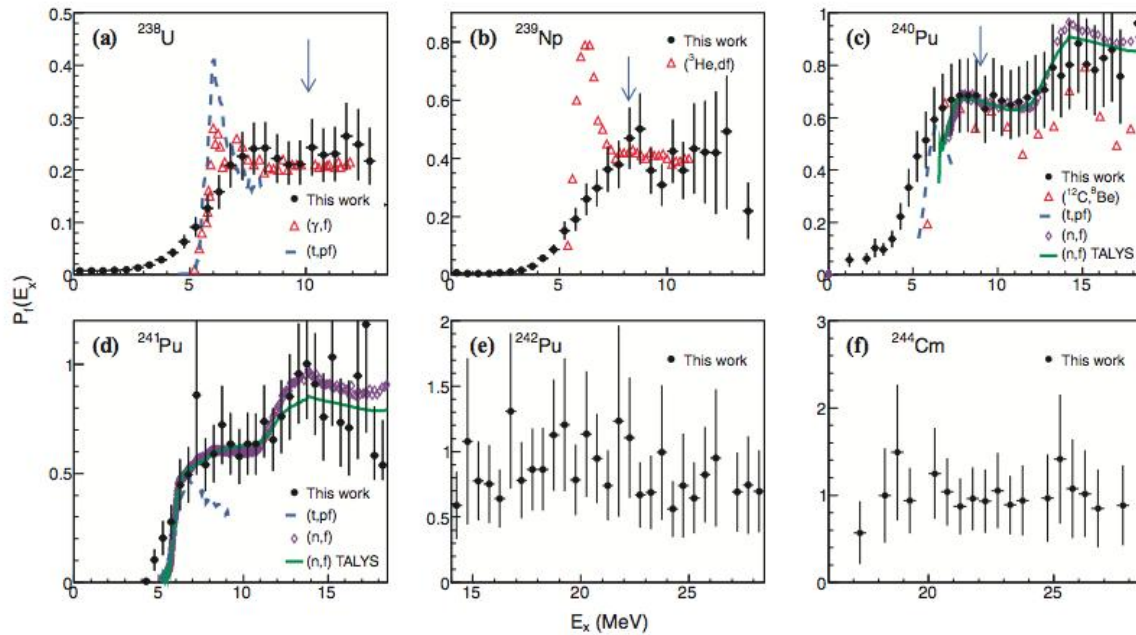
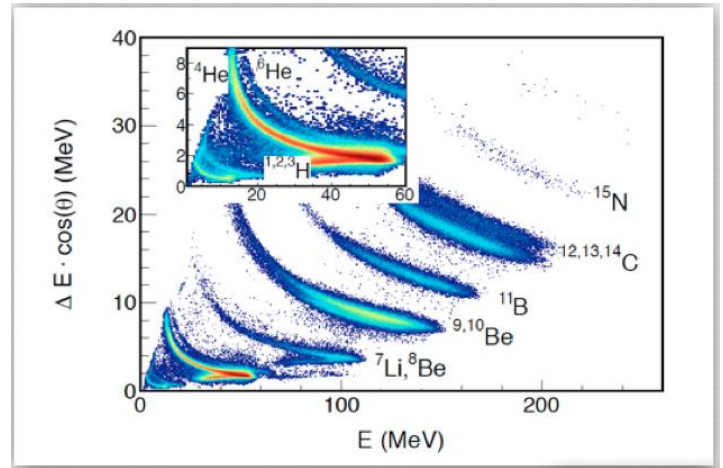
S. Pullanhiotan et al., NIM 593 (2008) 343
M. Rejmund et al., NIMA 646 (2011) 184

SPIDER dE-E Silicon telescope for the light ejectile determination



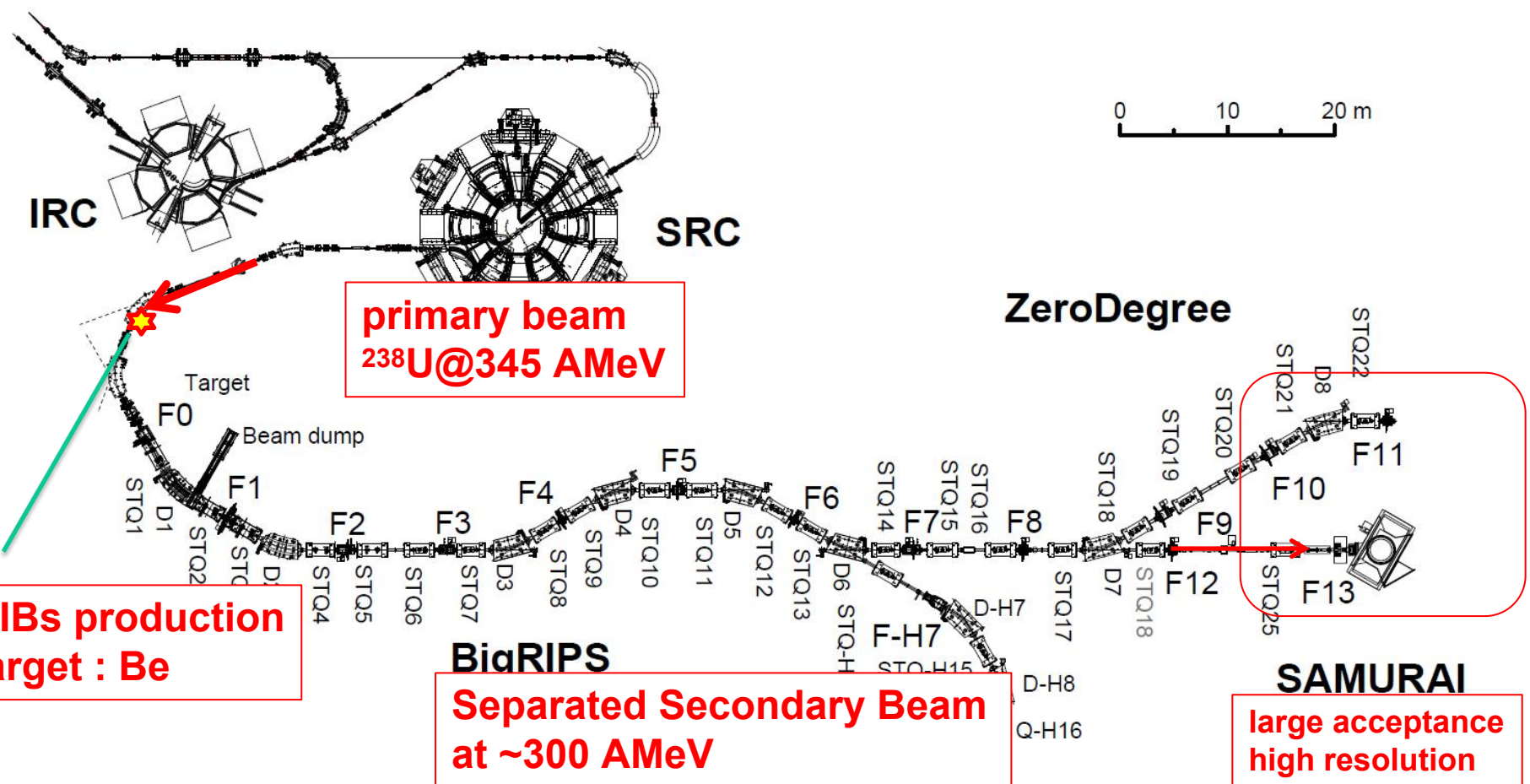
SPIDER ΔE - E, θ

C. Rodriguez-Tajes et al., PRC (2014) 024614

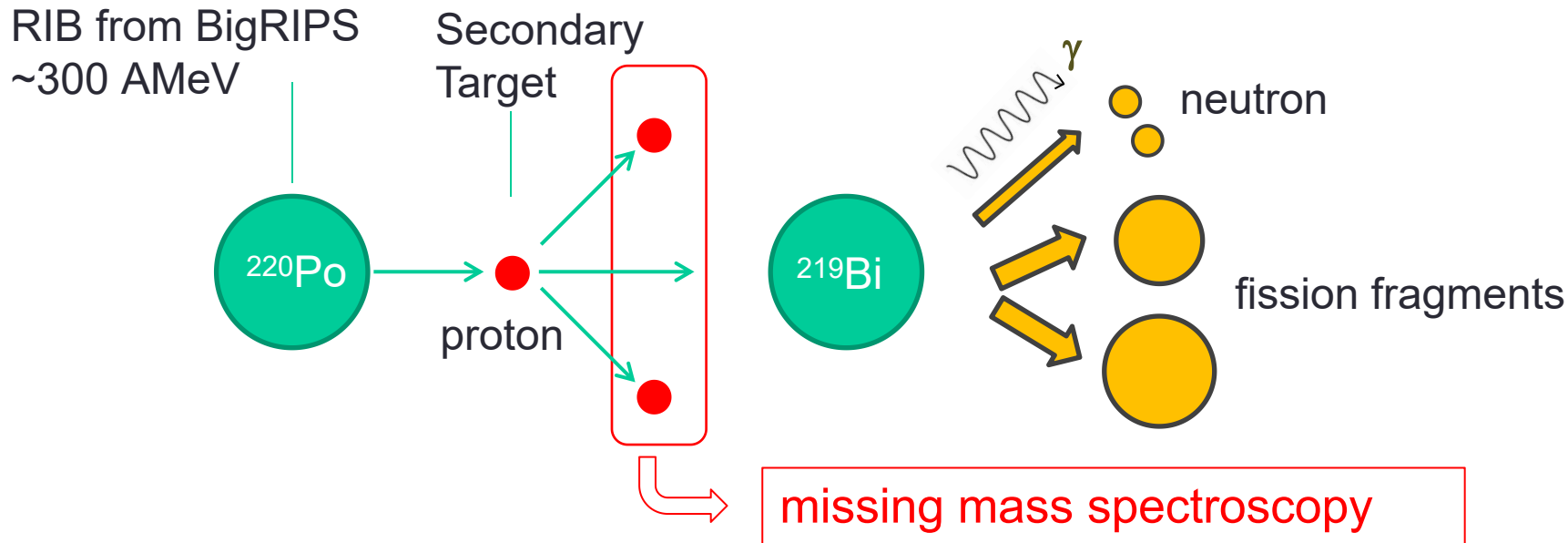


Fission Studies with BigRIPS and SAMURAI at RIBF@RIKEN (p,2p-fission method)

- 1st step the same as at GSI: Primary beam: ^{238}U at ~ 345 AMeV
- RIBs production on a Be target, separation with BigRIPS
- Separated RIBs are sent to SAMURAI for p,2p fission studies

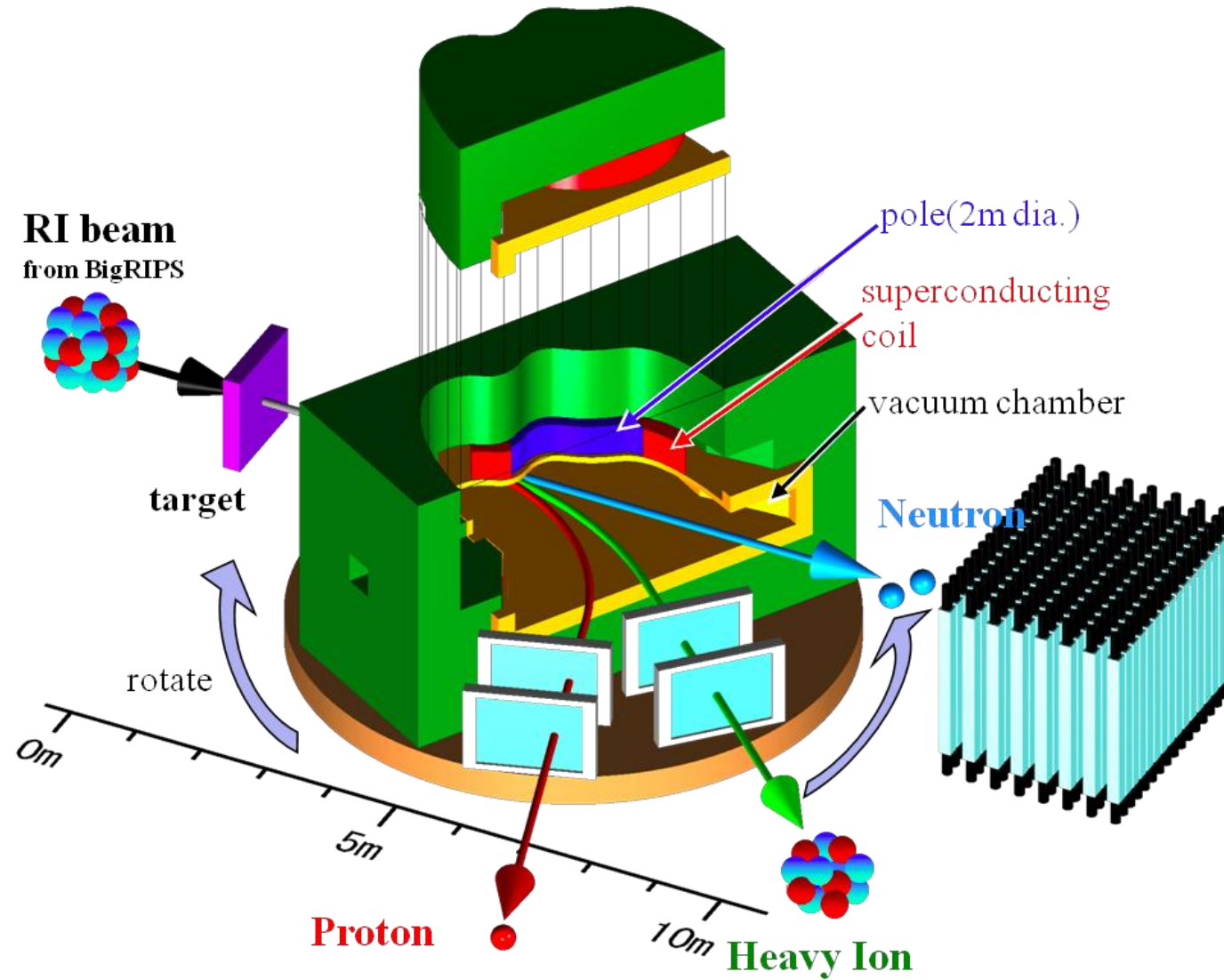


Method: Inverse kinematics with ($p, 2p$ -fission) reaction (similar idea with the p, pn -fission, but needs to measure also neutrons)

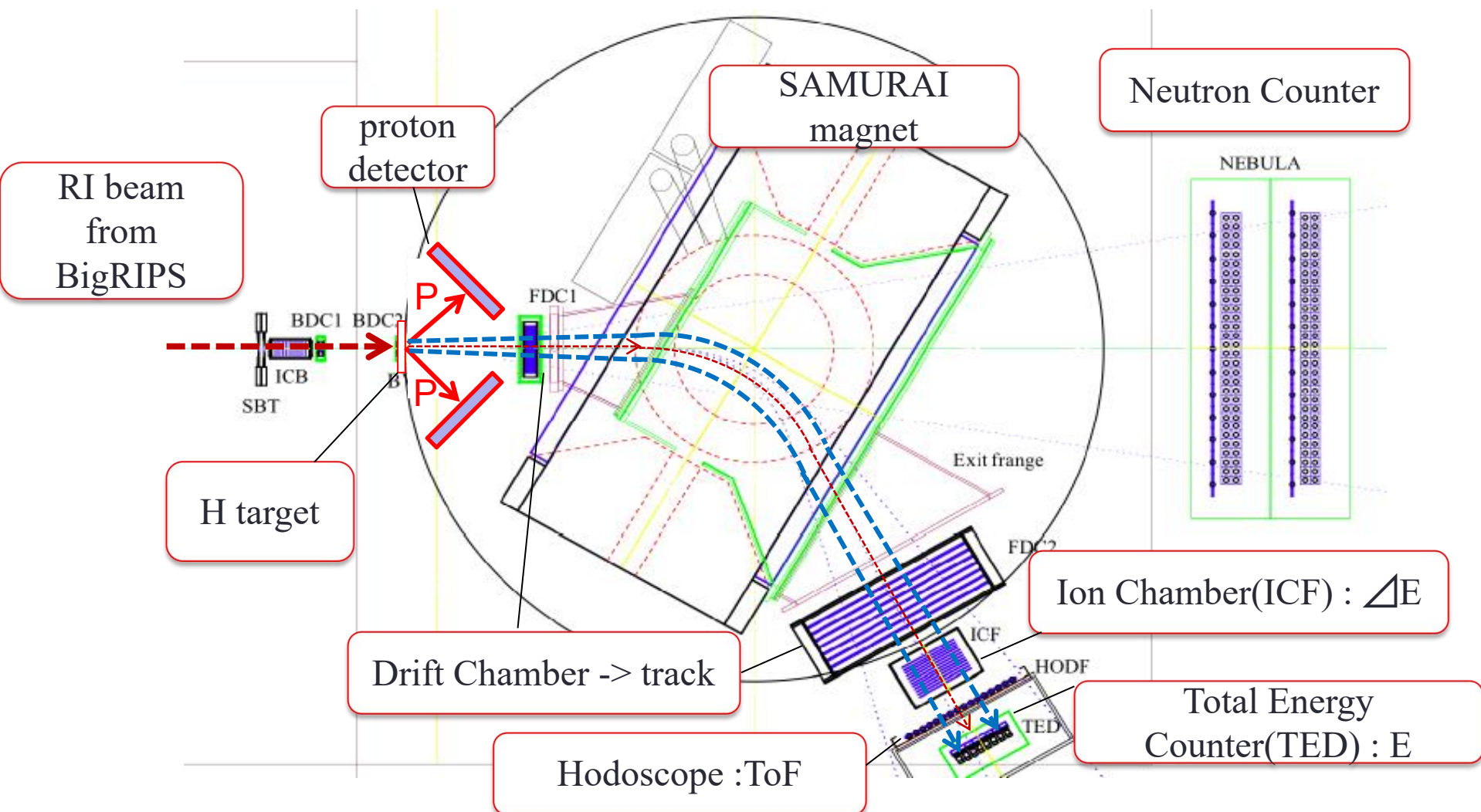


- proton knockout ($p, 2p$) reaction
 - cross section : large
 - high momentum transfer, large acceptance for forward-focused FF's
 - 2 proton measurement -> **low background**
- **Excitation energy is directly deduced even-by-even (!) by missing mass spectroscopy (recall, with Coulom, $E^* \approx 12$ MeV, fixed)**

SAMURAI (Superconducting Analyser for Multi-particles from Radio Isotope beams)



Method: Inverse kinematics with ($p, 2p$ -fission) reaction

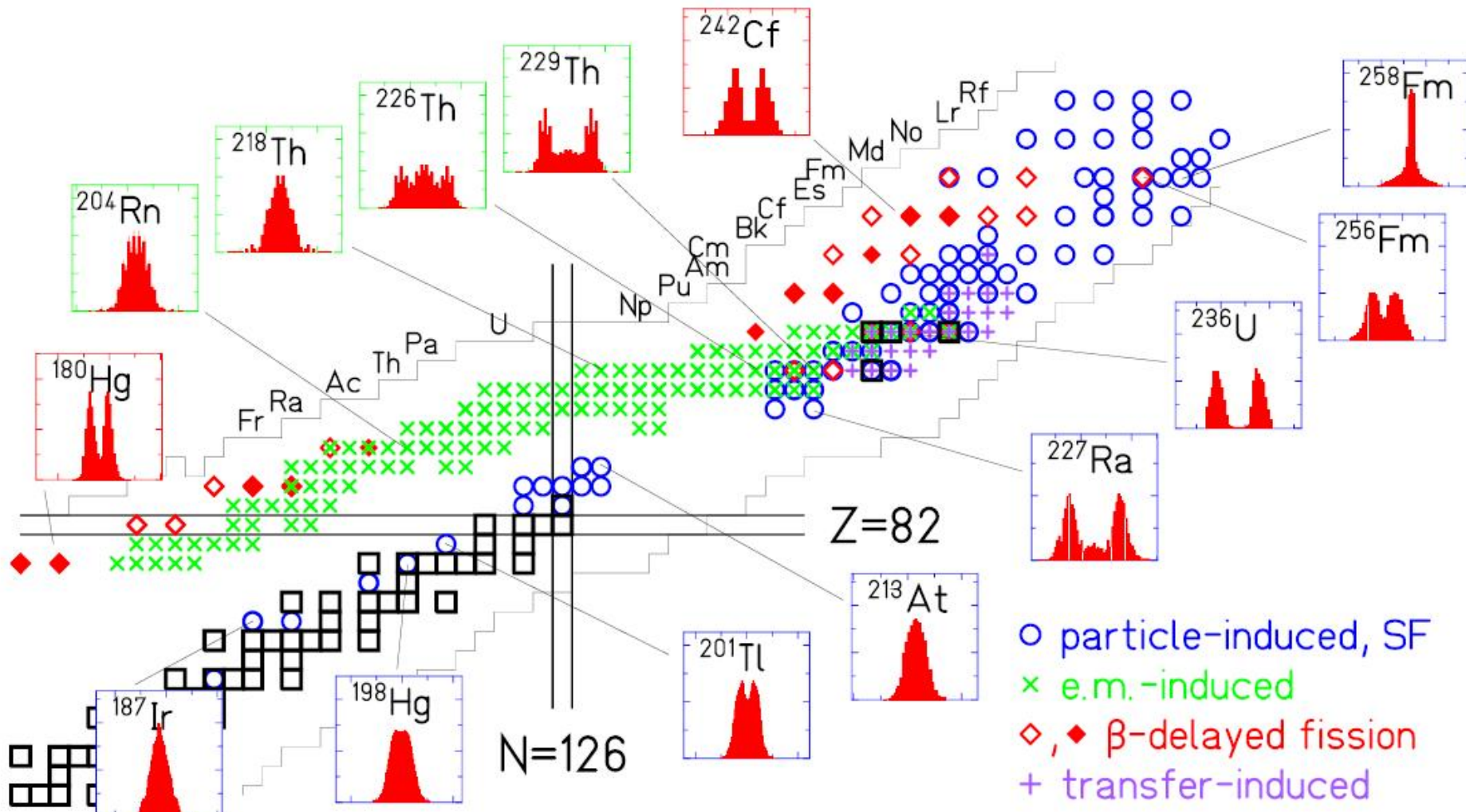


Charge(Z) and Mass(A) can be separated by $Bp - \Delta E - ToF(E)$

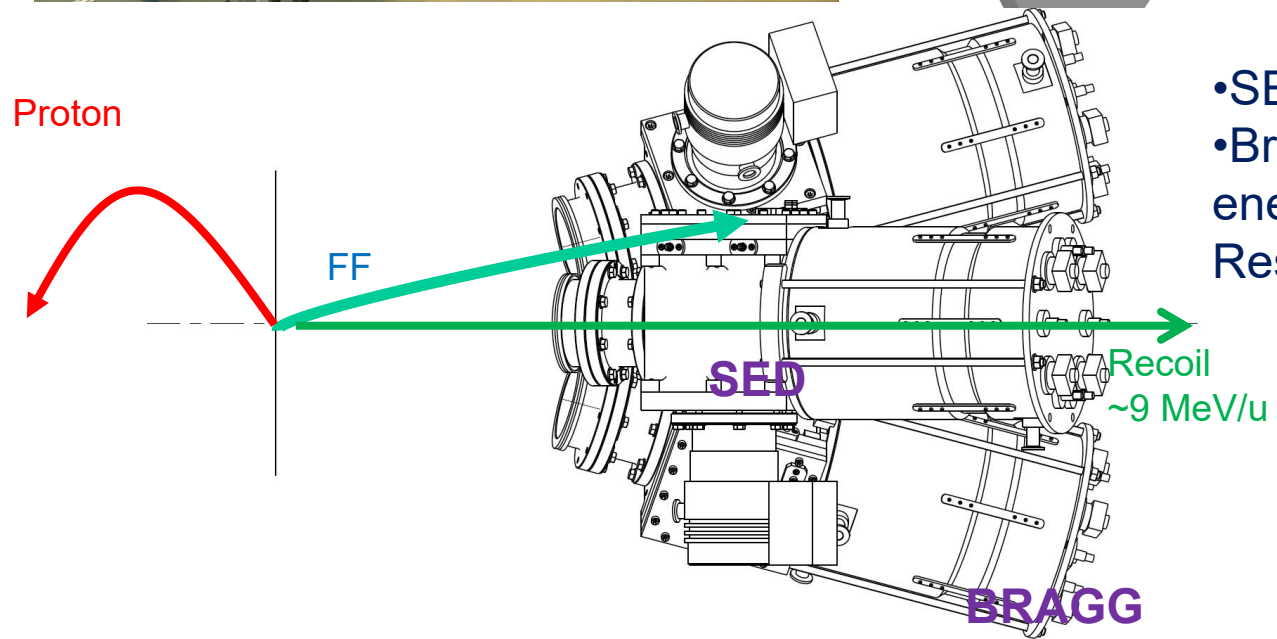
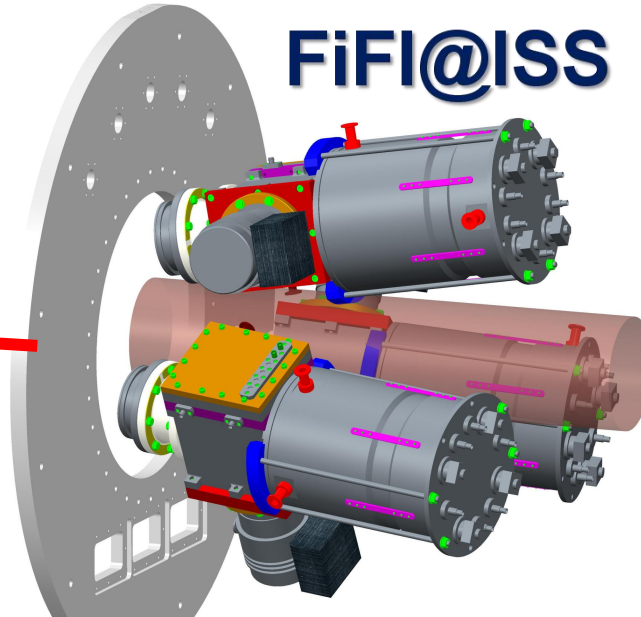
SAMURAI: Fragment Counters



Summary: Present Status of Fission Mass/Charge distribution measurements



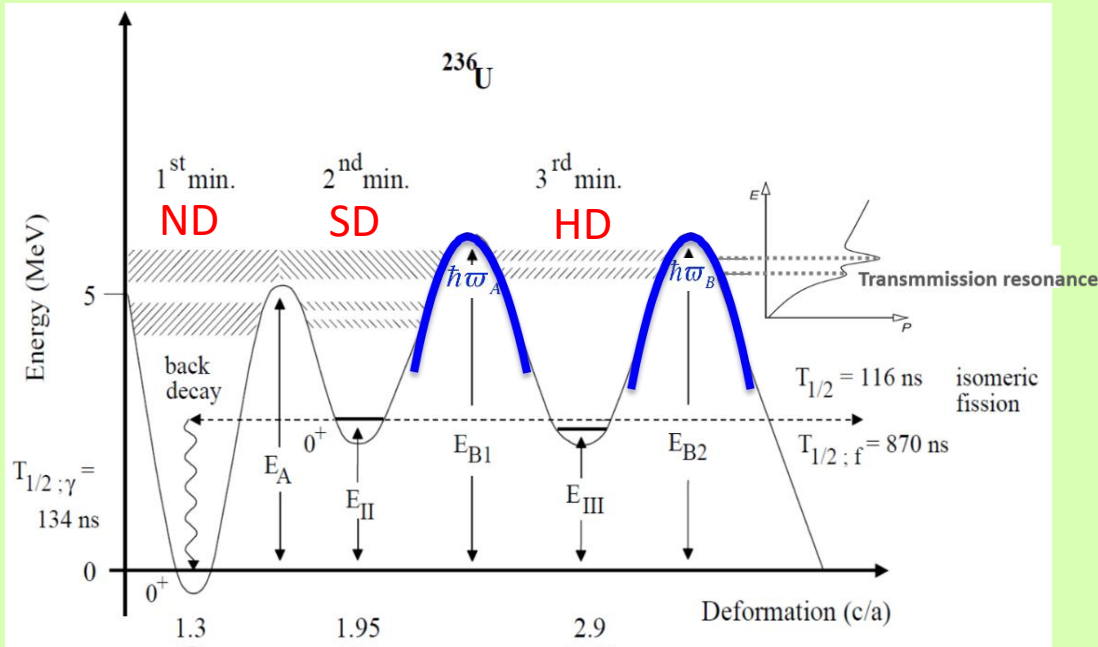
Fission-Fragment Detectors for ISS@ISOLDE



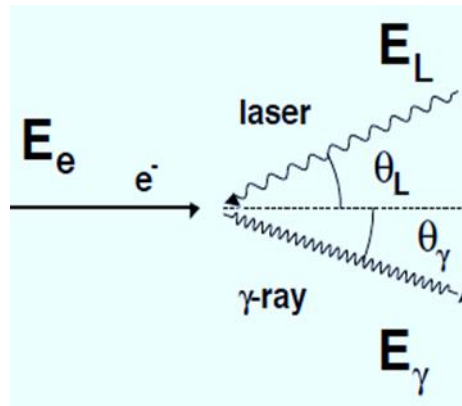
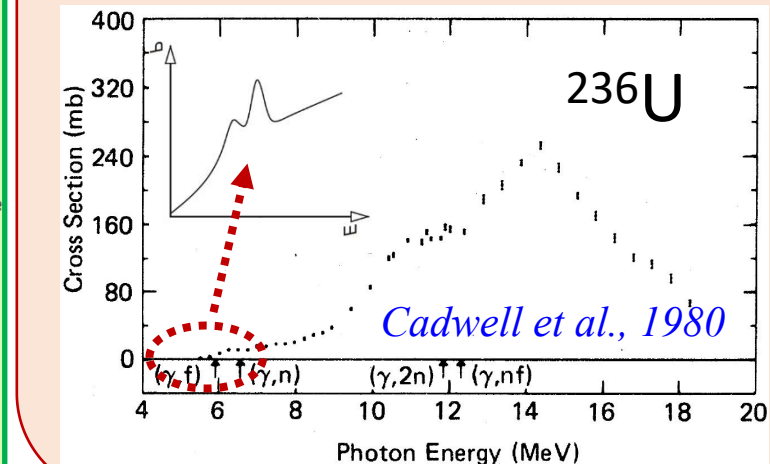
- SED MCP for ns FF timing
- Bragg ion chamber for FF energy measurement (~1MeV Resolution)

Fission studies with CBS brilliant gamma beams at ELI-NP

✓ The potential energy landscape



✓ Fission cross-section

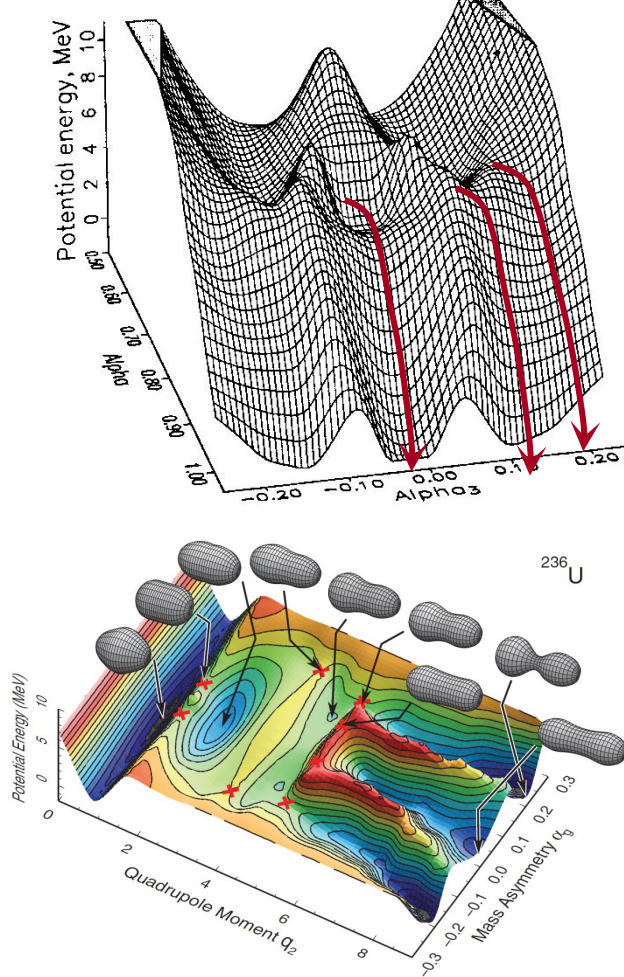
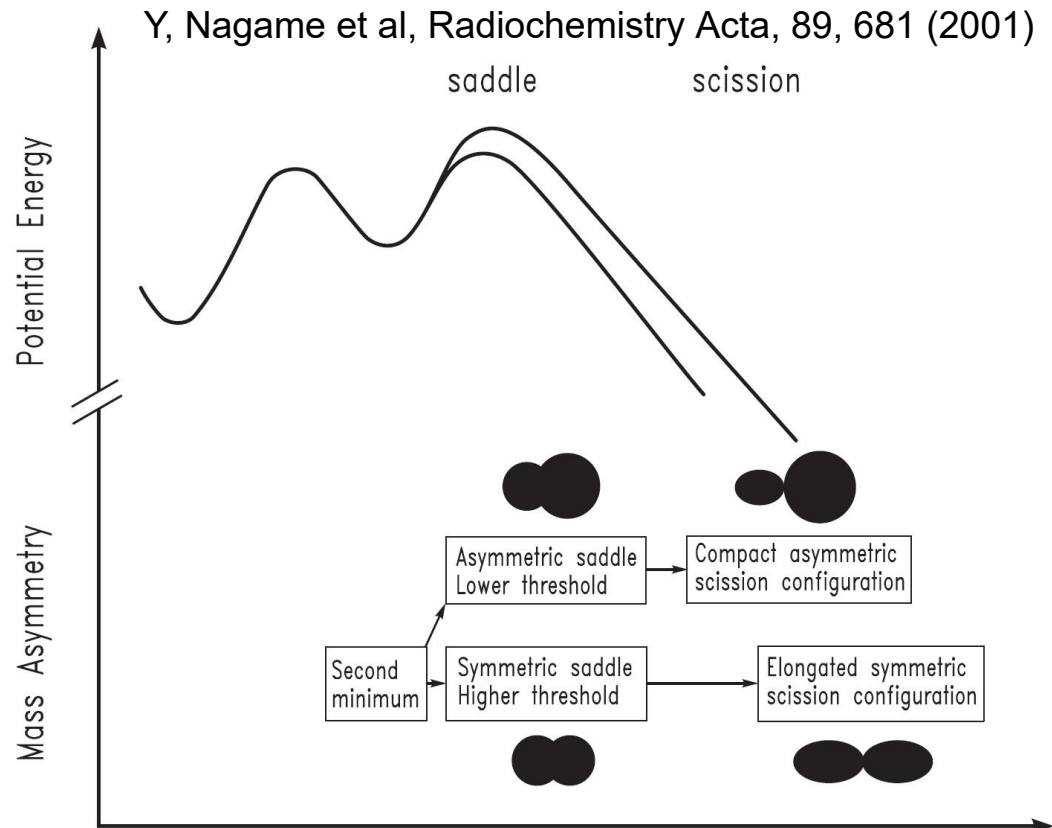


Compton Backscattering

First experiment - 2020(?): fission of neutron-rich Bi, Po and At nuclides

- Separated RIBs : ^{210}Bi (300 pps)
 ^{213}Po (270 pps)
 ^{219}At (130 pps)
- Estimation
- $N=1.1 \times 10^7$ fragment events per day for ^{218}Po
- $(p,2p)$ cross section ~ 100 ub/MeV at 1g/cm^2 H_2 target
-> $5*10^2$ events/day \cdot MeV

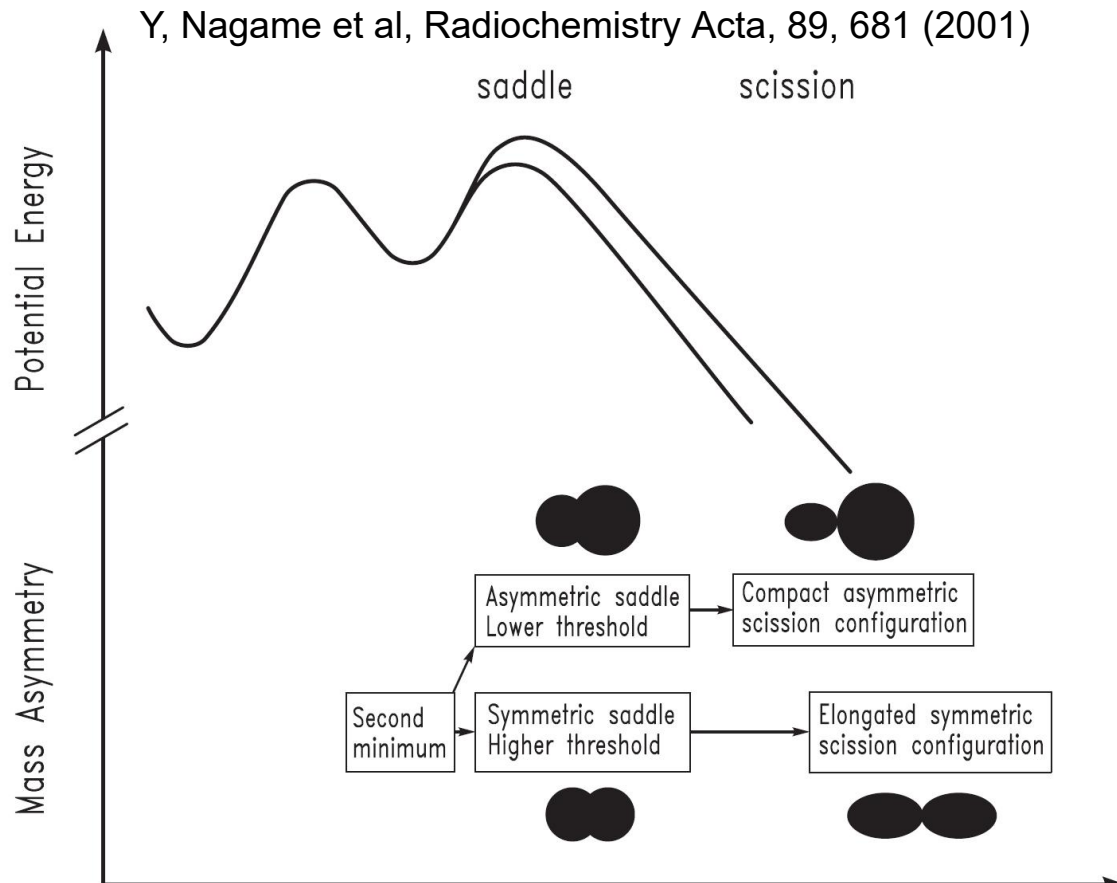
Multi-modal fission: competition between several modes



Each fission mode:

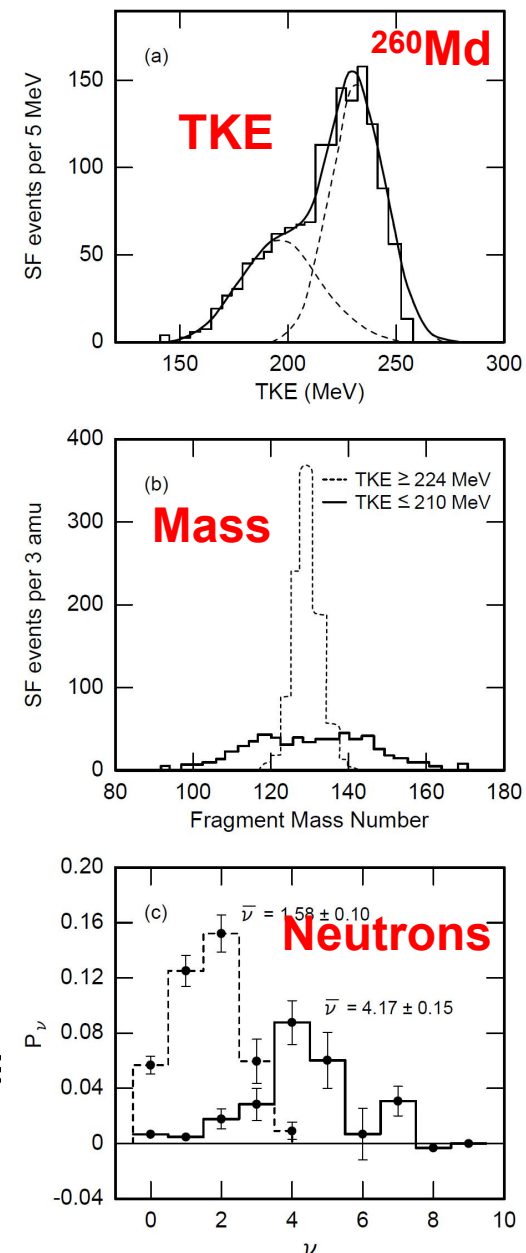
- proper path in the PES: **different mass distributions**
- different shell effects along the paths
- different scission configurations/deformations: **different TKE**

Multi-modal fission: competition between several modes



Evidenced by e.g.

- Skewed TKE distributions (two components)
- Complex (sometimes 3-peaks) FF's mass distributions
- Neutron multiplicities



Fission and r-process: influence of the fission mass distributions modelling

IOP Publishing

Rep. Prog. Phys. 80 (2017) 084901 (16pp)

Report on Progress

Impact of new data for neutron-rich nuclei on theoretical models of nucleosynthesis

Toshitaka Kajino^{1,2,3} and Grant J Mathews^{1,4}

¹ International Research Center for Big-Bang Cosmology and Element Genesis and Nuclear Energy Engineering, Beihang University, Beijing 100191, People's Republic of China

² Division of Theoretical Astronomy, National Astronomical Observatory of Japan, Mitaka, Tokyo, 181-8588, Japan

³ Department of Astronomy, Graduate School of Science, The University of Tokyo, Bunkyo-ku, Tokyo, 113-033, Japan

⁴ Center for Astrophysics, Department of Physics, University of Notre Dame, United States of America

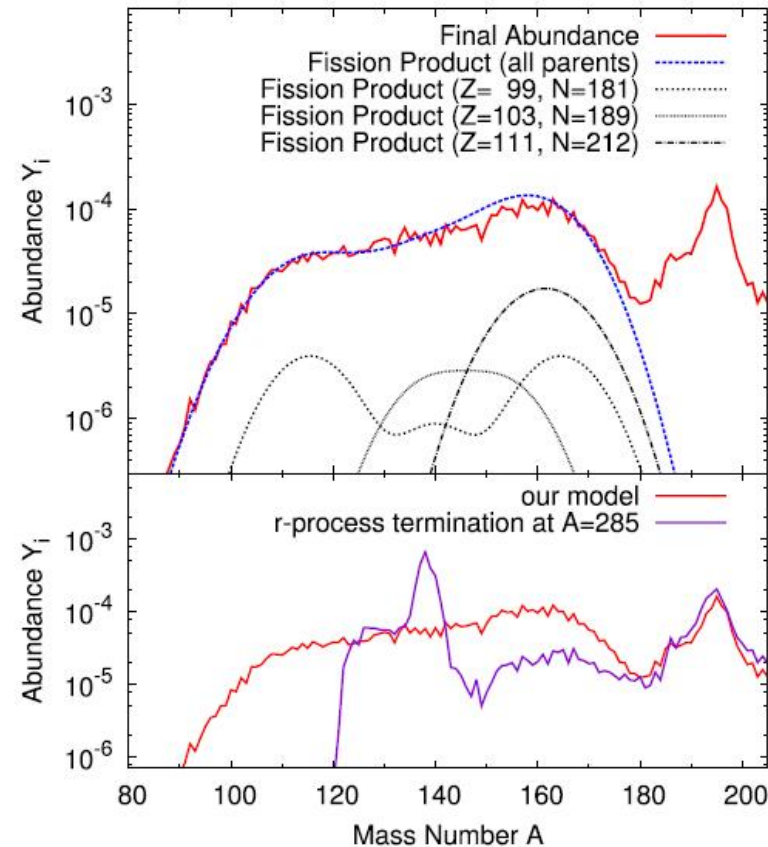
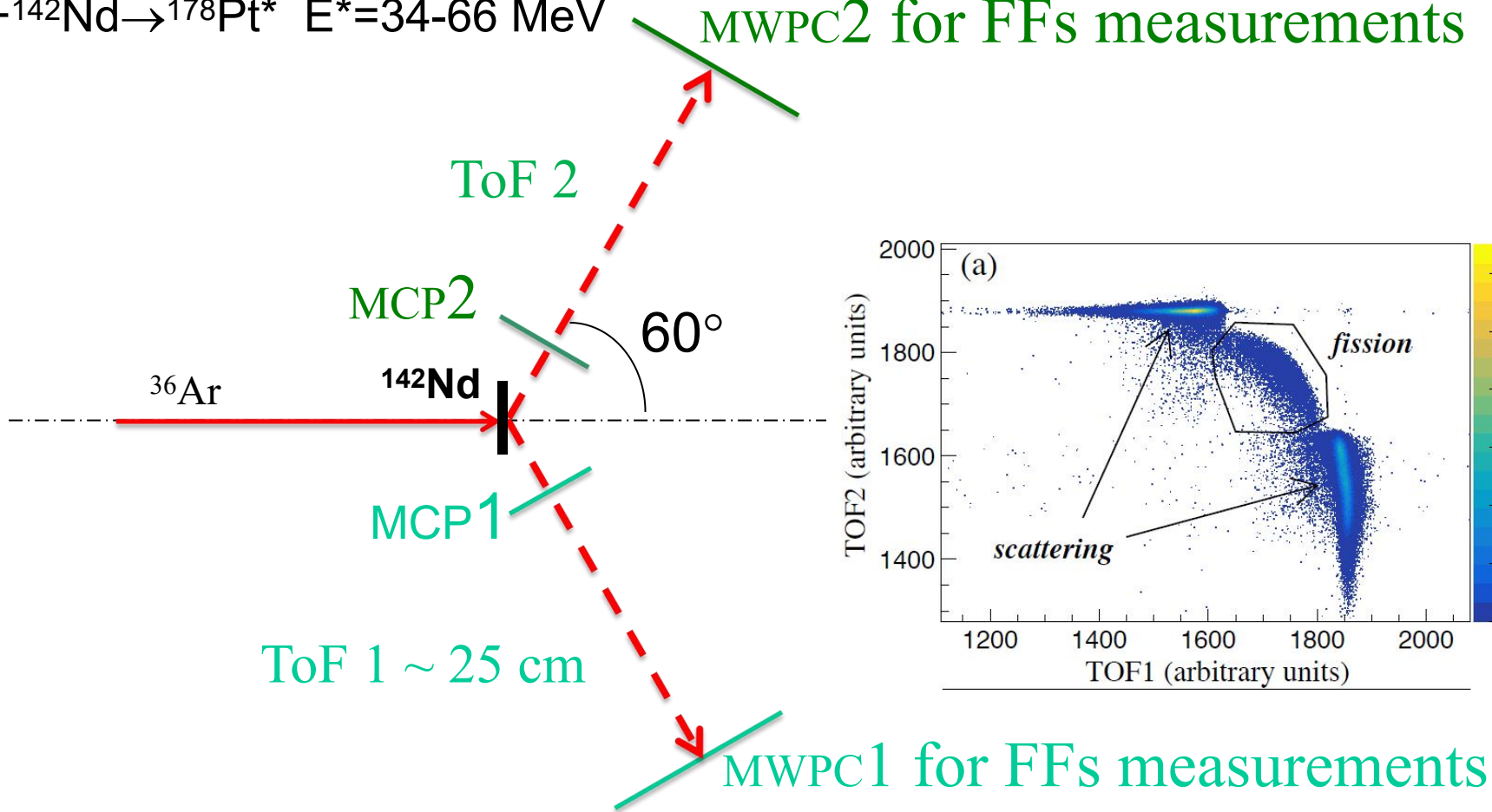


Figure 6. Illustration of the impact of fission yields and fission recycling on the final *r*-process abundances from Shibagaki *et al* (2016). Upper panel shows the relative contributions for 3 representative nuclei compared with the final abundance distribution. The lower panel shows the same final *r*-process yields compared with the distribution that would result if the termination of the *r*-process path were to occur at $A = 285$. Reproduced from Shibagaki *et al* (2016). © IOP Publishing Ltd. All rights reserved.

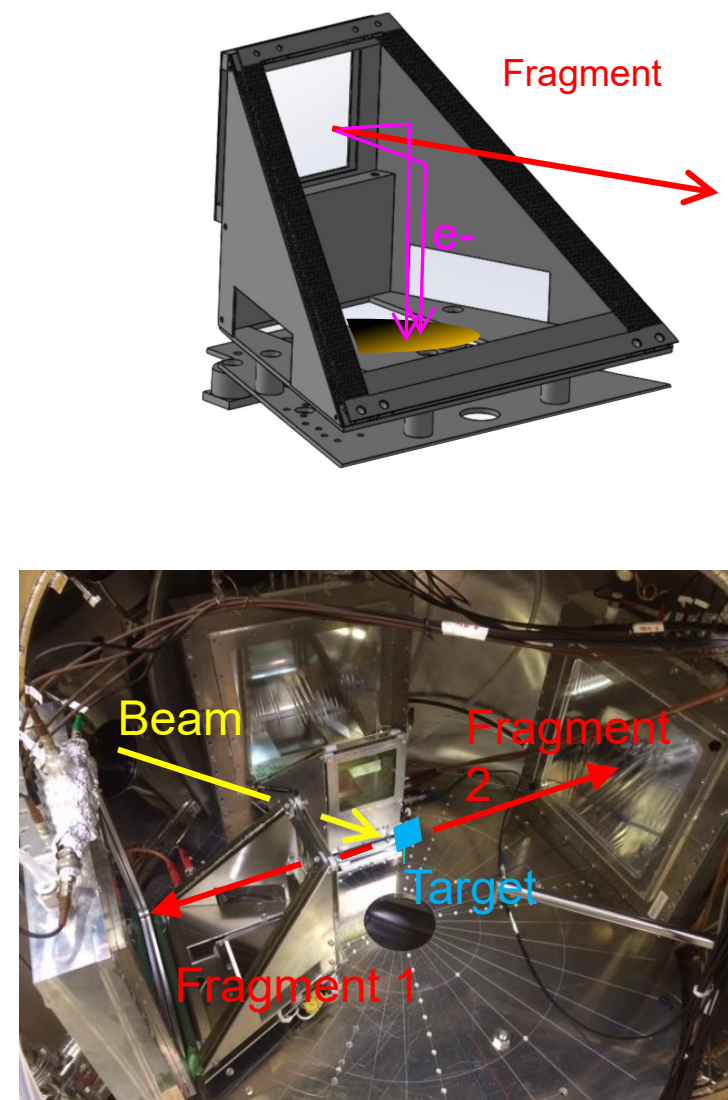
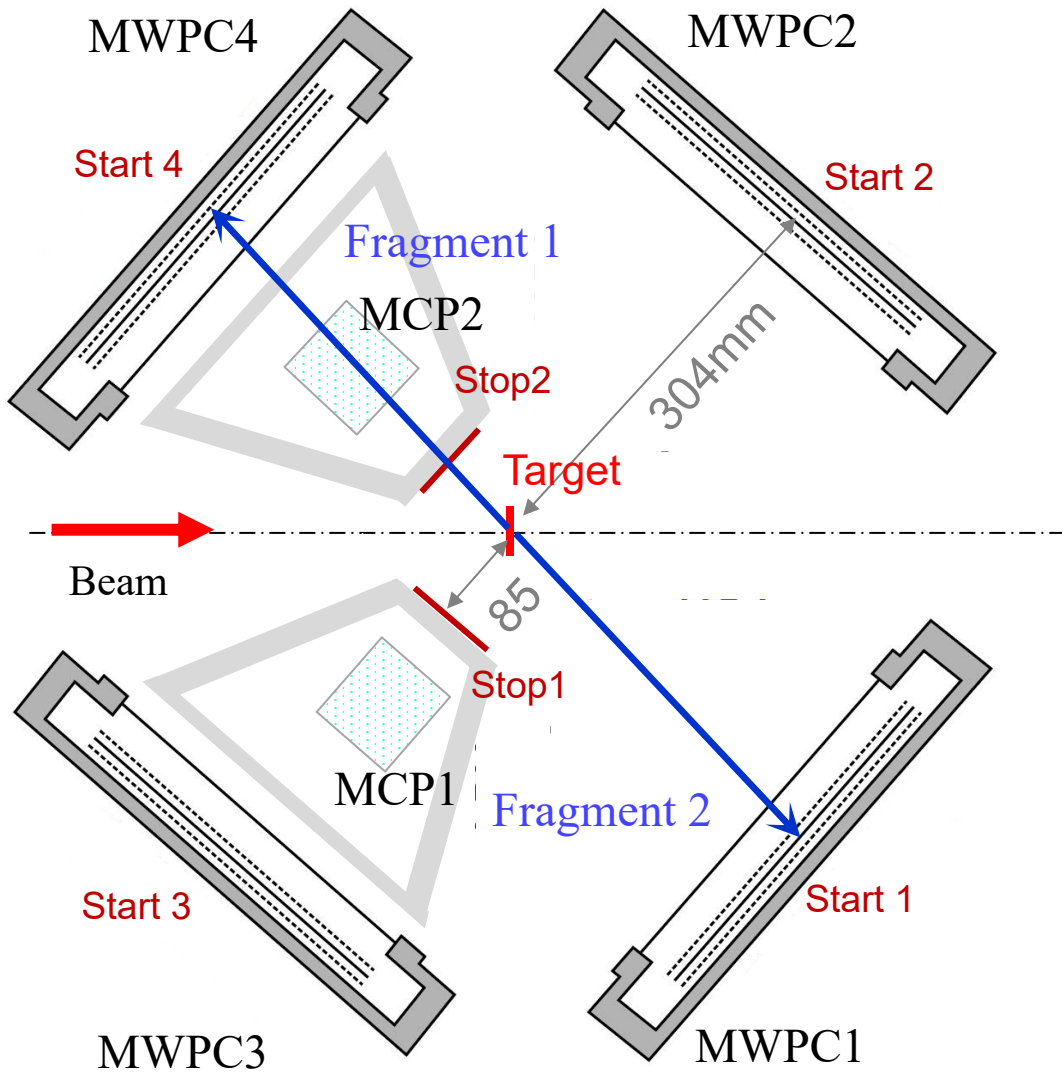
Fission of ^{178}Pt ($Z=78, N=100$): a factory to produce doubly-magic ^{100}Sn ($Z=N=50$) and ^{78}Ni ($Z=28, N=50$) in a single experiment? Fission experiments at the JAEA tandem

$^{36}\text{Ar} + ^{142}\text{Nd} \rightarrow ^{178}\text{Pt}^*$ $E^*=34\text{-}66 \text{ MeV}$

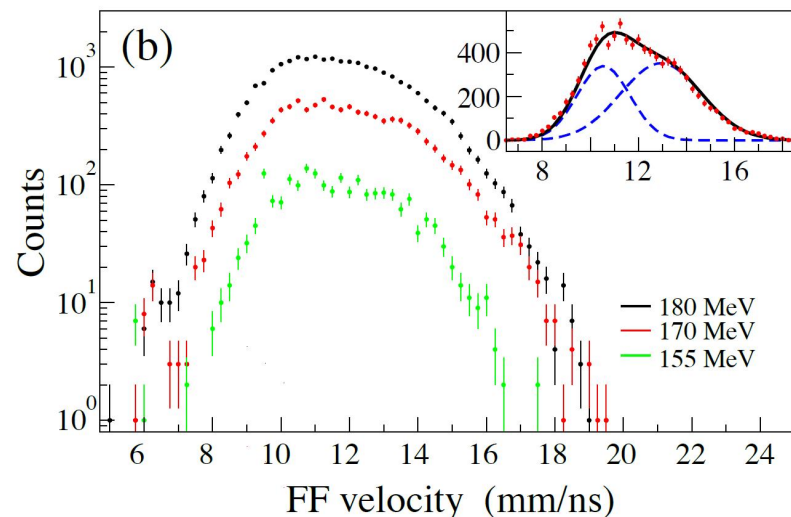


- Substantial improvement by using ToF detectors based on MCP (allows to measure velocities)
- In the next round – also neutron detectors

Fission setup at the JAEA tandem: 2 MCP ToF's + 4 MWPC's



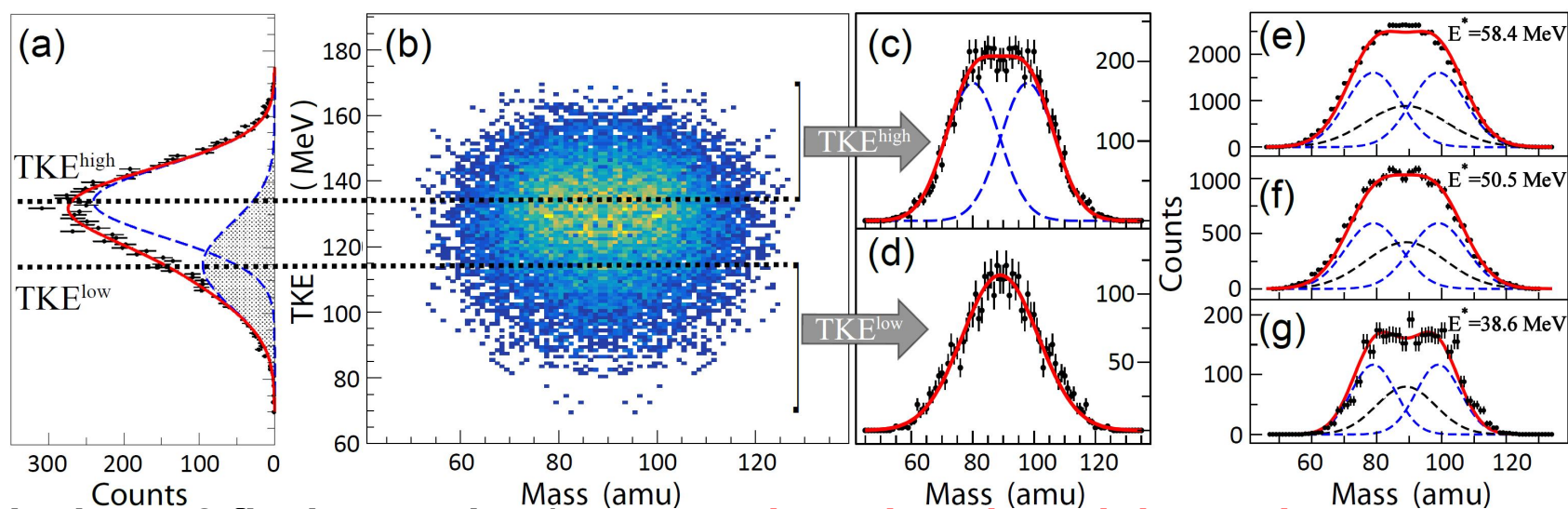
TKE vs Mass and FFs' Mass distributions for ^{178}Pt



a) Left-hand side plot: Fission fragments velocities.

Asymmetric distribution means that at least **an asymmetric fission modes contribute**

b) Bottom plot: Total Kinetic Energy vs Mass distributions. Asymmetry in TKE further confirms the presence of two modes



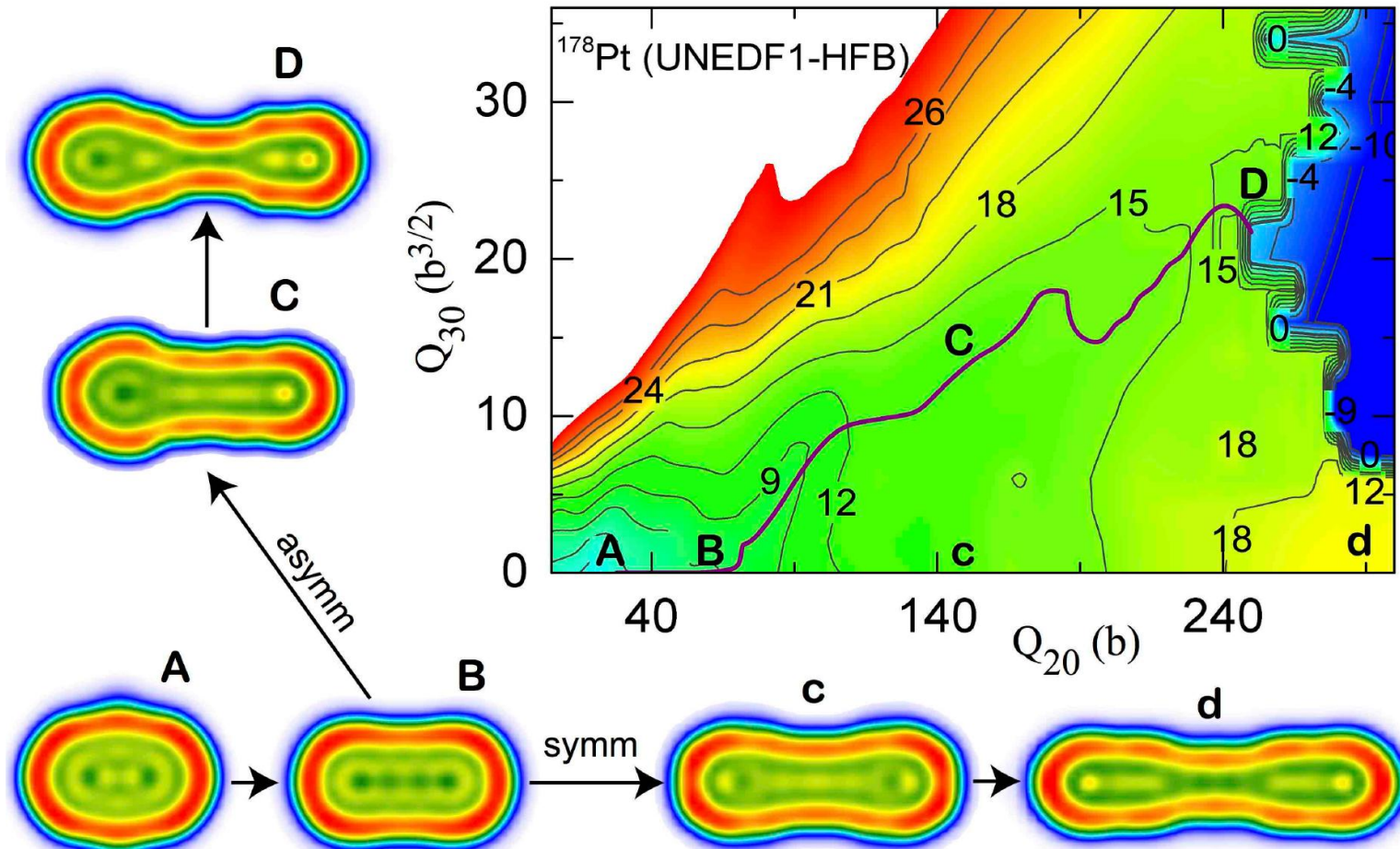
Conclusions: 2 fission modes (**pay attention – how broad the peaks are, mass resolution is ~ 3 u**)
 symmetric with $A_L = A_H = A_{\text{CN}}/2 = 89$

Asymmetric mode : $A_L = 79, A_H = 99$

Multimodal fission of ^{178}Pt

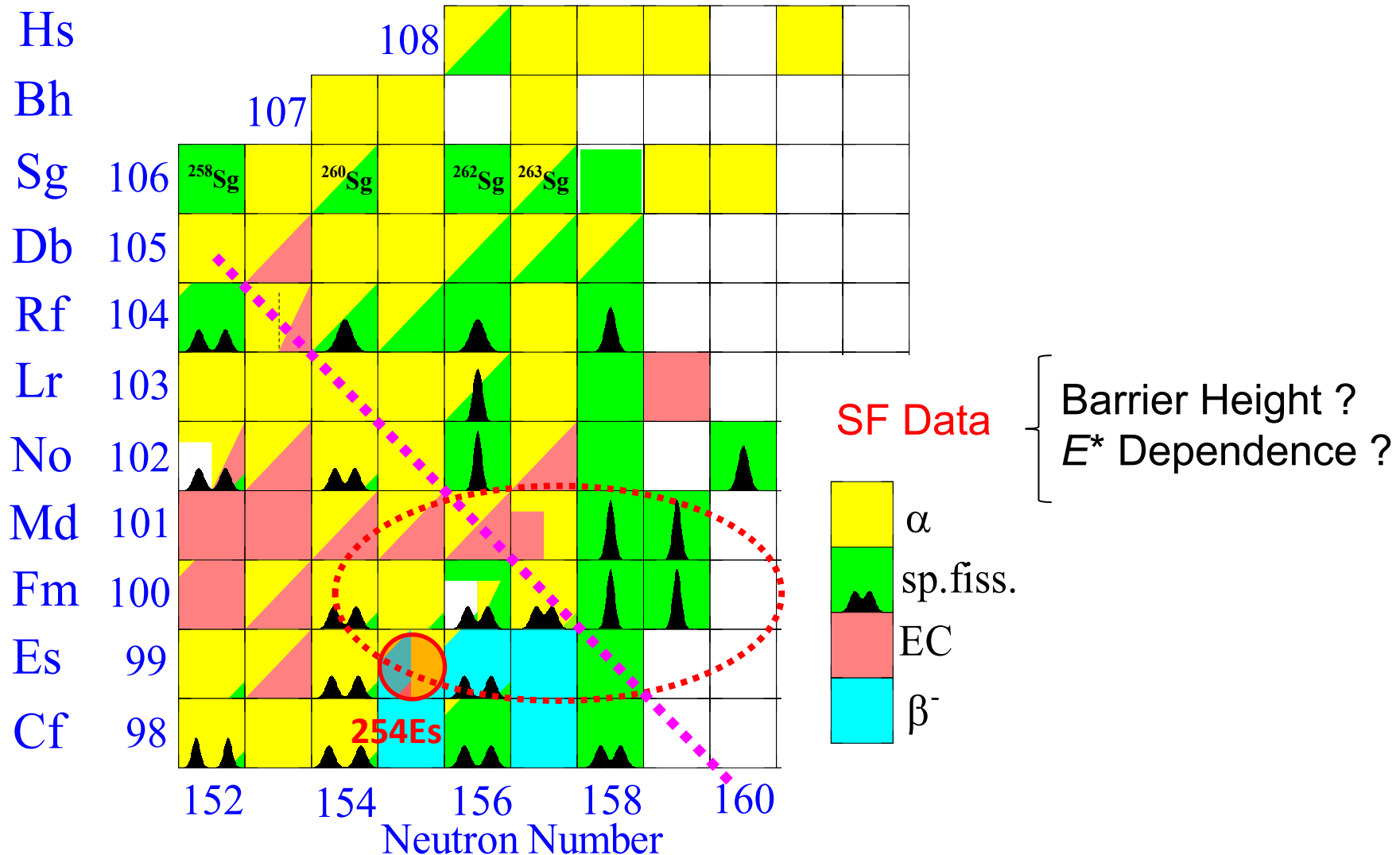
First observation of the competing fission modes in the sub-lead region

I. Tsekhanovich,¹ A.N. Andreyev,^{2,3} K. Nishio,³ D. Denis-Petit,⁴ K. Hirose,³ M. Makii,³ Z. Matheson,⁵ K. Morimoto,⁶ K. Morita,^{6,7} W. Nazarewicz,⁵ R. Orlandi,³ J. Sadhukhan,^{8,9} T. Tanaka,^{6,7} M. Vermeulen,³ and M. Warda¹⁰

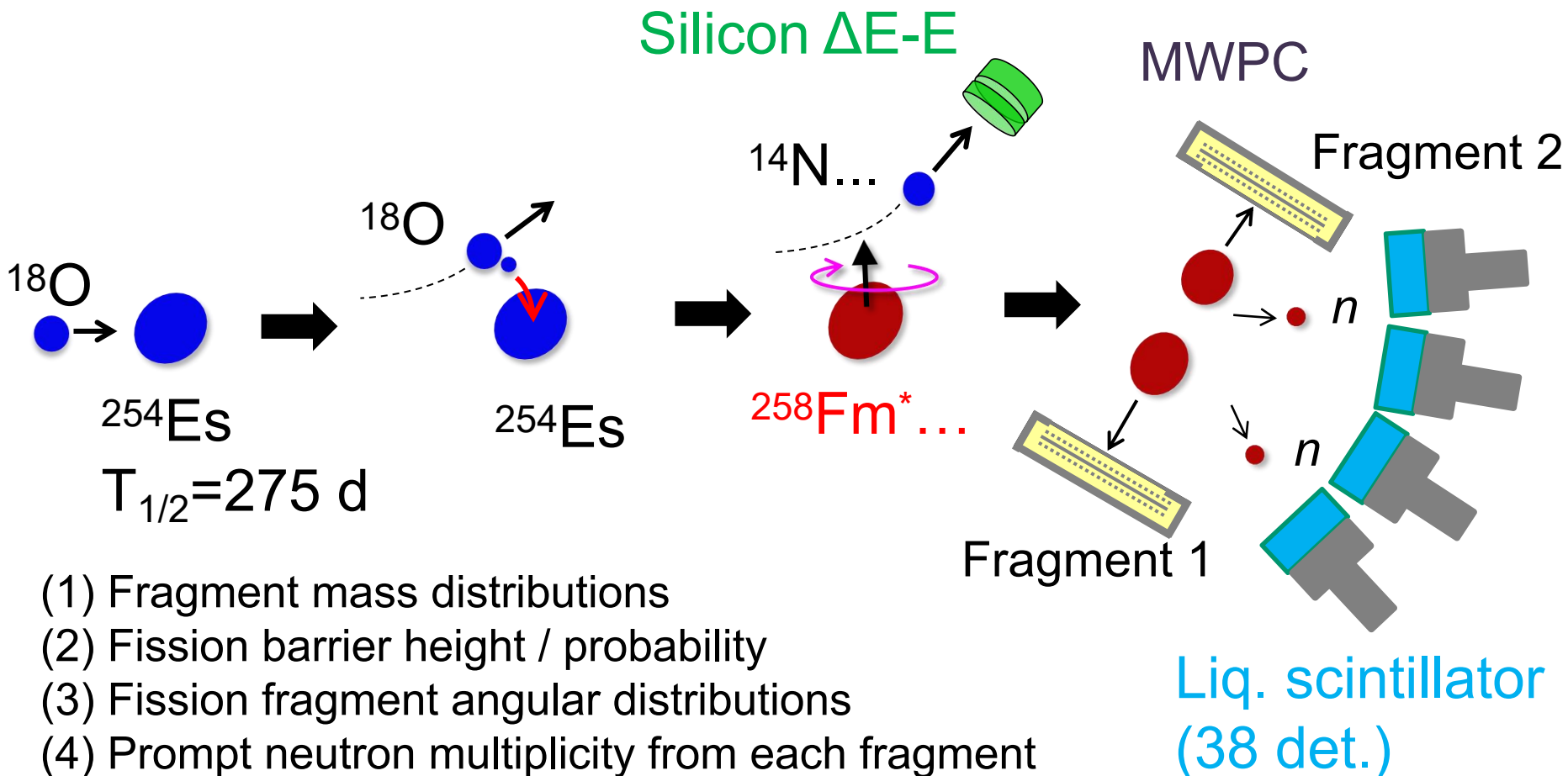


Strong collaboration with MSU (Michigan) and Polish Theory groups.

Transition from asymmetric to symmetric fission in heavy actinides (JAEA fission experiments)

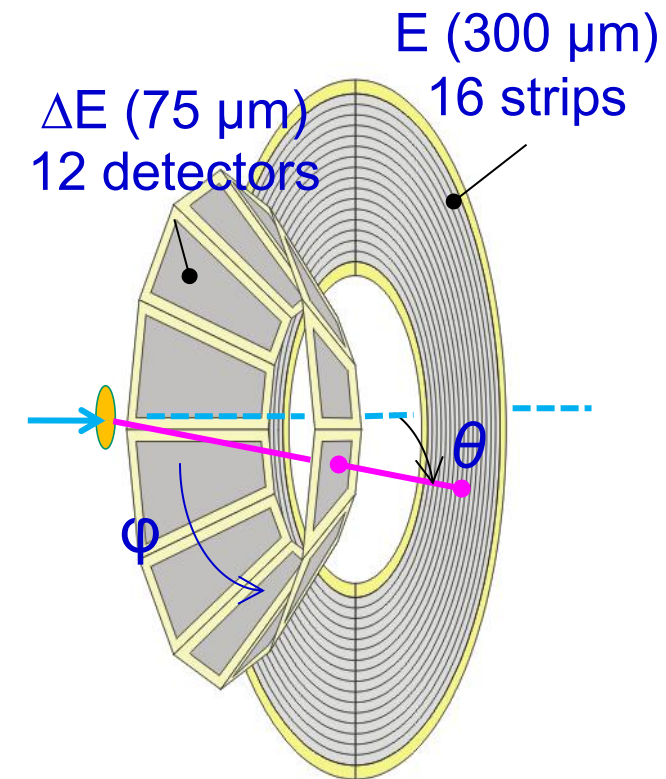
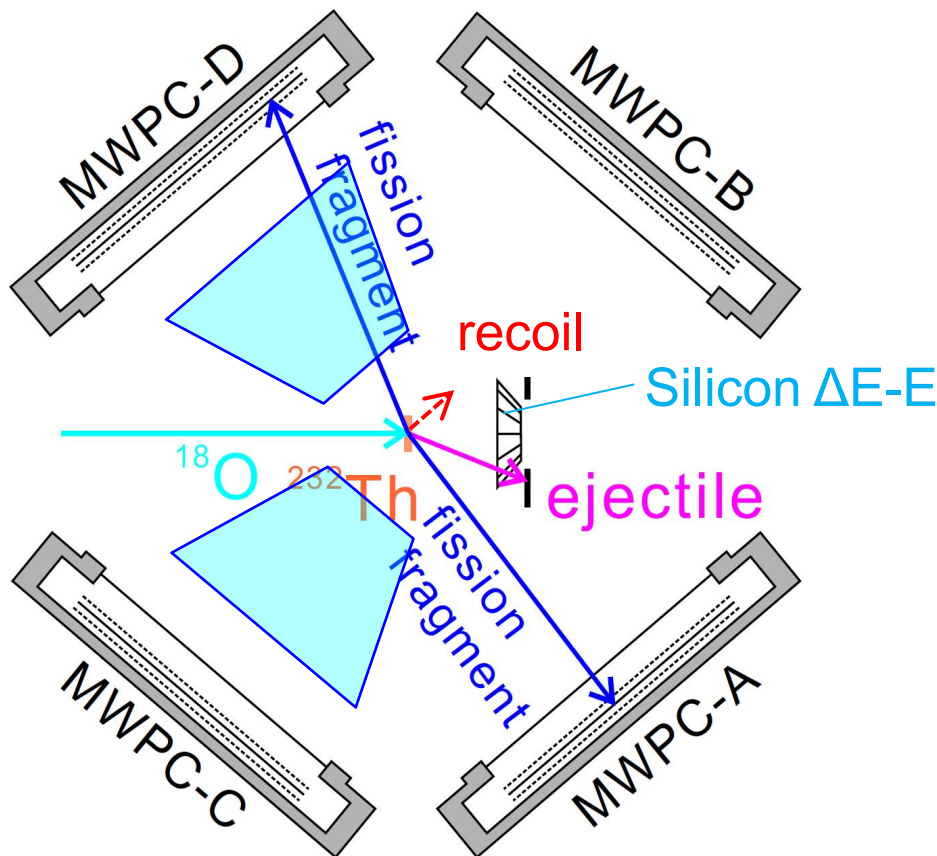


Multi-nucleon transfer (MNT) fission at JAEA(Tokai)



Measured and Planned experiments using ^{18}O beam and targets of ^{232}Th , ^{238}U , ^{248}Cm , ^{237}Np , ^{249}Cf , ^{243}Am , ^{231}Pa , ^{226}Ra , ^{254}Es

Experimental setup



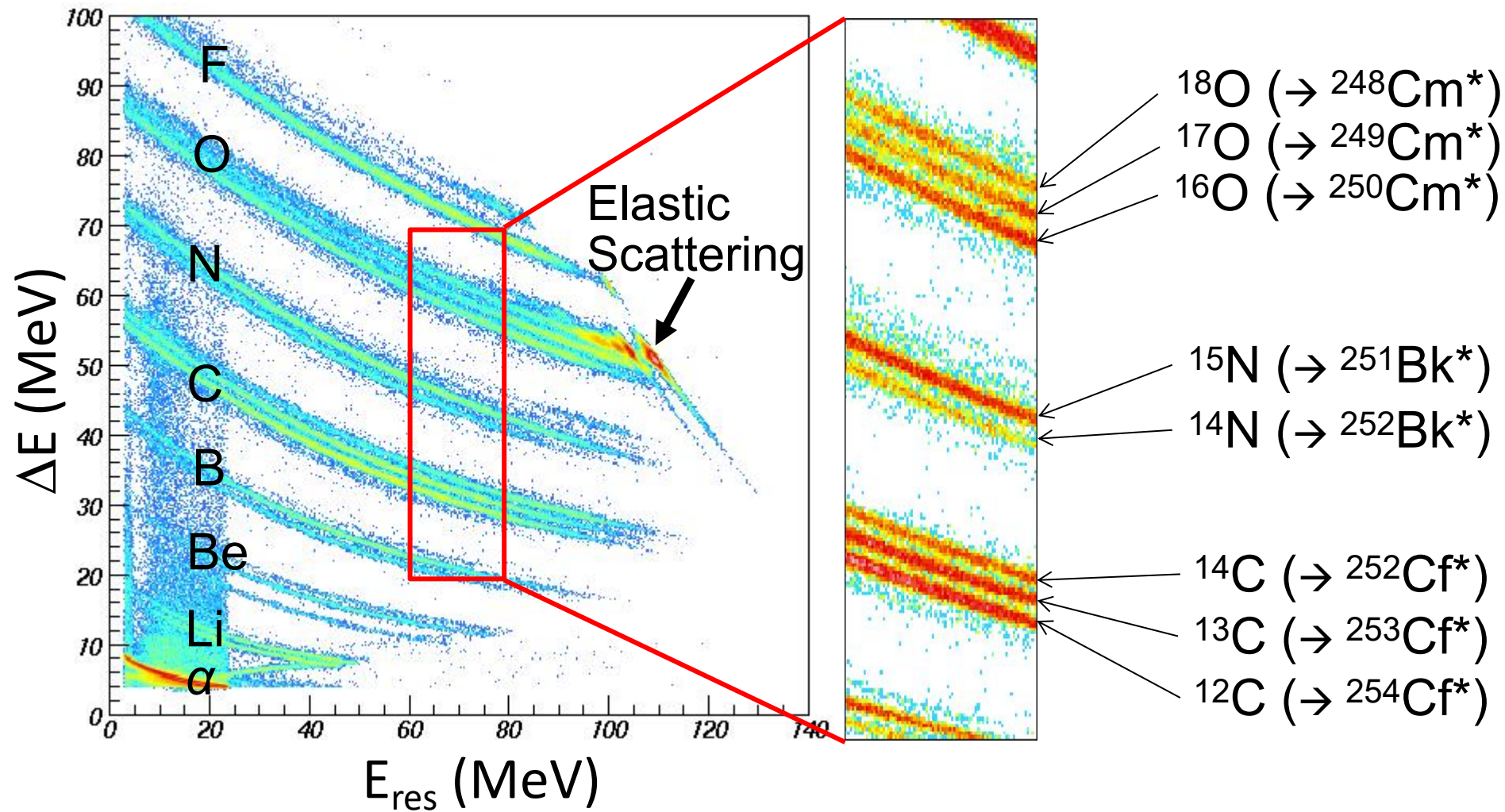
MCPs are added (T. Tanaka @ Kyushu univ./RIKEN)

START detector for the fragments.

→ TKE will also be obtained.

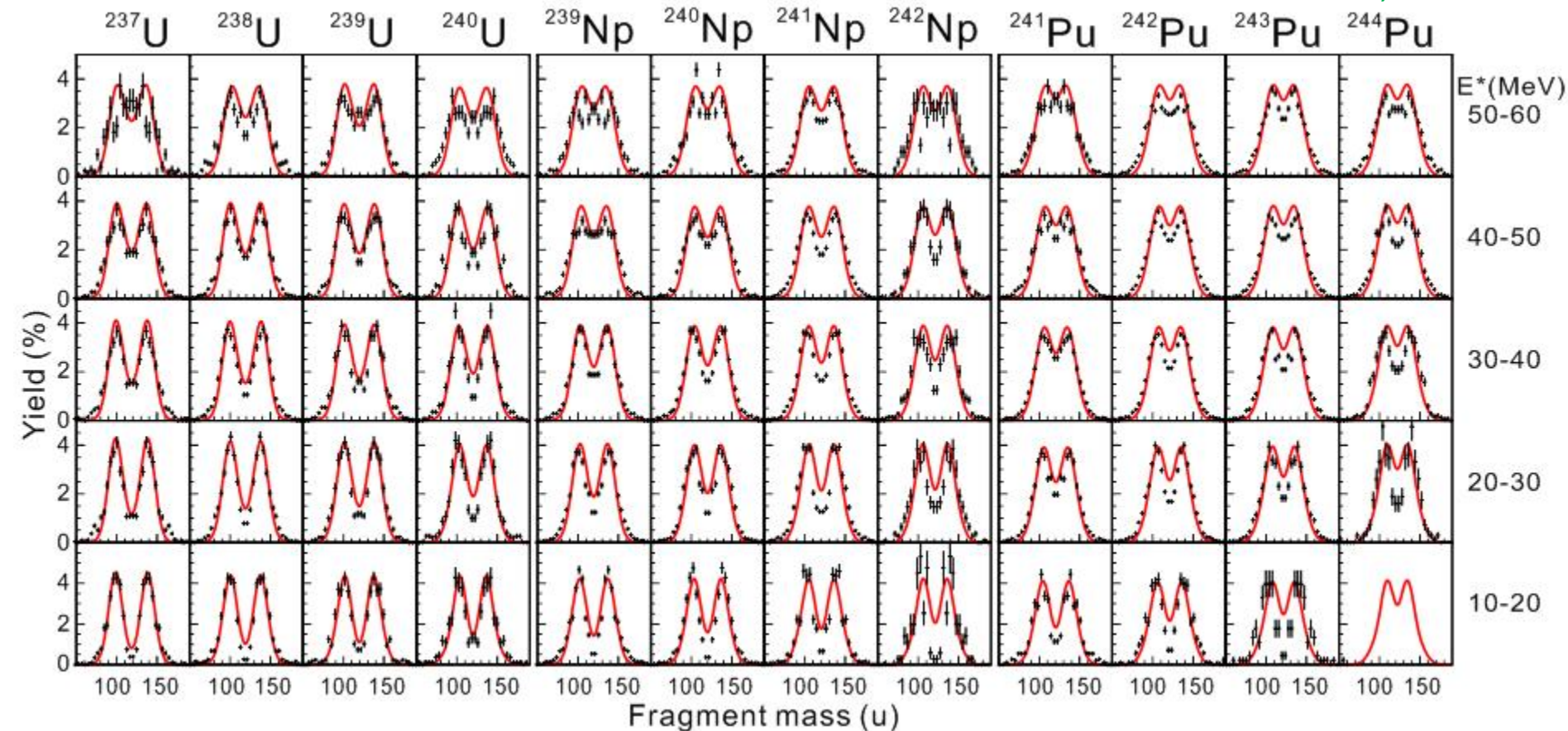
ΔE -E spectrum

$^{18}\text{O} + ^{248}\text{Cm}$ ($E_{\text{beam}} = 162\text{MeV}$)



Exp. and Calc. ($^{18}\text{O} + ^{238}\text{U}$)

Hirose et al. PRL, Nov 2017



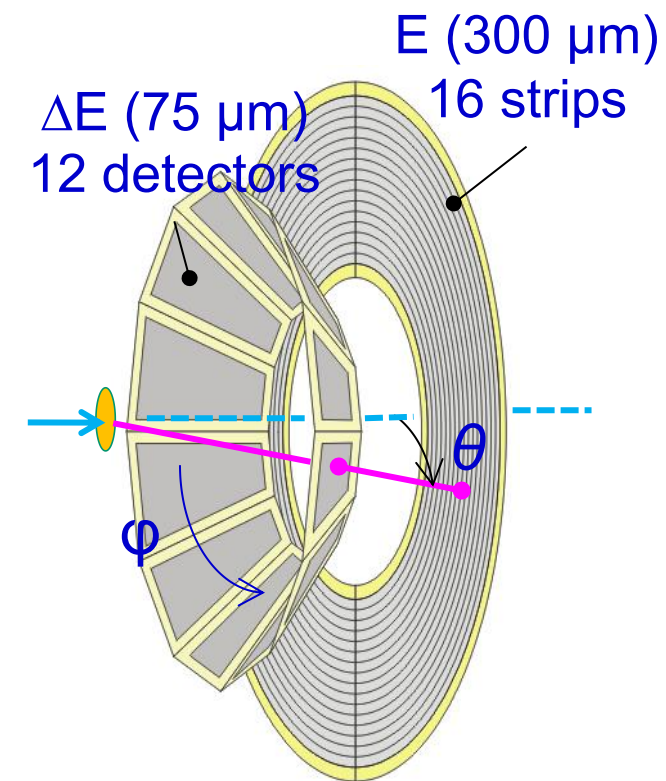
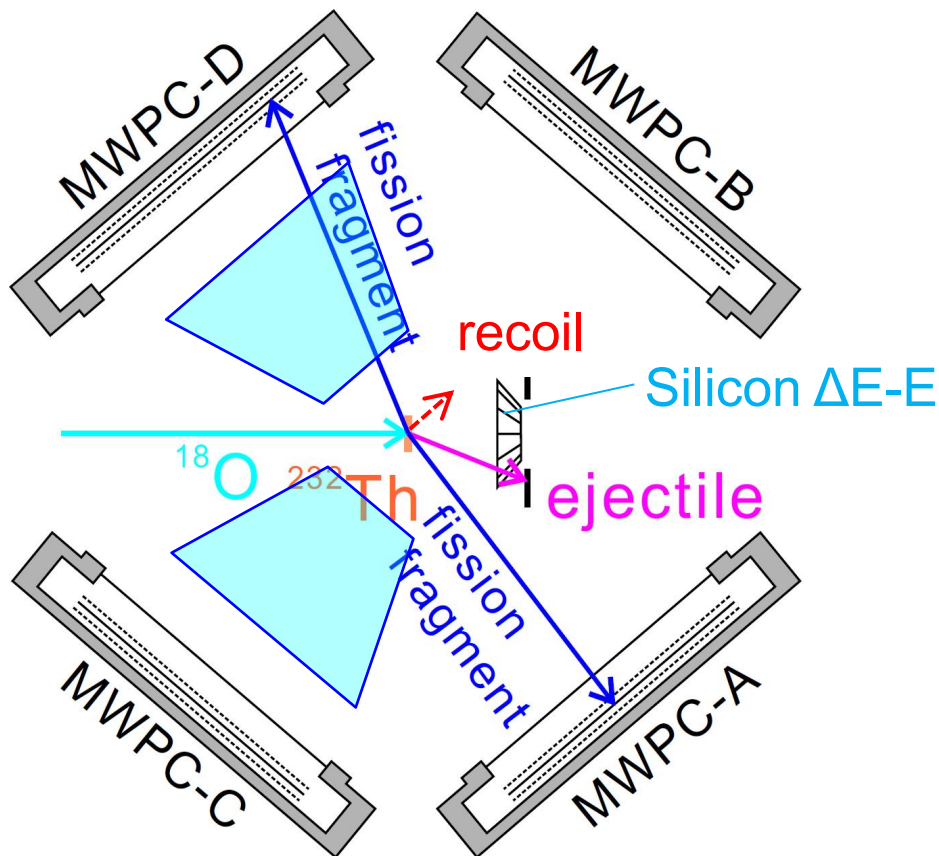
With multi-chance fission

The calculation well reproduces the experimental FFMD!

The asymmetric fissions observed in higher E_x is due to the multi-chance fission.

Note again the relatively poor FFs mass resolution ($\sim 3 \text{ u}$)

A Reminder: Experimental setup at JAEA



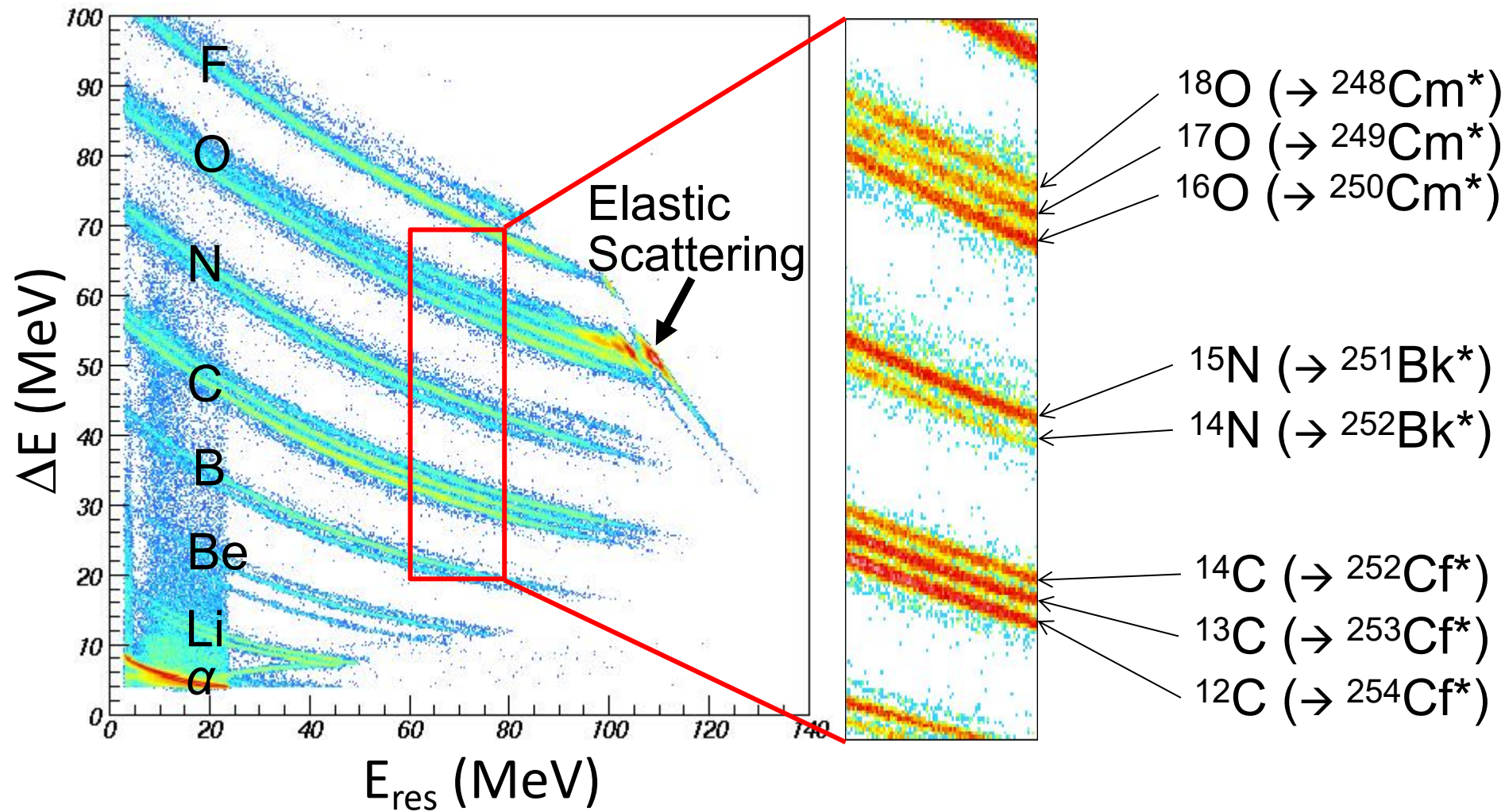
MCPs are added (T. Tanaka @ Kyushu univ./RIKEN)

START detector for the fragments.

→ TKE will also be obtained.

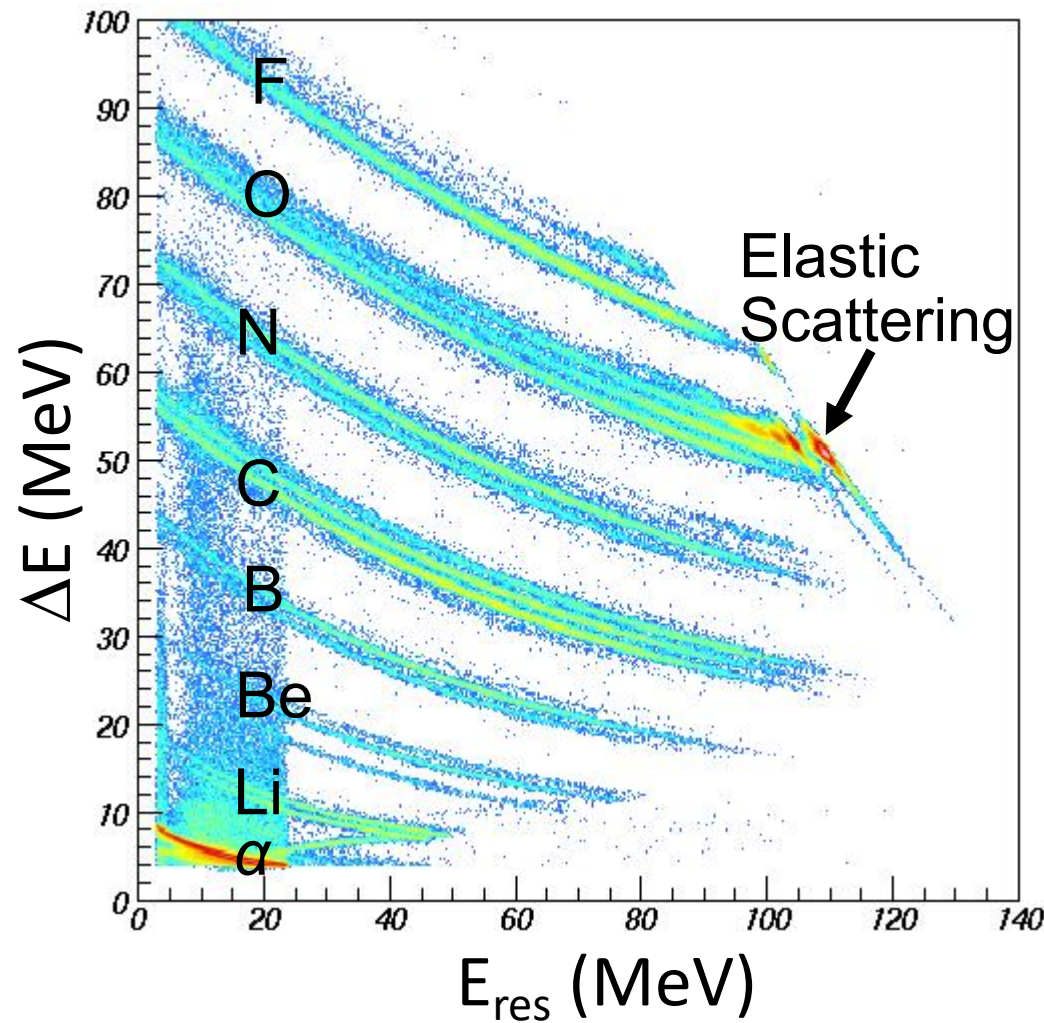
ΔE -E spectrum at JAEA

$^{18}\text{O} + ^{248}\text{Cm}$ ($E_{\text{beam}} = 162\text{MeV}$)

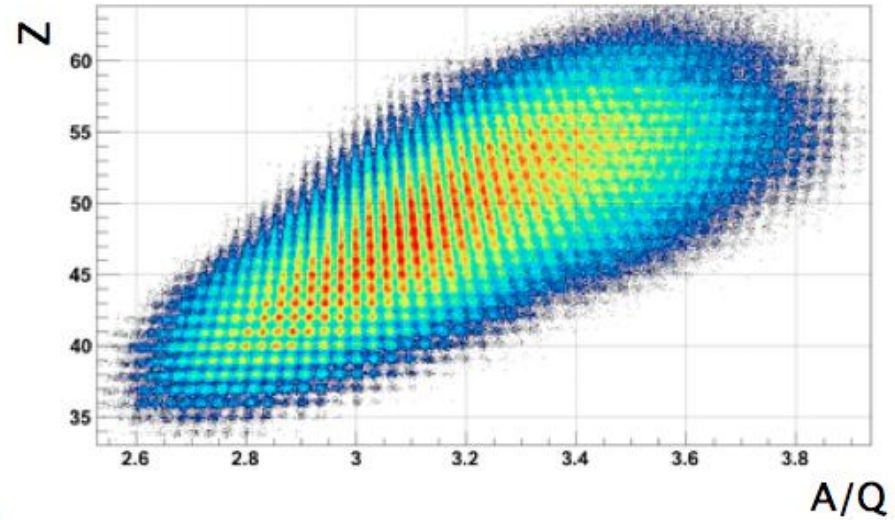
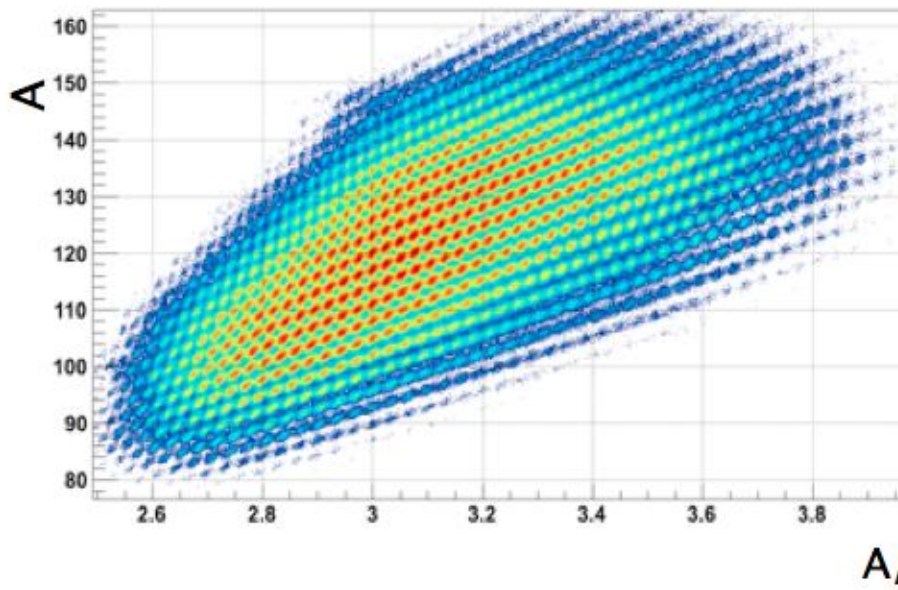
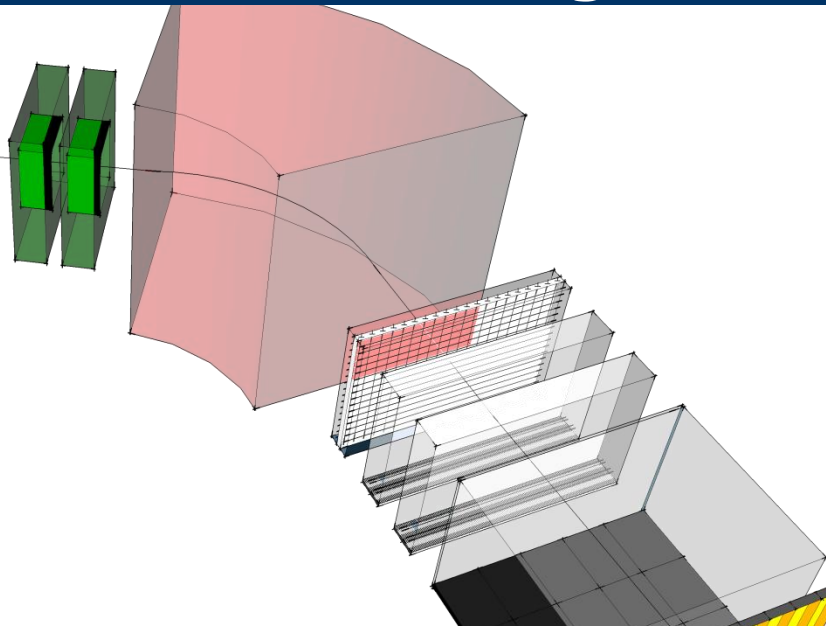
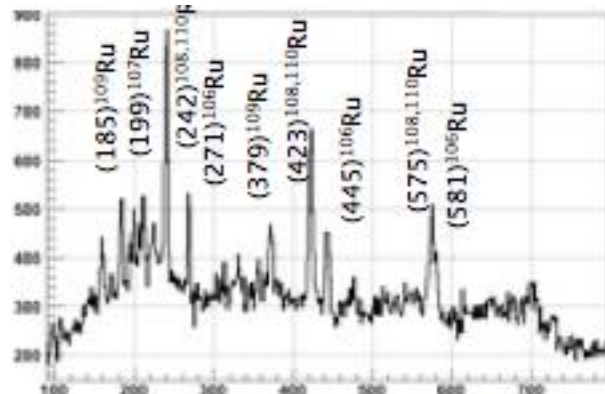
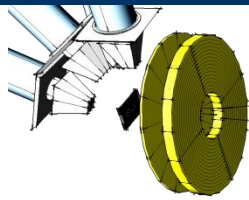


ΔE -E spectrum at JAEA

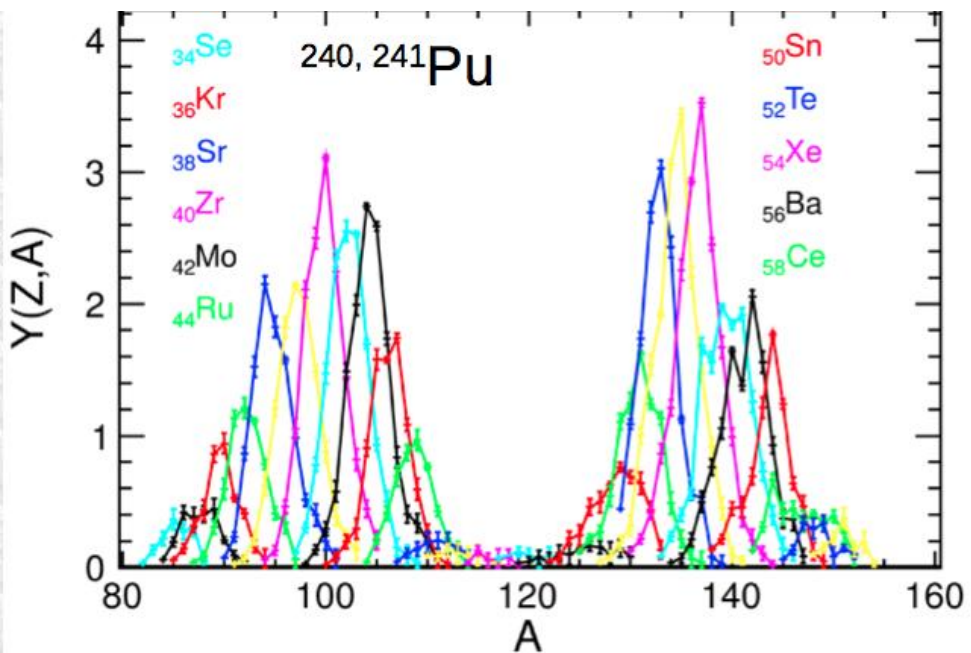
$^{18}\text{O} + ^{248}\text{Cm}$ ($E_{\text{beam}} = 162\text{MeV}$)



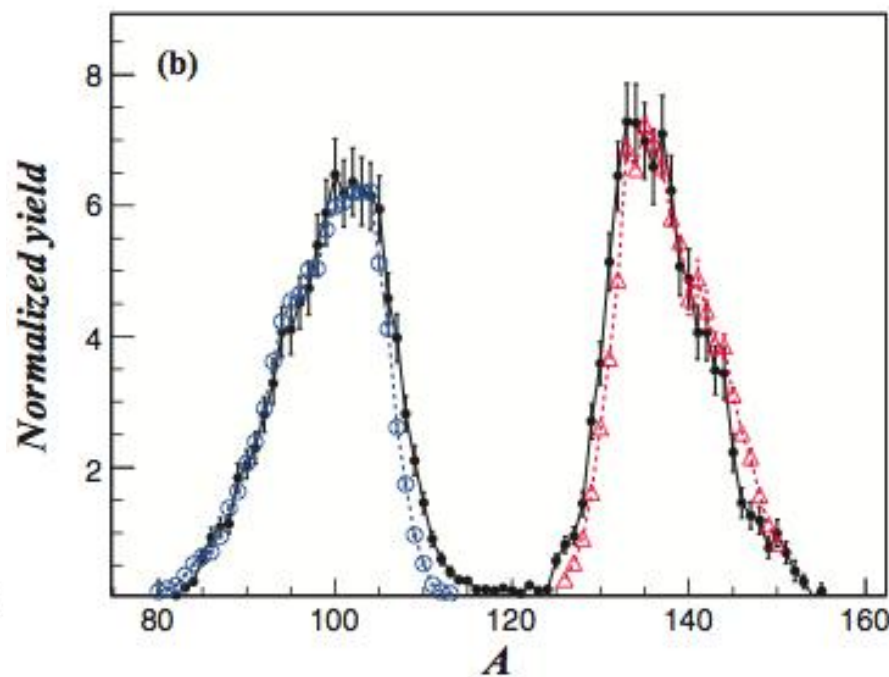
VAMOS magnet + Gas chamber for Z-A identification of fission fragments



Isotopic Distribution of Fission Fragments

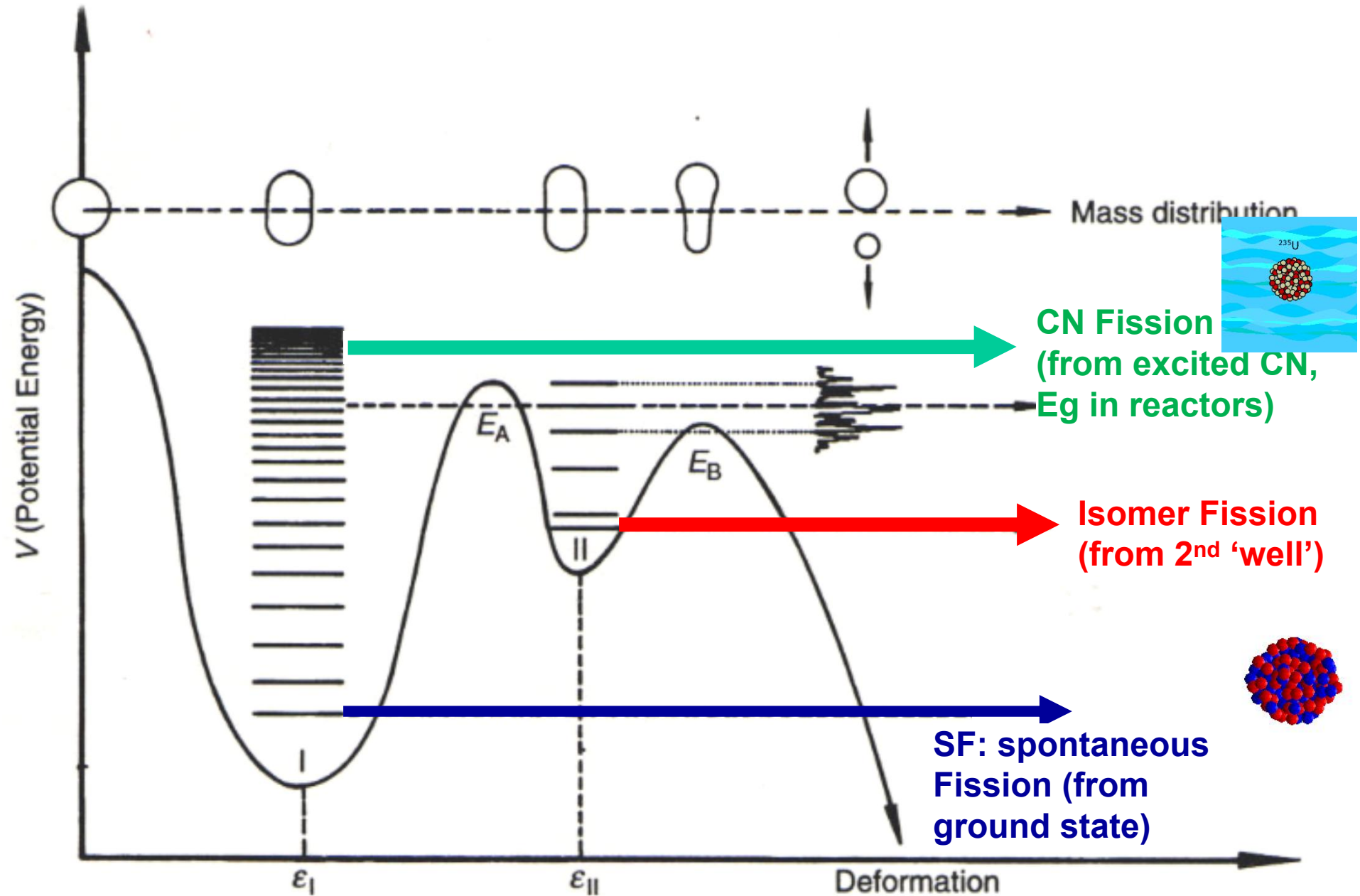


M. Caamaño et al., PRC 88 (2013) 024605



C. Schmitt et al., NPA430 (1984) A. Bail, PRC84 (2011)

Summary of fission modes (return to this later)



Outlook: Why 'new regions of fission'?

- Most of available fission data at low energy are from SF, **thus along the β -stability line**
- The theoretical fission models are also tuned there

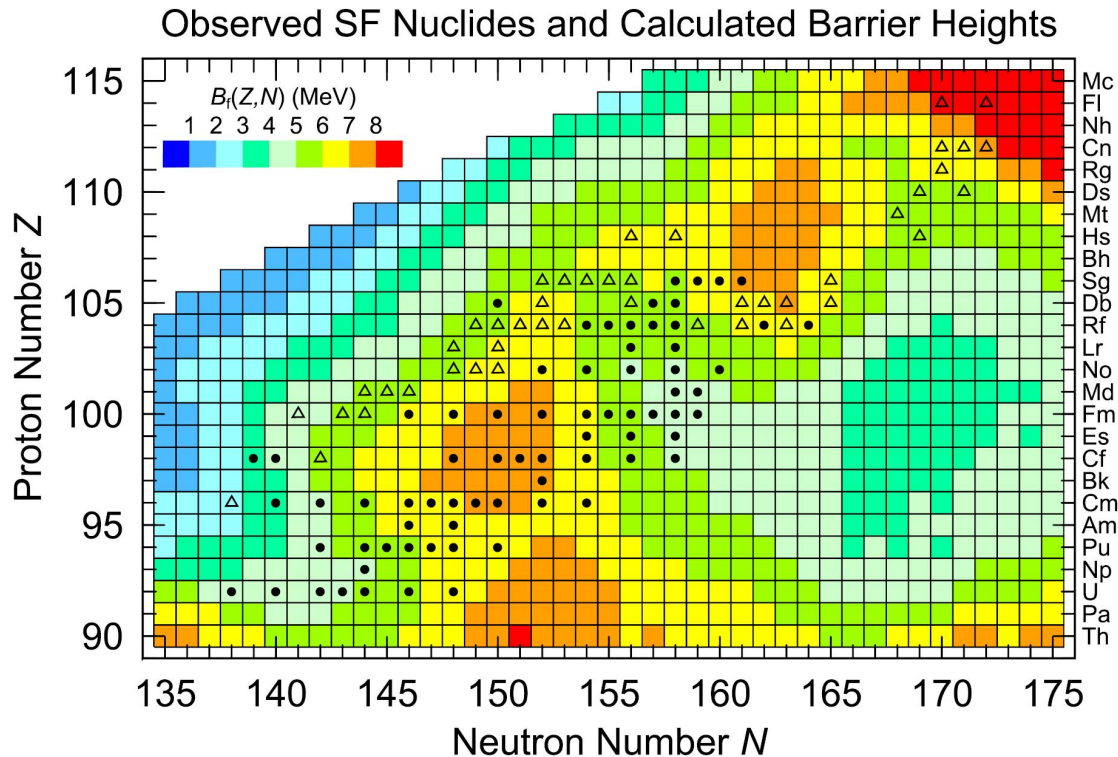
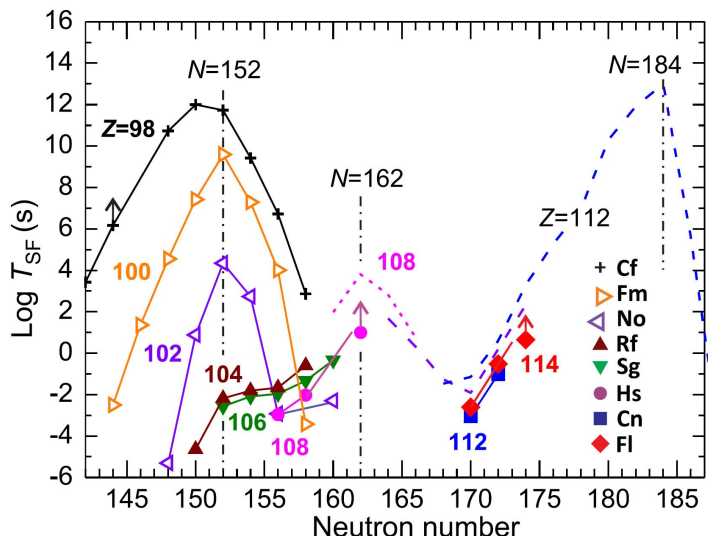


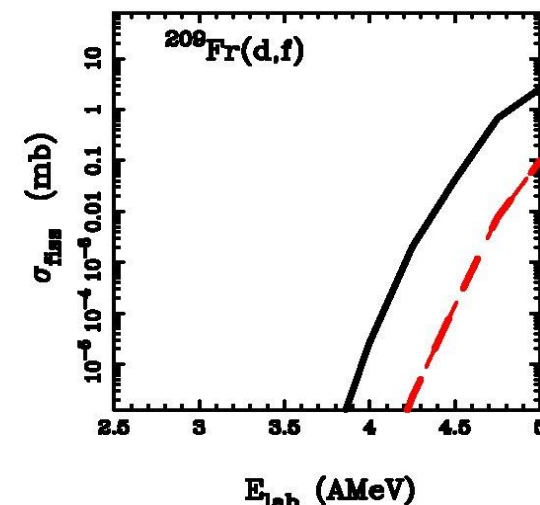
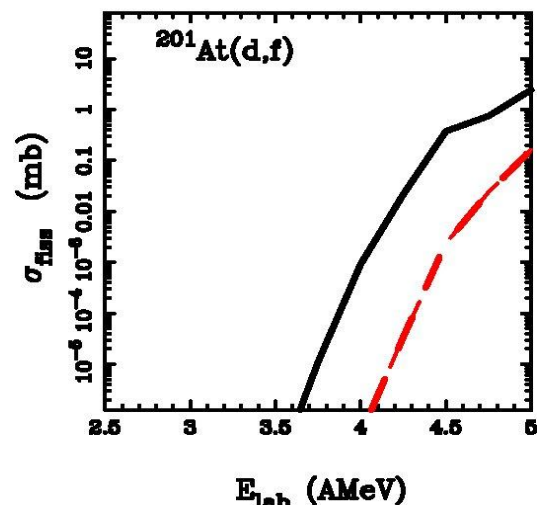
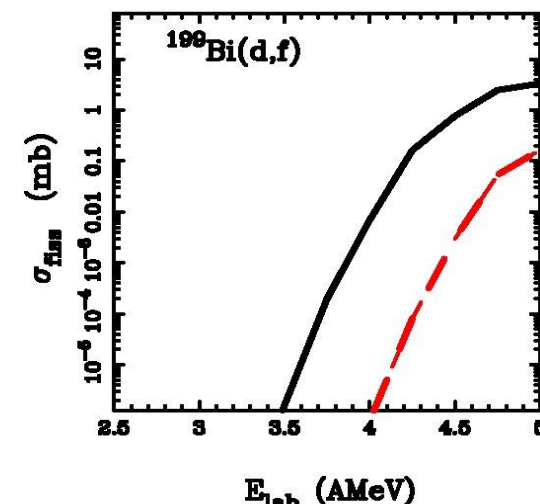
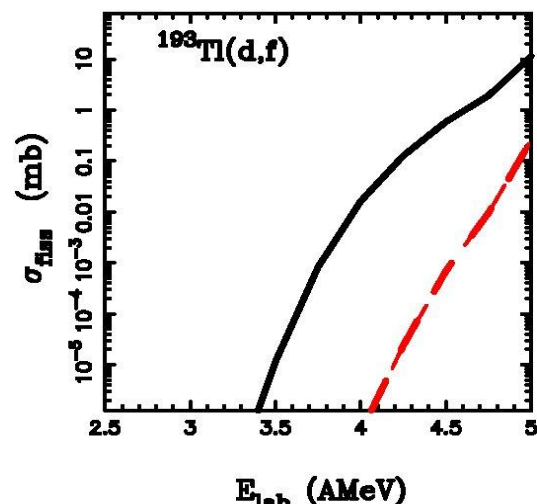
Figure 55. Presently known spontaneously fissioning isotopes (symbols) overlaid on the map of fission-barrier heights for the region above $Z = 90$, calculated within the macroscopic-microscopic model by Möller *et al* [9]. Open triangles and thick dots show the isotopes for which SF was discovered or their properties were re-studied since or before ~ 1995 , respectively. The

IS581 Experiment: (d,pf) transfer-induced fission of post-accelerated RIBs in inverse kinematics with ACTAR

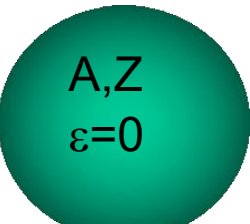
It is of primary interest to observe transfer-induced fission of odd elements such as Tl, Bi, At or Fr, since in this case the estimated fission barriers will not be influenced by uncertainty in estimation of the pairing gap in the saddle configuration.

Observed fission rates of these beams can be used to directly determine values of the fission barrier heights.

$$P_{\text{fis}}(E^*) = \frac{P_0}{1 + \exp\left(\frac{2\pi(B_f - E^*)}{\hbar\omega}\right)}$$



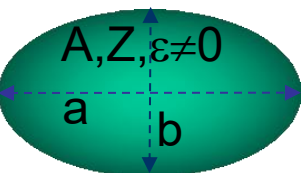
Fission Barrier in LDM



$$R = r_o A^{1/3}$$



Ellipsoidal deformation ϵ
 $a = R(1 + \epsilon)$
 $b = R(1 + \epsilon)^{-1/2}$



$$\text{BE} = \cancel{a_V A} - a_S A^{2/3} - a_C \frac{Z(Z-1)}{A^{1/3}} - \cancel{a_A \frac{(A-2Z)^2}{A}} + \delta(A, Z)$$

Volume $\sim R^3$ Surface $\sim R^2$ Coulomb $\sim 1/R$ Asymmetry $\sim (A-2Z)^2/A$ Pairing

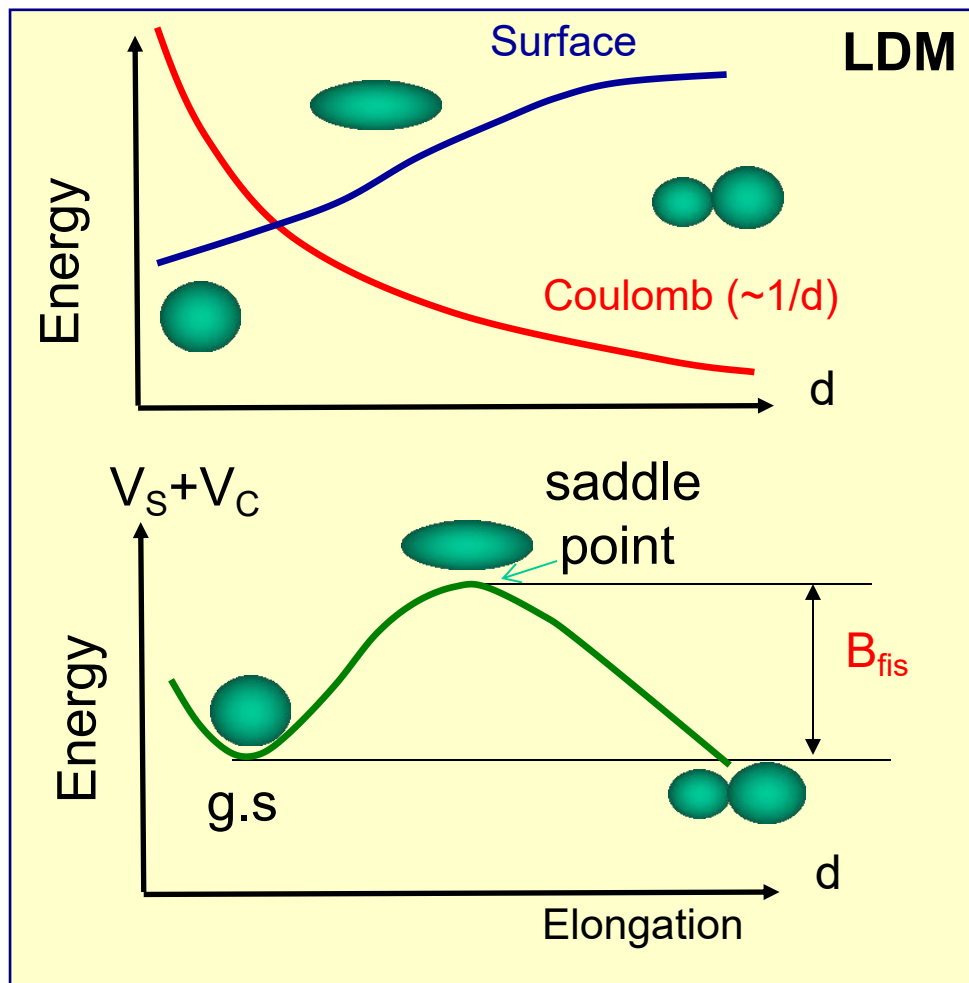
When deformed (assuming **incompressibility!** $R^3 = ab^2$):
 No need to remember expressions, but must know the trends!

- Volume, Asymmetry and Pairing \sim constant
- Surface term **increases** (thus tries to inhibit deformation) from $S = 4\pi R^2$ to $S = 4\pi R^2(1 + \frac{2}{5}\epsilon^2)$, thus BE decreases
- Coulomb **decreases** $\sim (1 - 1/5\epsilon^2)$, thus BE increases
- Difference in BE: $\Delta BE = BE(\epsilon=0) - BE(\epsilon)$

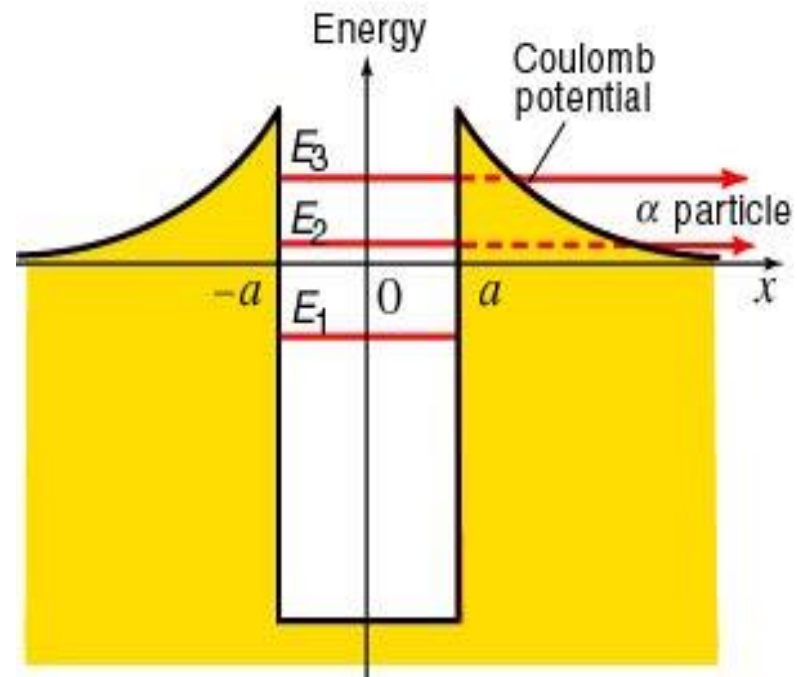
Thus, interplay between Surface and Coulomb terms is important when consider effects of deformation

Fission Barrier in 1D LDM ('Text-book' plot)

Competition between increasing Surface and decreasing Coulomb energies by increasing deformation leads to a local maximum in their difference called **Fission Barrier** (the top of the barrier is called the 'saddle point')



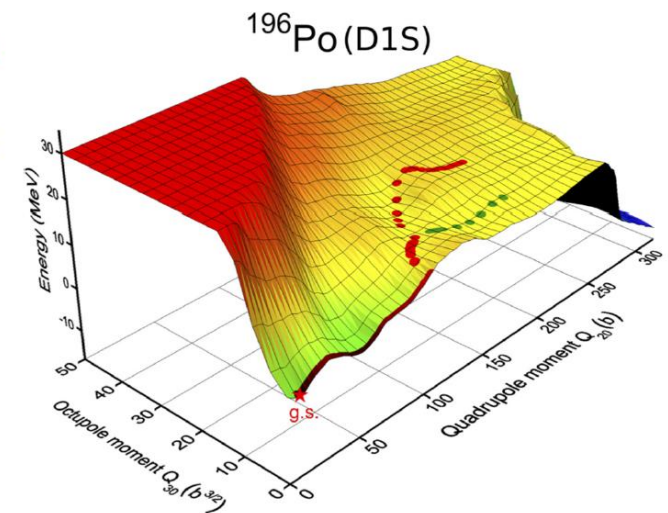
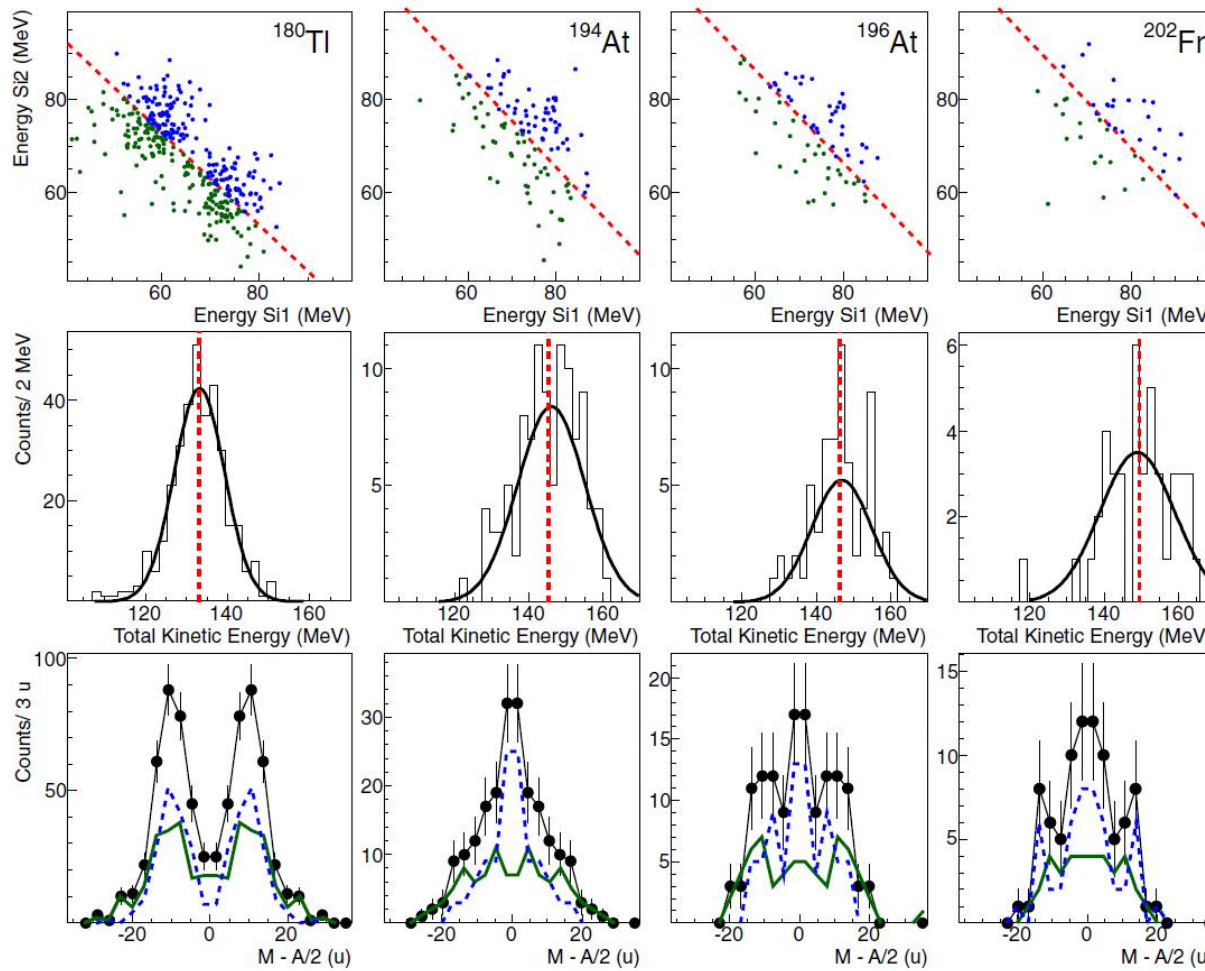
To be compared to alpha decay



NB: in both spontaneous fission and alpha decay, fission happens **via the tunnelling**

Extensive β DF program at ISOLDE (Tl-Bi-At-Fr): first glance in multimodal fission in the neutron-deficient lead region

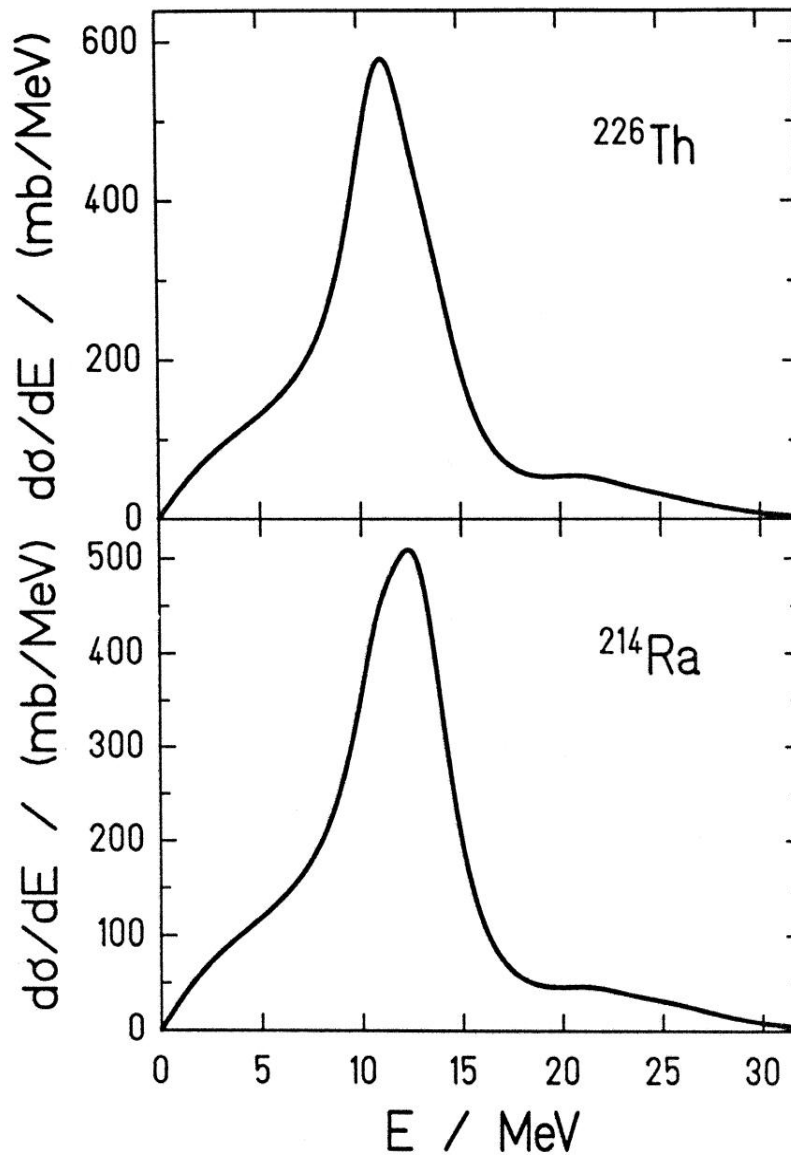
L.Ghys et al., PRC90 (2014)



J. D. McDonnell et al, PRC90, 2014

- One of the main issues: poor FF's mass resolution (~ 4 u) and absence of Z data
- Typical for most of 'low-energy' fission studies (eg. SF), FF's energies ~ 1 AMeV
- Need precise measurements of Z and A: e.g. SOFIA@GSI to rescue?!

Excitation Energy in Coullex-induced fission



- Low-energy excitation, on average $E^* \sim 12 \text{ MeV}$ (but no “fine” control of E^*)
- Thus shell effects must be conserved
- Can’t be applied for nuclei with high fission barrier ($> 12 \text{ MeV}$ or so)

Fig. 16. Calculated excitation-energy distributions of ^{226}Th and ^{214}Ra used as secondary projectiles after electromagnetic excitations in a lead target at 430 A MeV.

Fission of secondary beams after the EM excitation

Detailed studies of multi-modal fission

Black - experiment (Schmidt et al, NPA 665 (2000))

Red - calculations

